Fall 12-16-2016

DNA Polymerase Zeta-Dependent Mutagenesis: Molecular Specificity, Extent of Error-Prone Synthesis, and the Role of dNTP Pools

Olga V. Kochenova
University of Nebraska Medical Center

DNA POLYMERASE ζ -DEPENDENT MUTAGENESIS: MOLECULAR SPECIFICITY, EXTENT OF ERROR-PRONE SYNTHESIS, AND THE ROLE OF dNTP POOLS

by

Olga Kochenova

A DISSERTATION

Presented to the Faculty of
The University of Nebraska Graduate College
In Partial Fulfillment of the Requirements
For the Degree of Doctor of Philosophy

Cancer Research Graduate Program

Under the Supervision of Professor Polina V. Shcherbakova

University of Nebraska Medical Center
Omaha, Nebraska

October, 2016

Supervisory Committee:

Youri Pavlov, Ph. D. Tadayoshi Bessho, Ph. D.

Michel Ouellette, Ph. D.

DNA POLYMERASE ζ -DEPENDENT MUTAGENESIS: MOLECULAR SPECIFICITY, EXTENT OF ERROR-PRONE SYNTHESIS, AND THE ROLE OF dNTP POOLS

Olga V. Kochenova, Ph.D.

University of Nebraska, 2016

Supervisor: Polina V. Shcherbakova, Ph.D.

Despite multiple DNA repair pathways, DNA lesions can escape repair and compromise normal chromosomal replication, leading to genome instability. Cells utilize specialized low-fidelity **T**rans**l**esion **S**ynthesis (TLS) DNA polymerases to bypass lesions and rescue arrested replication forks. TLS is a highly conserved two-step process that involves insertion of a nucleotide opposite a lesion and extension of the resulting aberrant primer terminus. The first step can be performed by both replicative and TLS DNA polymerases and, because of non-instructive DNA lesions, often results in a nucleotide misincorporation. The second step is almost exclusively catalyzed by DNA polymerase ζ (Polζ). This unique role of Polζ allows the misincorporated nucleotide to remain in DNA, resulting in a mutation. Because of the low fidelity of Polζ, a processive copying of undamaged DNA beyond the lesion site by this polymerase is expected to be mutagenic. To restore faithful DNA replication, Polζ must be immediately replaced by an accurate replicative DNA polymerase. However, *in vivo* evidence for this is lacking.

To elucidate the late steps of TLS, we aimed to determine the extent of error-prone synthesis associated with mutagenic lesion bypass in yeast. We demonstrate that TLS tracts can span up to 1,000 nucleotides after lesion bypass is completed, leading to more than a 300,000-fold increase in mutagenesis in this region. We describe a model

explaining how the length of the error-prone synthesis may be regulated and speculate that Polζ could contribute to localized hypermutagenesis, a phenomenon that plays an important role in cancer development, immunity and adaptation.

To gain further insight into the mechanisms of Polζ-dependent mutagenesis, we determined how the increase in dNTP levels occurring in response to DNA damage in yeast affects Polζ function. Surprisingly, increasing the dNTP concentrations to "damage-response" levels only minimally affected the activity, fidelity and error specificity of Polζ, suggesting that, unlike the replicative DNA polymerases, Polζ is resistant to fluctuations in the dNTP levels. Importantly, we demonstrated that Polζ-dependent mutagenesis *in vivo* does not require high dNTP levels either. Altogether, our results suggest a novel function of Polζ in bypassing lesions or other impediments when dNTP supply is limited.

Table of Contents

Factors discussed in this dissertation

Gene	Function
APN1	apurinic/apyrimidinic endonuclease
APN2	apurinic/apyrimidinic endonuclease
DUN1	serine/threonine protein kinase
MEC1	genome integrity checkpoint protein
MMS2	E2 ubiquitin-conjugating enzyme
MSH2	DNA mismatch repair protein
NTG1	DNA *N*-glycosylase and AP lyase, *E. coli* endonuclease III homolog
NTG2	DNA *N*-glycosylase and AP lyase, *E. coli* endonuclease III homolog
OGG1	8-oxoguanine glycosylase and lyase
POL3	catalytic subunit of replicative DNA polymerase δ
POL31	accessory subunit of Polδ and Polζ
POL32	accessory subunit of Polδ and Polζ
RAD1	a structure-specific DNA endonuclease (with Rad10p) in nucleotide excision repair
RAD2	a structure-specific DNA endonuclease nucleotide excision repair

RAD5	ubiquitin ligase
RAD6	E2 ubiquitin-conjugating enzyme
RAD10	a structure-specific DNA endonuclease (with Rad1p) in nucleotide excision repair
RAD14	protein that recognizes and binds damaged DNA during nucleotide excision repair
RAD18	E3 ubiquitin ligase
RAD30	TLS DNA polymerase η
RAD51	strand exchange protein in homologous recombination
RAD53	DNA damage response protein kinase
REV1	deoxycytidyl transferase and TLS polymerase
REV3	catalytic subunit of TLS DNA polymerase ζ
REV7	accessory subunit of TLS DNA polymerase ζ
RNR1	major isoform of large subunit of ribonucleotide reductase
RNR2	small subunit of ribonucleotide reductase
RNR3	minor isoform of large subunit of ribonucleotide reductase
RNR4	small subunit of ribonucleotide reductase
SML1	ribonucleotide reductase inhibitor
UBC13	E2 ubiquitin-conjugating enzyme

Abbreviations

(6-4)PPs	(6-4) pyrimidine-pyrimidone photoproducts
A	adenine
AP	apurinic/apyrimidinic site or abasic site
BER	base excision repair
bp	base pair
C	cytosine
Can^R	canavanine-resistant
CPDs	*cys-sin* cyclobutane pyrimidine dimers
DRIM	Defective-Replisome-Induced Mutagenesis
dNTP	deoxynucleoside triphosphate
F	phenylalanine
G	guanine
h	hour
HR	homologous recombination
HPV	human papillomavirus
HU	hydroxyurea
K	lysine
Leu	leucine
L	leucine (amino acid code)

min	minute
MMR	DNA mismatch repair
NDP	nucleoside diphosphate
NER	nucleotide excision repair
nt	nucleotide
Polδ	replicative DNA polymerase δ
Polε	replicative DNA polymerase ε
Polη	TLS DNA polymerase η
Polζ	TLS DNA polymerase ζ
PCNA	proliferating cell nuclear antigen
RFC	replication factor C
RNR	ribonucleotide reductase
RPA	replication protein A
SC	synthetic complete
ssDNA	single-stranded DNA
T	thymine
TLS	translesion synthesis
Ura	uracil
UV	ultraviolet light
YPDAU	yeast extract peptone dextrose adenine uracil

List of Tables and Figures

Acknowledgment

There are so many people to thank for helping and supporting me during these six years of Graduate School.

First of all, I would like to express my deepest appreciation to my advisor, Polina Shcherbakova, who has been a great mentor over the years. Since the very beginning, she has always been a personal and professional role model that shaped me into a scientist I am today. I am very thankful for your support, guidance, encouragement and inspiration over the years. Thank you for patiently reading through everything I have written and for always providing me with valuable suggestions that helped me a lot to improve my writing skills. Thank you for always being open to discussions, having time and patience to explain concepts to me and for letting me test all, even crazy, ideas.

My supervisory committee comprising of Dr. Tadayoshi Bessho, Dr. Michel Ouellette, and Dr. Youri Pavlov has played an important role in my graduate career. I appreciate their patience, constructive criticism and great suggestions. I am especially thankful to Dr. Youri Pavlov for always being cheerful and encouraging, for his enthusiasm and expressing a great interest in my research. I am also very grateful to Dr. Joyce Solheim for always being warm and supportive during my Graduate School.

I was extremely fortunate to work alongside amazing labmates: Matt, Tony, Artem, Corinn, Yinbo, Liz, Krista, Irina, Hollie, Dan, Miriam, Stephanie, Chelsea and Xuan. Thank you all for your friendship, great conversations and fun time in and outside the lab.

I would like to thank our long-term collaborators Dr. Peter M J Burgers and his post-doctoral fellow Rachel Bezalel-Buch (Washington University in St. Louis, MO) for preparations of Polζ, Dr. Andrei Chabes and his graduate student Phong Tran (Umeå University, Sweden) for measurements of dNTP pools.

I owe a debt of gratitude to my undergraduate advisors, Dr. Sergey G Inge-Vechtomov and Dr. Elena Stepchenkova, who have played an important role in my scientific career. I would not be where I am today without the opportunities they had provided for me.

I am very thankful to the administrative staff of Eppley Institute: Ed Ramspott, Barb, Darcy, Diane, Misty and Michele for making the time I spent in Eppley easier for me. Also I would like to thank Dan Teet for all his assistance with visa and immigration-related issues. I am grateful to the Cancer Research Graduate Program for financial support through my first year and the Program of Excellence Graduate Assistantship from UNMC Graduate Studies for support through my third and fourth years.

My journey through graduate school would not be as enjoyable as it was without love and support of my family and friends. I would especially like to thank my mother, Nina Kochenova, and my late father, Vadim Kochenov, for giving me the opportunities to follow my dreams and for always believing in me. My sister, Irina, has always been there for me. Thank you for always finding a way to cheer me up. Also, I would like to express my sincerest gratitude to my husband Anton for being so understanding and caring, for never doubting my abilities and for being so patient about us living apart for these six years. Finally, I would like to thank my wonderful friends outside the lab: Nastya, Vasilisa, Olga, Dima, Hardeep, Anton S., Anton P. and Masha for their support and encouragement. I would like to specifically thank Masha for her assistance with drawing chemical structures of DNA lesions for my dissertation.

Finally, I would like to thank Chelsea and Stephanie for a critical reading of sections of this dissertation.

Chapter 1. Introduction

1.1 Types of DNA damage and repair pathways

All types of DNA damage can be divided into two major groups, endogenous and exogenous, based on the nature of DNA-damaging factors. Endogenous DNA damage mostly results from spontaneous alterations in DNA structure due to hydrolytic and oxidative reactions, the consequences of cell metabolism (reviewed in (Friedberg et al, 2006)). One of the most common types of endogenous DNA damage is the loss of exocyclic amino groups, or spontaneous deamination. Deamination can occur through pH- and temperature-dependent reactions, and also through enzymatic activity of specialized DNA editing enzymes, deaminases (Lindahl, 1993, Lindahl & Nyberg, 1974, Rebhandl et al, 2015). Because of changes in pairing properties of the altered bases, products of deamination can lead to mutagenesis during replication (Lindahl, 1974). In addition, subsequent processing of deaminated bases by specialized DNA glycosylases, may give rise to another highly mutagenic DNA lesion, apurinic/apyrimidinic (AP) sites (reviewed in (Boiteux & Jinks-Robertson, 2013, Lindahl, 1979)). AP sites also can be formed by spontaneous loss of purine or pyrimidine base from DNA due to cleavage of the *N*-glycosyl bond (Friedberg et al, 2006, Lindahl & Barnes, 2000, Lindahl & Nyberg, 1972). Formation and mutagenic properties of AP sites will be reviewed in details in the Subsection 1.1.1.

Other common types of endogenous DNA damage result from oxidative stress. Reactive oxygen species, generated as by-products of aerobic metabolism, can produce various oxidized lesions such as thymine glycol, 7,8-dihydro-oxoguanine, and various modified bases in DNA (reviewed in (Friedberg et al, 2006)).

On the contrary, exogenous DNA damage is a result of exposure of living cells to various environmental chemical and physical agents that can alter DNA (reviewed in

(Friedberg et al, 2006)). The most common types of exogenous sources of DNA damage are ionizing radiation, ultraviolet (UV) radiation, alkylating agents, and cross-linking chemicals. Exposure of DNA to these agents may result in the formation of single-strand breaks, bulky DNA adducts, alkylated bases, and DNA-DNA or protein-DNA crosslinks.

DNA damage can impair various processes in living cells, including faithful transmittance of genetic material and gene expression. In addition, it can cause cell death, or, on the contrary, provoke uncontrollable cell division (Hoeijmakers, 2009). To avoid all of these destructive consequences of exogenous and endogenous DNA damage, cells evolved multiple pathways that remove lesions from DNA and restore the original sequence (Figure 1.1). Collectively, these processes are known as DNA repair pathways.

One of the most frequently utilized repair pathways is base excision repair (BER) that deals with single-strand breaks, modified or mispaired bases in DNA such as uracil, 7,8-dihydro-oxoguanine, products of alkylation, and thymine - guanine mispairs (reviewed in (Boiteux & Jinks-Robertson, 2013, Friedberg et al, 2006, Zharkov, 2008)). BER is initiated by specialized DNA glycosylases that recognize particular classes of modified bases in DNA and cleave *N*-glycosyl bonds leaving an AP site in DNA. The resulting AP sites are processed by AP lyases or endonucleases that initiate a short- or long-patch BER, followed by ligation of the resulting nick.

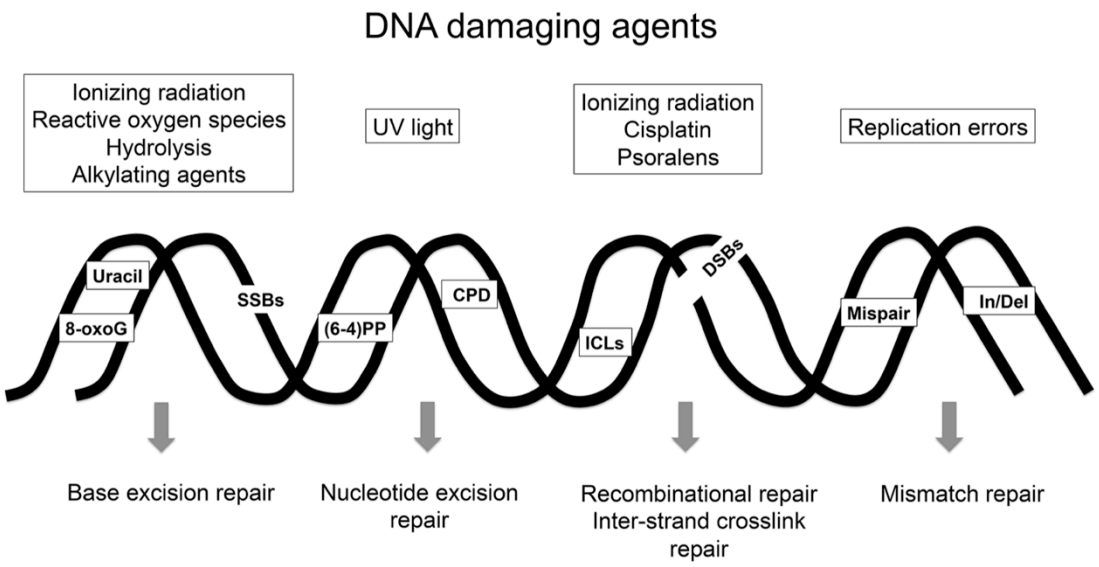

Figure 1.1 Types of DNA damage and repair pathways.

Most common types of DNA damaging agents (top), examples of DNA lesions that they induce (middle), and DNA repair pathways dealing with these lesions (bottom) are shown. Abbreviations: 8-oxoG - 7,8-dihydro-oxoguanine, SSBs - single-strand breaks, (6-4)PP – (6-4) pyrimidine-pyrimidone photoproduct, CPD - *cys-sin* cyclobutane pyrimidine dimer, ICLs - interstrand crosslinks, DSBs – double-strand breaks, In/Del – insertion/deletion mismatch.

Nucleotide excision repair (NER) removes bulky DNA lesions resulting from UV irradiation or exposure to chemical DNA damaging agents. Bulky lesions can significantly affect DNA replication and transcription by blocking DNA and RNA polymerases (reviewed in (Boiteux & Jinks-Robertson, 2013, Friedberg et al, 2006, Scharer, 2013)). NER consists of two pathways depending on mechanism of lesion recognition and factors that participate in this step. In global genome NER, bulky lesions are directly recognized by multiprotein complexes across the whole genome. In contrast, transcription-coupled NER is initiated by the stalling of RNA polymerase at the lesion site and, therefore, functions only on the transcribed strand. After recognition of a lesion, multiple proteins bind to the damage site and form a so-called preincision complex that unwinds DNA duplex around the lesion. This allows specific endonucleases to perform incisions on both sides of the lesion and release a lesion-containing single-stranded DNA fragment. The remaining gap is filled and ligated by DNA polymerases and DNA ligase, respectively.

Many DNA repair intermediates can be converted into another cytotoxic lesion – double-strand breaks. Double-strand breaks are particularly dangerous to cells, because they can lead to replication fork collapse, chromosome rearrangements or loss, and eventually, cell death. Double-strand breaks are repaired by homologous recombination (HR) pathway or non-homologous end-joining in higher eukaryotes (Kowalczykowski, 2015, Waters et al, 2014). The first step of HR involves resection of the double-strand break to produce single-stranded regions and is mediated by helicases and exonucleases. Next, single-stranded ends invade a homologous DNA molecule to initiate new DNA synthesis. Finally, this leads to formation of Holliday junctions and either nucleolytic resolution or topological dissolution of these structures. In contrast, non-homologous end joining does not require invasion of the homologous region, but

directly promotes ligation of the double-strand break. The first step of non-homologous end joining involves recognition and binding of the ends of the double-strand break by a multisubunit protein complex to promote end bridging. The next step assures formation of ligatable DNA ends through their processing by nucleases or DNA polymerases. During the last step, DNA ligase complex ligates processed DNA ends.

Interstrand crosslink repair removes lesions that covalently bind two DNA strands and block replication and transcription (reviewed in (Duxin & Walter, 2015, McVey, 2010). Although the underlying principle of interstrand crosslink repair is generally conserved among species, different organisms utilize various subsets of proteins and different combinations of repair pathways to deal with these lesions. For example, interstrand crosslinks are repaired by combination of NER and HR in bacteria and yeast. First, nucleases catalyze incisions on both sides of the crosslink, creating a gap. Such gaps contain so-called unhooked crosslinks, and can be either filled by specialized DNA polymerases or repaired by HR. During the last step, the unhooked crosslink is removed by NER. Interstrand crosslink repair is more complicated in higher eukaryotes. The choice of DNA repair pathway depends on the stage of the cell cycle. Outside of S-phase, interstrand crosslinks are recognized and repaired by the NER pathway. In contrast, during S-phase, repair of crosslinks is initiated by the convergence of two replication forks at the lesion. This promotes recruitment of a specialized complex (Fanconi Anemia complex) that introduces incisions on both sides of the lesion in one of the crosslinked strands. The resulting gap in one strand and double-strand break in another are filled by specialized DNA polymerases and repaired through HR, respectively. Later, the remaining unhooked adduct is removed by NER.

Although DNA damage is a considerable source of mutations in DNA, mutations can arise during replication of undamaged DNA when DNA polymerases misincorporate

a nucleotide. In addition to misincorporation of deoxyribonucleotides, replication errors often can result from primer-template misalignments that can lead to formation of insertion-deletion loops. Both single-nucleotide mismatches and insertion-deletion loops are recognized and removed by components of the DNA mismatch-repair (MMR) pathway (reviewed in (Fishel, 2015)). Briefly, mismatches or insertion-deletion loops are recognized by MMR machinery, and then a short patch of DNA including the incorrect nucleotide(s) is excised from the duplex. Later, the gap is filled by DNA polymerases. In addition to replication errors, MMR can also act on some modified deoxyribonucleotides in double-stranded DNA.

In the next two subsections, AP sites and UV-induced lesions, as well as repair pathways that deal with removal of these lesions in yeast, will be discussed in more detail.

1.1.1 Abasic site

It has been estimated that approximately 10,000 apurinic sites and 500 apyrimidinic sites may be generated in a mammalian cell daily, which makes AP sites the most frequent endogenous DNA damage (Figure 1.2) (Tropp, 2012). The main source of AP sites is a spontaneous hydrolysis of *N*-glycosyl bond that happens at considerable rates in living cells (Lindahl & Nyberg, 1972, Loeb & Preston, 1986, Shapiro, 1981). Pyrimidine nucleosides are bound to deoxyribose through more stable *N*-glycosyl linkage, and, therefore, the loss of cytosine and thymine happens at a much lower rate than that of adenine and guanine (Lindahl & Karlstrom, 1973). The remaining deoxyribose residues can acquire an open aldehyde form that can be later converted to single-strand break. AP sites, as well as the resulting single-strand breaks, are repaired by BER (reviewed in (Boiteux & Guillet, 2004, Zharkov, 2008)). In yeast, AP

endonucleases Apn1 and Apn2 are involved in the repair of the majority of AP sites, with Apn1 being responsible for the excision of 97% of all AP sites. Although Apn2 is involved in the repair of only 3% of AP sites in wild-type cells, it can compensate for Apn1 deficiency *in vivo* (Johnson et al, 1998, Popoff et al, 1990). AP endonucleases cut on the 5'-side of AP site producing 3'-OH end and a 5'-deoxyribose-phosphate. Polβ in mammalian cells or Polε/Polδ in yeast remove 5'-blocking end and incorporate a single nucleotide to fill the gap. In addition, AP sites can be processed by AP lyase activity of any of the three known DNA *N*-glycosylases/AP lyases in yeast: Ogg1, Ntg1, and Ntg2. AP lyase activity catalyzes cleavage on the 3' side of the AP site producing a 5'-phosphate end and 3'- deoxyribose-phosphate. After removal of 3'-blocking ends by AP endonuclease, repair is completed by DNA polymerase and DNA ligase activities (reviewed in (Boiteux & Guillet, 2004, Friedberg et al, 2006, Lindahl, 1979, Zharkov, 2008)).

If left unrepaired, AP sites can produce single base substitutions (reviewed in (Boiteux & Guillet, 2004)). It has been shown that in *Escherichia coli* (*E. coli*) there is a strong preference for dATP incorporation across from AP sites, so called "A-rule". In yeast and human cells, AP sites also have mutagenic potential, but AP sites in eukaryotes can produce a greater variety of nucleotide substitutions. It appears that the "A-rule" is still followed in eukaryotes, but predominant insertion of dCTP or dGTP can also be observed depending on the sequence context or genetic assay used (Avkin et al, 2002, Cabral Neto et al, 1994, Chan et al, 2013, Gentil et al, 1992, Gibbs & Lawrence, 1995, Gibbs et al, 2005, Haracska et al, 2001, Kunz et al, 1994, Neto et al, 1992, Weerasooriya et al, 2014, Zhao et al, 2004). More specifically, early studies in yeast utilized genetic assays, in which a natural site-specific AP site or its artificial analog, tetrahydrofuran were located on a gapped-duplex or a single-stranded plasmid,

respectively (Gibbs et al, 2005, Zhao et al, 2004). At least for the sequence contexts used in these systems, it was observed that the preferred nucleotide inserted opposite AP site is dCTP. On the contrary, when natural or artificial AP sites were located in the duplex DNA, the majority of mutations at this site resulted from A incorporation opposite the lesions. The studies of mutations induced by methyl methanesulfonate in the *apn1 apn2* background revealed the following frequencies of nucleotide incorporation opposite the AP sites: dATP (64%), dCTP (14%), dGTP (11%), and dTTP (11%) (Haracska et al, 2001). Additionally, Pagès et al. observed preferable dATP incorporation opposite a site-specific tetrahydrofuran in a double-stranded plasmid (Pages et al, 2008), regardless of the lesion location in the leading or lagging strand. Finally, chromosomal AP sites generated by sequential action of cytosine deaminase and uracil *N*-glycosylase in yeast also predominately induced C to T substitutions, indicative of an dATP incorportion across from the AP sites (Chan et al, 2013). The relative frequencies of dATP or dCTP insertion at particular sites were significantly affected by the sequence context, with some motives having a stronger preference for dCTP insertion. Altogether these studies suggest that artificial and endogenously generated AP sites have the same mutagenic potential. However, the specificity of nucleotide incorporation opposite AP sites can vary depending on the lesion location in the gapped/ single-stranded plasmids or in the dsDNA. This observation suggests the involvement of different proteins to the copying of damaged templates during replication of single-stranded and double-stranded DNA.

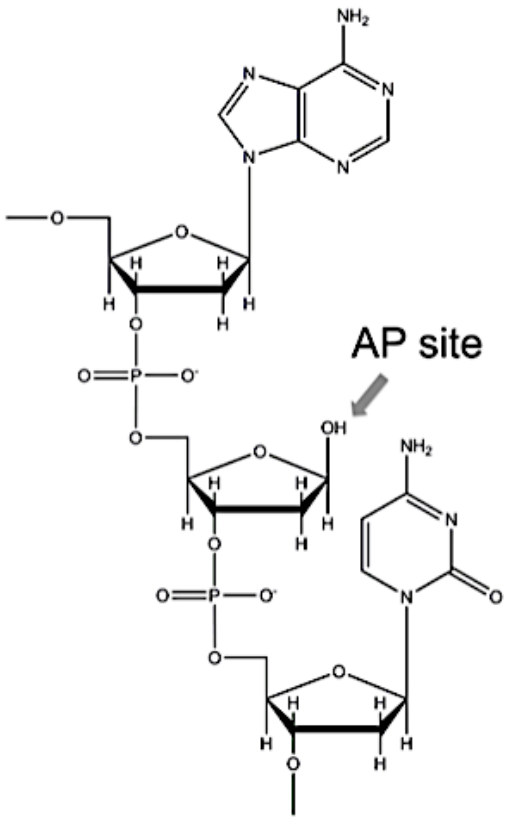

Figure 1.2 Illustration of an AP site in DNA.

The arrow indicates an abasic deoxyribose in DNA backbone.

1.1.2 UV-induced lesions

UV radiation induces various types of DNA lesions with *cys-sin* cyclobutane pyrimidine dimers (CPDs) and (6-4) pyrimidine-pyrimidone photoproducts ((6-4)PPs) being the most frequent types of lesions (Figure 1.3). The overall ratio of CPDs and (6-4)PPs formation in UV-irradiated DNA was estimated to be 3:1 (Mitchell & Nairn, 1989). While both of these lesions can be formed at any of the adjacent pyrimidine dinucleotides: TT, TC, CT, and CC (Ravanat et al, 2001), some dinucleotides are more prone to forming photolesions than others, depending on the surrounding sequence context and doses of UV irradiation. Generally, TT and TC sites are more susceptible to photoreaction than CT and CC sites. In addition, CPDs are predominately observed at TT sites, while (6-4)PPs are more frequently formed at TC sites (Brash & Haseltine, 1982, Mitchell et al, 1992, Mitchell et al, 1990, Pfeifer et al, 1991).

Biochemical and genetic studies of NER components in yeast significantly contributed to elucidating the mechanism of UV photolesions repair. Removal of UV-induced lesions is a complex process that involves the following steps: 1. Damage recognition by Rad14 protein; 2. Unwinding of DNA by multiprotein complex TFIIH; 3. Excision of a short DNA fragment containing the lesion by Rad1-10 and Rad2; 4. Gap filling by replicative polymerases and ligation of the resulting nick by DNA ligase I (reviewed in (Boiteux & Jinks-Robertson, 2013, Rastogi et al, 2010, Scharer, 2013)). Most of the UV-induced lesions are removed very quickly after UV irradiation by global genome NER and transcription-coupled NER. Studies in yeast showed that at 4 hours post-UV irradiation approximately 80% and nearly 100% of CPDs are removed by NER from non-transcribed and actively transcribed strands, respectively (Tremblay et al, 2008). Although NER operates across the whole genome, the efficiencies of UV photolesions removal vary for different genomic regions. The removal of (6-4)PPs and

CPDs on the transcribed strand occurs at similar rates as they presumably inhibit RNA polymerase with similar efficiencies. However, (6-4)PPs are removed faster than CPDs on the non-transcribed strand (Tijsterman et al, 1999). It was proposed that because of the more profound DNA structure distortion and/or nucleosome destabilization that (6-4)PP creates, they can be recognized by global genome NER faster than CPDs (Kim & Choi, 1995, Mann et al, 1997, Taylor et al, 1988, Tijsterman et al, 1999). The latter idea is supported by the fact that the removal of CPDs by global genome NER is greatly affected by the positioning of nucleosomes, and sites with a slower rate of CPDs removal coincide with the position of nucleosome cores (Tijsterman et al, 1999).

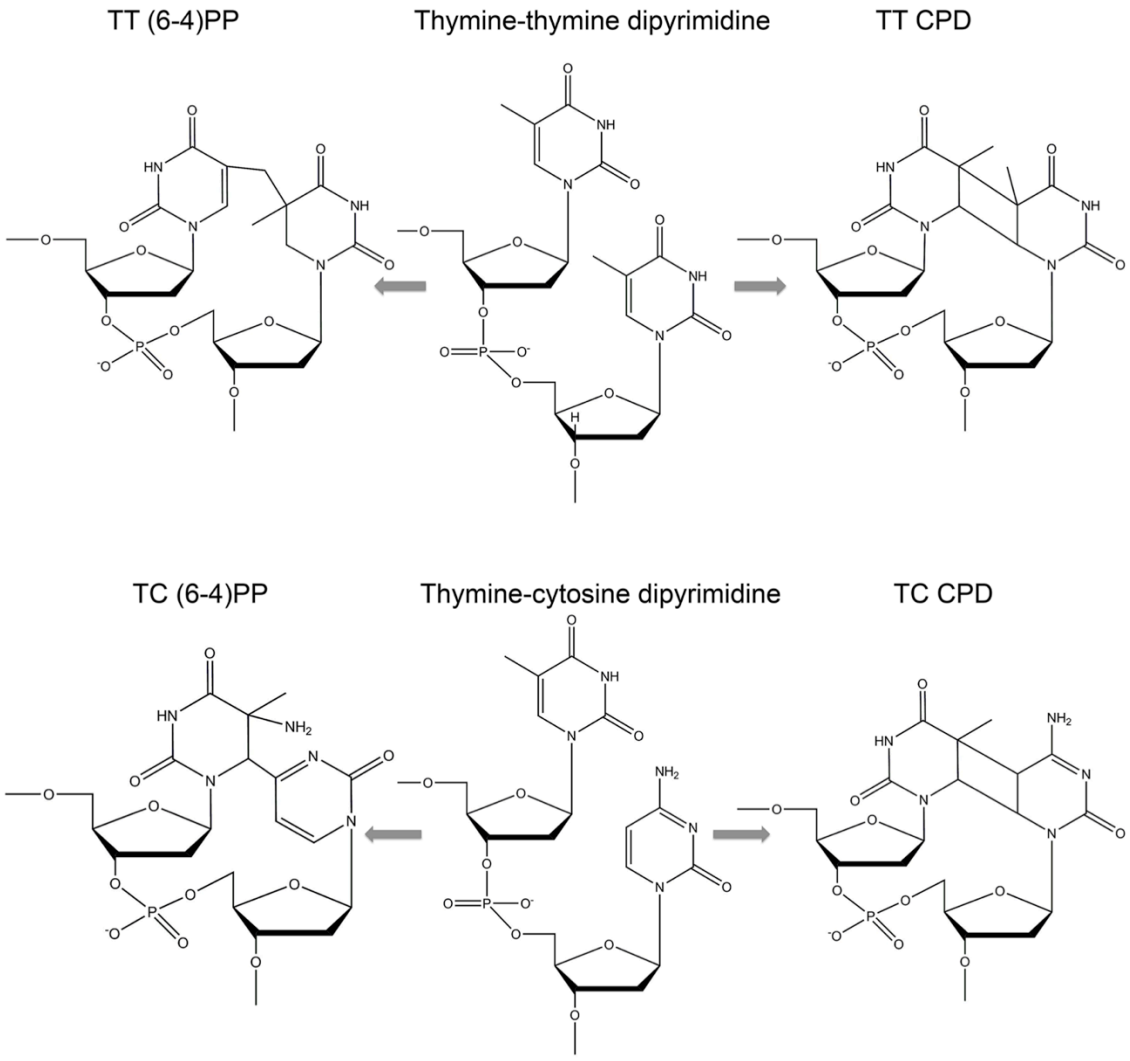

Figure 1.3 Illustration of (6-4)PPs (left) and CPDs (right) using thymine-thymine (top part) and thymine-cytosine (bottom part) dipyrimidine sites as examples.

1.2 DNA damage tolerance pathways

Although cells developed multiple mechanisms to remove lesions from DNA and restore its original sequence, additional pathways are frequently required that would allow the cell to temporarily tolerate lesions in DNA during replication. Lesions that are not removed prior to the S phase of cell cycle can cause replication fork collapse, because the highly selective active sites of replicative DNA polymerases cannot accommodate unusual DNA structures (Broyde et al, 2008, McCulloch & Kunkel, 2008). Therefore, several mechanisms exist that help cells to complete DNA replication by resuming stalled replication without removing the blocking lesion. These pathways are usually referred to as DNA damage tolerance pathways or the post-replication repair pathways (reviewed in (Boiteux & Jinks-Robertson, 2013, Budzowska & Kanaar, 2009, Waters et al, 2009)). Two main subpathways, translesion synthesis (TLS) and HR-mediated template switching, are responsible for bypassing lesions at stalled replication forks. Although the two subpathways share some common regulatory factors, they utilize completely different mechanisms to deal with the lesion. The template switching relies on recombination-based mechanisms involving newly synthesized strand of the sister chromatid as a template and, therefore, is very accurate (Branzei & Szakal, 2016, Budzowska & Kanaar, 2009). On the contrary, TLS requires the function of specialized low-fidelity DNA polymerases to bypass a lesion and is highly error-prone (Figure 1.4) (Waters et al, 2009).

Both TLS and template switching require post-translational modifications of proliferating cell nuclear antigen (PCNA), a processivity factor for DNA polymerases (Ulrich & Walden, 2010). Upon induction of DNA damage, PCNA is monoubiquitylated

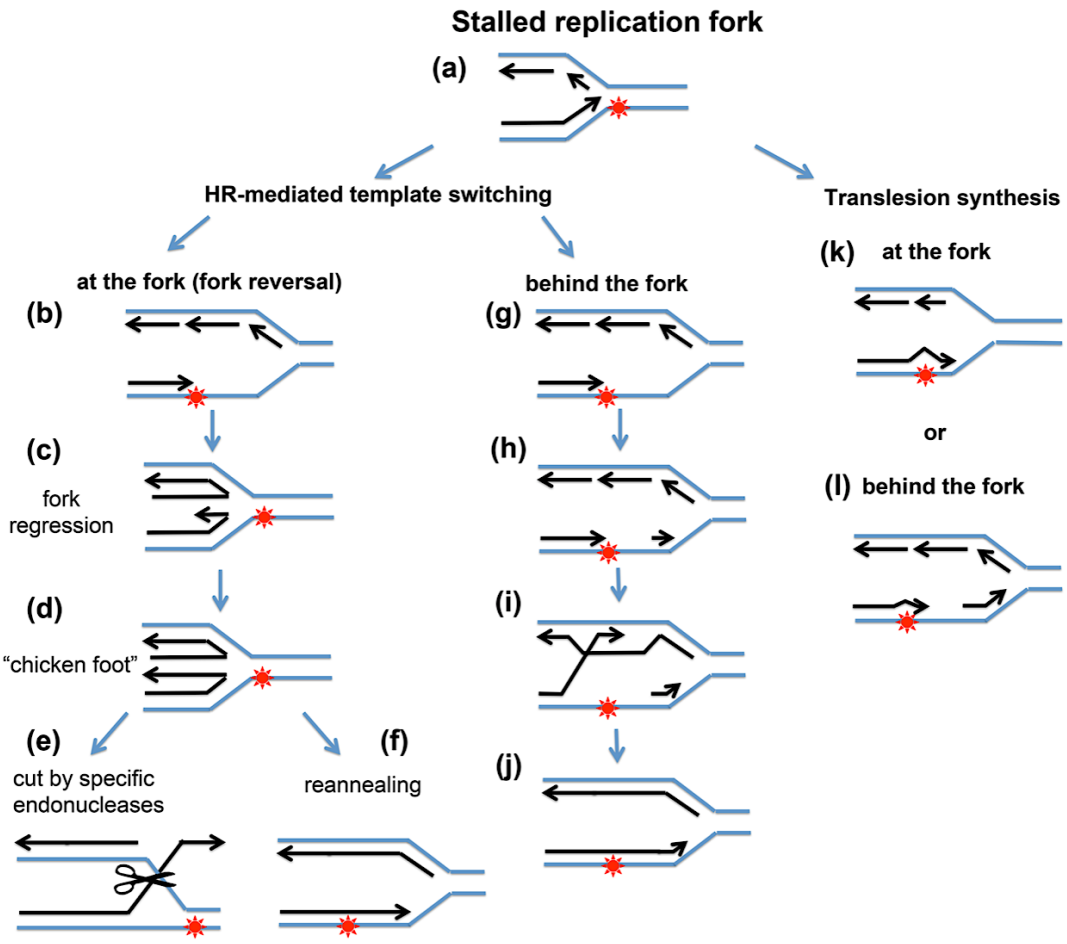

Figure 1.4 DNA damage tolerance pathways.

Stalling of leading strand replication at the lesion site (red star) **(a)** can lead to uncoupling of the leading and lagging strand synthesis **(b, g)**. The template switching at the fork (left part) is initiated by the fork regression **(c)**, which provides a template for DNA synthesis and leads to the formation of a "chicken foot" structure **(d)**. The "chicken foot" structure can be resolved by the action of structure-specific endonucleases **(e)** or through a strand realignment **(f)**. Alternatively, the stalled replication forks can be rescued by HR-mediated template switch behind the fork (middle part). After replication fork uncoupling **(g)**, DNA synthesis can be re-initiated downstream of the stalled replisome, leaving a single-stranded gap **(h)**. The strand invasion **(i)** to the sister chromatid initiates DNA synthesis. Later, the newly synthesized strand realigns with its original template **(j)**. Finally, two models of TLS (right part) propose that rescue of stalled replication forks by TLS can occur in the context of ongoing replication **(k)** or in the gaps **(l)**. In both cases, specialized DNA polymerases bypass a lesion by directly incorporating a nucleotide opposite the lesion site, often resulting in a mutation.

at lysine 164 (K164) by Rad6-Rad18 complex to promote TLS, and subsequent K63-linked polyubiquitylation at this residue by Ubc13-Mms2/Rad5 regulates template switching (Haracska et al, 2004, Hoege et al, 2002, Kannouche et al, 2004, Stelter & Ulrich, 2003). Since polyubiquitylation requires a monoubiquitylated PCNA as a substrate, Rad6-Rad18 deficiency compromises all post-replicative repair. Interestingly, inactivation of PCNA polyubiquitylation leads to a strong mutator phenotype, indicating that HR-mediated template switching is a preferable pathway to rescue stalled replication forks.

1.2.1 Lesion bypass by template switching

HR can promote lesion bypass via two possible mechanisms, template switching at the fork, also known as fork reversal, or template switching behind the fork (left and middle parts of the Figure 1.4, respectively) (reviewed in (Boiteux & Jinks-Robertson, 2013, Budzowska & Kanaar, 2009, Ulrich, 2011). While initiation of both processes requires a strand-exchange protein Rad51, E2/E3 monoubiquitylation complex Rad6-Rad18, and ubiquitin-conjugating complex Ubc13-Mms2, the subsequent steps are regulated by distinct factors. More specifically, fork reversal and formation of a “chicken-foot” structure is facilitated by the activity of Mph1 helicase and, presumably, Rad5 (Figure 1.4 (c, d)). The template switching behind the fork requires the Shu complex that couples damage tolerance to HR (Choi et al, 2010). While it has been proposed that fork regression can happen on both strands, HR-mediated template switch behind the fork is mostly used for the damage bypass on the lagging strands (Boiteux & Jinks-Robertson, 2013). However, the HR-mediated template switch behind the fork is possible on the leading strand as well, assuming the re-priming of replication can occur downstream of the lesion.

1.2.2 Translesion synthesis

In the case of TLS, a damaged nucleotide is used as a template by TLS polymerases (Figure 1.4 (k, l)). An open active site and/or an ability to perform primer loop-out at abnormal templates allow the TLS polymerases to replicate over a great variety of DNA lesions and catalyze synthesis on damaged templates (Lee et al, 2015, Sale et al, 2012, Yang, 2014). However, low fidelity of specialized polymerases involved in lesion bypass and miscoding potential of the lesion itself make TLS a highly error-prone process.

In higher eukaryotes, there are multiple DNA polymerases that are involved in TLS including the Y-family enzymes Polη, Polι, Polκ, and Rev1, the A-family polymerases Polν and Polθ, the B-family enzyme Polζ, and PrimPol (Helleday, 2013, Hogg et al, 2011, Sale, 2013, Takata et al, 2015, Wan et al, 2013, Waters et al, 2009). The yeast *Saccharomyces cerevisiae* (*S. cerevisiae*) has only homologs of Polη, Rev1 and Polζ (Boiteux & Jinks-Robertson, 2013, Waters et al, 2009). According to the current model of TLS, upon replisome stalling at the lesion site, replicative polymerase dissociates from the primer terminus (Figure 1.5). PCNA monoubiquitylation by Rad6-Rad18 complex recruits TLS DNA polymerases to bypass a road-blocking lesion (Waters et al, 2009).

Lesion bypass by TLS polymerases is achieved through a two-step process that involves insertion of a nucleotide opposite the lesion and extension of the resulting aberrant primer terminus (Figure 1.5). The insertion of a nucleotide across from the lesion can be performed by any of the TLS polymerases or, with lower efficiency, by replicative DNA polymerases. The type of the DNA lesion determines the choice of polymerase that

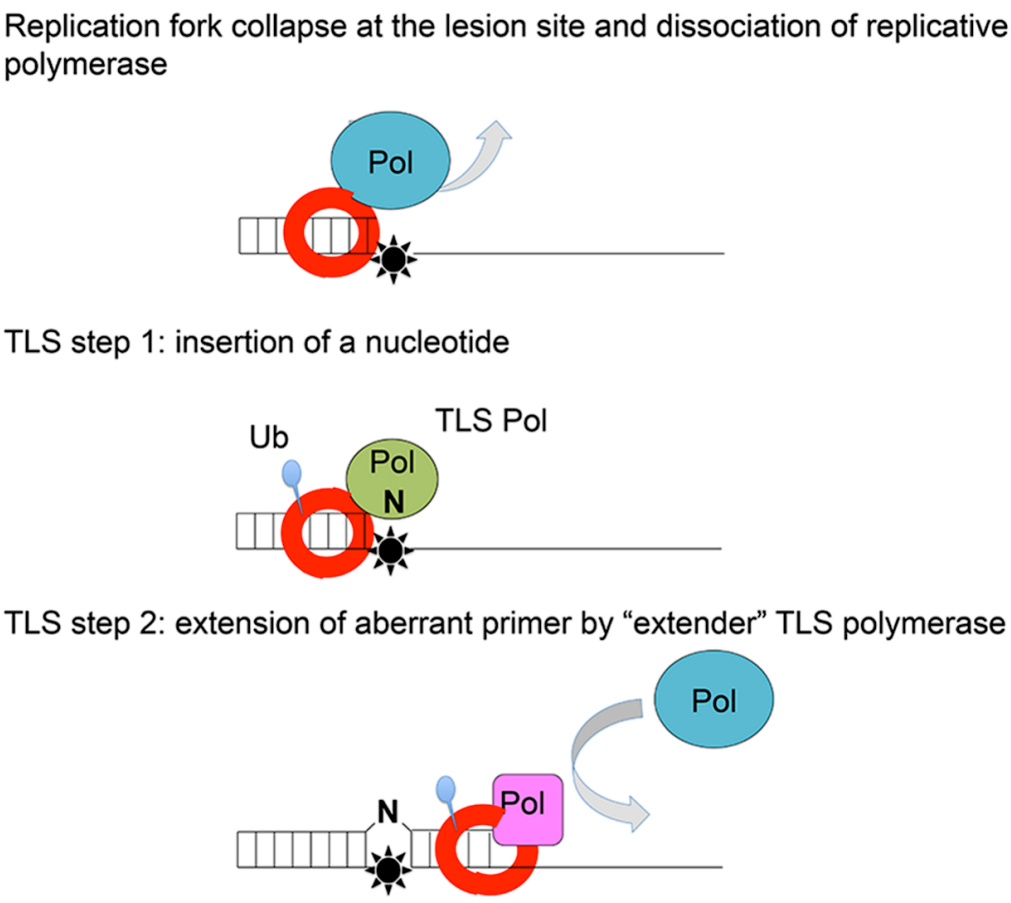

Figure 1.5 A two-step TLS model.

Stalling of replisome at the lesion site (black star) leads to replicative polymerase (blue circle) dissociation from the PCNA (red ring). PCNA ubiquitylation (Ub) recruits TLS polymerases to insert a nucleotide (N) across from the lesion site. The “inserter” DNA polymerase then hands off the aberrant primer terminus to the” extender” TLS polymerase (purple square) in order to complete lesion bypass. The subsequent switching to replicative DNA polymerase restores faithful replication.

will perform a nucleotide insertion. The second step requires a specialized “extender” TLS polymerase that is able to efficiently utilize mispaired or aberrant primer termini (Lawrence, 2004, Livneh et al, 2010, Prakash et al, 2005). It has been proposed that the “extender” polymerase incorporates several nucleotides beyond the lesion site to prevent the removal of the TLS tract by the exonuclease activity of replicative polymerase (discussed in more details in the Section 3.1 and in (Fujii & Fuchs, 2004)).

While the molecular details of the insertion and extension steps have been studied extensively for a variety of lesions, the late steps of TLS remain poorly understood. Specifically, it is not known when and where the switch back to replication by accurate DNA polymerases occurs after the lesion bypass is completed. The high infidelity of the TLS polymerases suggests that their participation in replication past the lesion site must be limited.

1.2.2.1 Translesion Synthesis DNA Polymerases in yeast

Polζ is a key player in mutagenic TLS in *S. cerevisiae* as it is the only polymerase known to be capable of efficient extension of nucleotides incorporated opposite lesions. This unique role of Polζ allows the altered DNA sequence to remain in the newly synthesized strand, leading to conversion of the misincorporation into a mutation. Therefore, Polζ-deficient cells have substantially reduced spontaneous and DNA damage-induced mutagenesis (Lawrence, 2004, Makarova & Burgers, 2015).

Yeast Polζ is comprised of four subunits encoded by the *REV3*, *REV7*, *POL31* and *POL32* genes (Johnson et al, 2012, Makarova et al, 2012, Zhong et al, 2006). Despite being a member of the B family DNA polymerases (Braithwaite & Ito, 1993, Ito & Braithwaite, 1991), Polζ lacks exonuclease activity and is at least two orders of magnitude less accurate than the replicative polymerases Polε and Polδ (Zhong et al,

2006). In addition to its four subunits, the function of Polζ in TLS also requires Rev1, a protein that interacts with both replicative and TLS polymerases (Acharya et al, 2005, Acharya et al, 2009, D'Souza & Walker, 2006, Guo et al, 2003, Murakumo et al, 2001, Ohashi et al, 2004, Tissier et al, 2004) and possesses deoxycytidyl transferase activity (Nelson et al, 1996a). The essential role of Rev1 is structural and likely involves recruiting Polζ to the lesion site and enhancing its lesion bypass capability (Waters et al, 2009). The catalytic activity of Rev1, although not important for the overall efficiency of TLS, is utilized during the bypass of some lesions and helps to shape the mutagenic specificity of bypass (Chan et al, 2013, Kim et al, 2011, Otsuka et al, 2005, Pages et al, 2008, Wiltrout & Walker, 2011, Zhou et al, 2010). For example, the Rev1 deoxycytidyl transferase is responsible for the high frequency of dCTP incorporation observed *in vivo* during the bypass of AP sites (Chan et al, 2013, Kim et al, 2011).

Polη is the third known TLS DNA polymerase in yeast, encoded by the *RAD30* gene (McDonald et al, 1997). The fidelity of Polη on undamaged templates is among the lowest determined for DNA polymerases *in vitro* (Johnson et al, 2000b, Matsuda et al, 2000, Washington et al, 1999). However, the moderate increase in the level of spontaneous mutagenesis in yeast cells overexpressing Polη, suggests that the access of Polη to replication of undamaged DNA is largely restricted (Pavlov et al, 2001a). Despite the low fidelity, Polη was shown to be involved in accurate bypass of TT CPDs (Abdulovic & Jinks-Robertson, 2006, Gibbs et al, 2005, Kozmin et al, 2003, Yagi et al, 2005). Polη-deficient cells show increased sensitivity to UV irradiation and elevated mutagenesis, suggesting that in the absence of Polη CPDs can be bypassed in an error-prone manner by Polζ-dependent TLS (Abdulovic & Jinks-Robertson, 2006, Lawrence & Hinkle, 1996). While reducing mutagenic potential of TT CPDs, Polη was shown to be involved in mutagenic bypass of TT (6-4)PPs in wild-type yeast and cytosine-containing

pyrimidine photolesions in Polζ-deficient strains (Bresson & Fuchs, 2002, Kozmin et al, 2003, Zhang & Siede, 2002).

1.3 The role of dNTP pools in DNA damage bypass

The efficient response to DNA damage requires activation of signaling cascades that regulate DNA repair processes and induce temporary arrest of the cell cycle progression. This provides extra time for removal or bypassing a lesion and allows the cell to enter mitosis with completely replicated chromosomes (Zhou & Elledge, 2000). In yeast *S. cerevisia*e, the slowdown or arrest of the cell cycle in response to DNA damage is achieved through the activation of protein kinases Mec1/Rad53/Dun1 (Baldo et al, 2012). In addition to slowing down the progression through S phase, Mec1/Rad53/Dun1 pathway activates ribonucleotide reductase (RNR), the enzyme that catalyzes the first step in *de novo* synthesis of dNTPs (Andreson et al, 2010, Chabes et al, 2003, Reichard, 1988). During normal S-phase the tight regulation of RNR activity provides optimal dNTP levels that allow efficient DNA replication (Labib & De Piccoli, 2011). Failure to provide balanced dNTP supply may promote genome instability by either reducing the fidelity of DNA polymerases or by slowing down fork progression (Ahluwalia & Schaaper, 2013, Gon et al, 2011, Kumar et al, 2011, Kumar et al, 2010, Mertz et al, 2015, Schaaper & Mathews, 2013, Tse et al, 2016, Watt et al, 2016). Conversely, dNTPs pools expand approximately six- to eight-fold after treatment with DNA damaging agents, such as UV light, methyl methanesulfonate and 4-nitroquinoline 1-oxide (Chabes et al, 2003). This is achieved by Mec1/Rad53/Dun1-mediated degradation of RNR inhibitor Sml1 and by inducing expression of genes encoding the RNR subunits (Figure 1.6) (Andreson et al, 2010, Huang et al, 1998, Zhao et al, 2001). The expansion of dNTP pools significantly improves cell survival during DNA damage (Chabes et al, 2003), and is proposed to facilitate lesion bypass by replicative DNA polymerases, as

well as TLS DNA polymerases (Chabes et al, 2003, Sabouri et al, 2008). In agreement with this view, higher dNTP concentrations enhance the efficiency of lesion bypass by various DNA polymerases *in vitro* (Haracska et al, 2000, Haracska et al, 2001, Johnson et al, 2001, Johnson et al, 2000a, Sabouri et al, 2008, Stone et al, 2011). In addition, studies in *E. coli* suggested that high dNTP levels stimulate TLS *in vivo* by shifting a balance between proofreading and polymerization activities of replicative DNA polymerase III toward the elongation mode allowing the TLS tract to remain in DNA (Gon et al, 2011). However, it has not been established whether elevated dNTP pools can enhance TLS polymerases activity *in vivo*. While facilitating lesion bypass, high dNTP levels could conceivably further reduce the fidelity of TLS DNA polymerases leading to accumulation of more mutations in the genome.

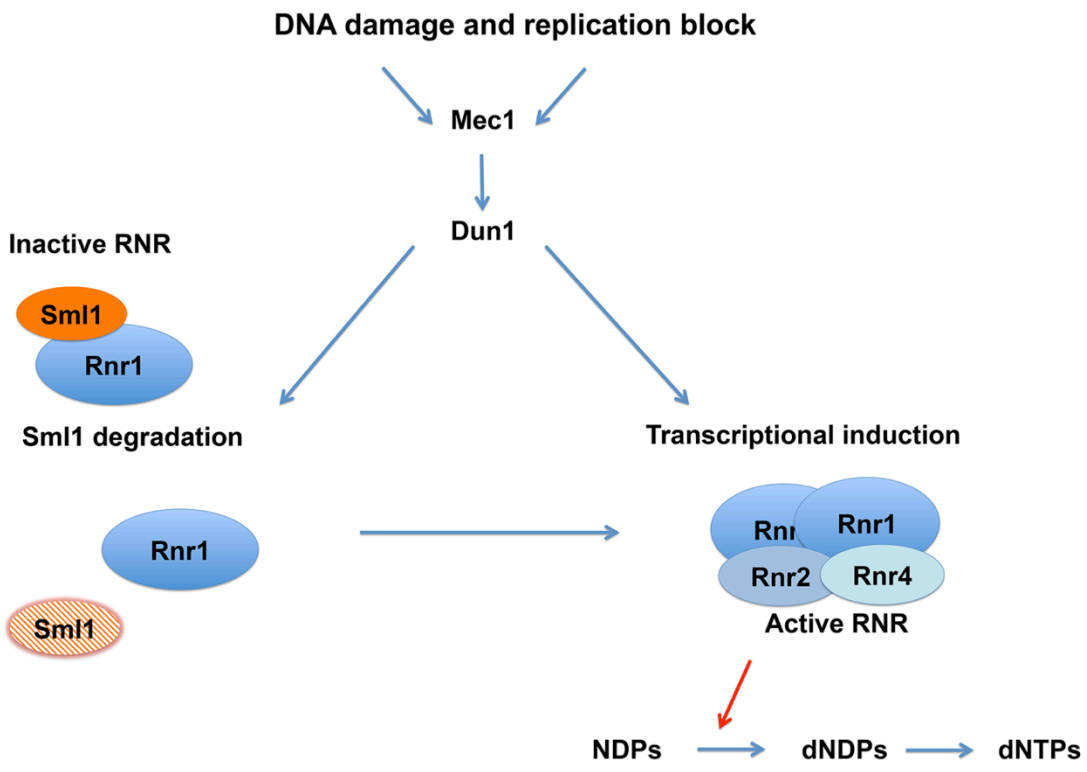

Figure 1.6 The mechanisms of RNR activation in response to DNA damage and replication block.

Prior to activation of DNA damage response by Mec1/Rad53/Dun1 kinases, the large subunit of RNR complex, Rnr1, is inactivated by Sml1 binding (left part). In response to DNA damage, Sml1 is degraded, which allows an assembly of an active RNR complex via binding of two Rnr1 subunits to Rnr2 and Rnr4 subunits. In addition to Sml1 degradation, Dun1 kinase promotes increased production of the RNR complex through transcriptional induction (right part). Active RNR catalyzes conversion of NDPs to dNDPs.

1.4 Participation of DNA polymerase ζ in replication of undamaged DNA

Besides the important role in TLS, Polζ and Rev1 are recruited to replicate undamaged DNA when the normal replication is impaired because of a mutation affecting one of the components of replisome (Northam et al, 2006, Northam et al, 2014, Northam et al, 2010). Defective replisomes stall more frequently at DNA sequences that are prone to formation of short hairpin structures. Such stalling triggers the recruitment of Rev1 and Polζ that help to bypass these structures (Northam et al, 2014). Increased participation of the error-prone Polζ in the replication of undamaged DNA leads to substantial elevation of the rate of spontaneous mutation leading to a phenomenon called Defective-Replisome-Induced Mutagenesis (DRIM). DRIM can be induced by mutations in almost any component of the replisome. It can be promoted by defects in DNA polymerases α, δ and ε (Northam et al, 2006, Pavlov et al, 2001b, Shcherbakova et al, 1996), in non-catalytic replisome components (Aksenova et al, 2010, Becker et al, 2014, Garbacz et al, 2015, Grabowska et al, 2014, Kraszewska et al, 2012, Northam et al, 2006) or replication-coupled chromatin remodeling factors (Kadyrova et al, 2013), as well as by treatment of wild-type cells with hydroxyurea (HU), a well-known replication inhibitor (Northam et al, 2010). Similar to TLS, DRIM requires monoubiquitylation of PCNA by Rad6-Rad18 (Northam et al, 2006), suggesting that the recruitment of Polζ-Rev1 to stalled defective replisomes is regulated in the same way as in the case of lesion bypass.

One of the best-studied genetic models of DRIM in yeast is the *pol3-Y708A* mutant. This mutation leads to an alanine substitution for Tyr708 at the active site of Polδ (Pavlov et al, 2001b). A slow growth phenotype, HU sensitivity and constitutive

PCNA monoubiquitylation in the *pol3-Y708A* strains suggest the existence of replication stress in these mutants. Moreover, approximately 90% of the spontaneous mutagenesis in this strain is dependent on Polζ indicating its significant contribution to DNA replication in this mutant, which makes it a good model for studies of Polζ-dependent mutagenesis during replication of undamaged DNA. Measurement of the size of dNTP pools in logarithmically growing wild-type and *pol3-Y708A* strains showed a seven-fold increase in the total dNTP level in the *pol3-Y708A* mutant in comparison to the wild-type strain (Figure 8.1 (A)). The increases for individual dNTPs range from approximately six- to nine-fold and are similar to those observed during DNA damage response (Chabes et al, 2003). This finding is in accord with the view that TLS polymerases always function in situations when dNTP pools are elevated. However, it still remains unknown whether this expansion of dNTP pools stimulates Polζ activity and/or is essential for Polζ-dependent mutagenesis.

1.5 Dissertation overview

The work described in this dissertation addresses two important aspects of TLS-associated mutagenesis: possible contribution of TLS polymerase ζ to mutagenesis beyond the lesion site, and the effect of intracellular dNTP fluctuations occurring during DNA damage response on the level and specificity of Polζ-dependent mutagenesis. Overall, the results in this dissertation support the following statements: (1) mutagenic bypass of plasmid-borne and chromosomal lesions is associated with untargeted mutagenesis in the adjacent DNA region, (2) untargeted mutagenesis likely results from the processive copying of undamaged DNA by Polζ, (3) Polζ is remarkably resistant to the fluctuations in dNTP pools naturally occurring in response to DNA damage. Based on our findings, we provide a model explaining how the length of Polζ-dependent error-

prone synthesis can be regulated during TLS in yeast and propose a novel function of Polζ in rescuing stalled replication forks when dNTP supply is low.

Chapter 3 of this dissertation describes a genetic system that can be used for phenotypical identification of the products of mutagenic TLS across from a site-specific plasmid-borne AP site. A survey of the region downstream of the lesion site (in respect to the direction of TLS) for the presence of additional mutations revealed that the bypass of a single AP site is associated with untargeted mutagenesis within at least 200 bp from the lesion. The occurrence of the untargeted mutations in the bypass products indicates error-prone polymerase activity in this region.

Chapter 4 of this dissertation describes a genetic system for selection of the products of TLS through a site-specific chromosomal UV lesion. This chapter presents evidence that, as in the case of AP site bypass, Polζ-dependent bypass of UV-induced lesion is accompanied by more than 300,000-fold increase in mutation rate in the region downstream from the lesion site. This indicates that the untargeted mutagenesis is a common phenomenon associated with Polζ-dependent TLS regardless of the lesion type. In addition, experiments described in this chapter investigate whether Polζ or another TLS polymerase is responsible for the generation of untargeted mutations beyond the lesion site.

Experiments described in Chapter 5 of this dissertation thoroughly characterize the effect of the increase in dNTP levels occurring during DNA damage response on Polζ-dependent mutagenesis. Biochemical experiments described in this chapter provide evidence that four-subunit Polζ ($Pol\zeta_4$), as well as five-subunit complex, $Pol\zeta_4$-Rev1 ($Pol\zeta_5$), are remarkably insensitive to the changes in dNTP levels. Furthermore, experiments in this chapter demonstrate that the high dNTP levels are not required for

Polζ-dependent lesion bypass or Polζ-dependent copying of undamaged DNA *in vivo.* We provide evidence that high dNTP levels facilitate function of replicative polymerases upon DNA damage or replication stress, while Polζ is uniquely capable of rescuing perturbed DNA replication in the absence of dNTP pools expansion.

Chapter 2. Materials and Methods

2.1 Strains and plasmids

The haploid *S. cerevisiae* strains PS1001/PS1002 (*MATα ade5 lys2-Tn5-13 trp1-289 his7-2 leu2-3,112 ura3Δ apn1Δ::loxP apn2Δ::loxP*) and OK29/30 (*MATα ade5-1 lys2::InsE$_{A14}$ trp1–289 his7-2 leu2-3,112 ura3-G764A-LEU2*) were used to determine the extent of the error-prone synthesis during AP site and UV lesion bypass, respectively. PS1001 and PS1002 are two independent isolates of the same genotype derived from CG379Δ (Shcherbakova et al, 1996, Shcherbakova & Pavlov, 1996) and obtained by D. L. Daee in the Dr. Shcherbakova laboratory by replacement of the *APN1* and *APN2* genes by the *loxP-LEU2-loxP* and *loxP-kanMX-loxP* cassettes, respectively (Kochenova et al, 2015). The *LEU2* and *kanMX4* markers were removed by expressing Cre recombinase as described in (Guldener et al, 1996). OK29 and OK30 are two independent isolates of the same genotype derived from E134 (*MATα ade5-1 lys2::InsE$_{A14}$ trp1-289 his7-2 leu2-3,112 ura3-52*) (Shcherbakova & Kunkel, 1999)) as follows. First, the E134^{+} strain was obtained by M. R. Northam in the Dr. Shcherbakova laboratory by substituting the *ura3-52* allele in E134 with a wild-type copy of the *URA3* gene. Next, the *ura3-G764A* mutation was created by site-directed mutagenesis in a yeast integrative vector containing the *URA3* and *LEU2* genes cloned into pUC18 (Shcherbakova & Pavlov, 1993), yielding pUC18-*ura3-G764A-or1*. Finally, OK29 and OK30 were obtained by substituting the wild-type chromosomal *URA3* gene of E134^{+} with the PCR-amplified *ura3-G764A-LEU2* cassette. The primers for amplification had 20 bp of homology to pUC18 regions flanking the *ura3-G764A* and *LEU2* genes on the 3' end and 45 bp of homology to the 3' and 5' untranslated regions of the chromosomal *URA3* gene on the 5' end. The *rev3*Δ, *rad30*Δ and *msh2*Δ derivatives of OK29/30 and *msh2*Δ derivatives of PS1001/1002 were obtained by transformation with PCR-

generated DNA fragments carrying the *kanMX* cassette flanked by a short sequence homology to the *REV3*, *RAD30* or *MSH2* genes. The *rev3-L979F* derivatives of OK29/30 strains were constructed by using *SnaB*I-cut pREV3Cav2-L979F plasmid, (Sakamoto et al, 2007), and the presence of the mutation was confirmed by DNA sequencing.

To study the genetic interaction of the *pol3-Y708A* allele and Dun1 deficiency, first, the *DUN1* gene was replaced with *kanMX4* cassette in the haploid strains 1B-D770 (*MATa ade5-1 lys2-Tn5-13 trp1-289 his7-2 leu2-3,112 ura3-4*) and E134 (Shcherbakova & Kunkel, 1999). Next, *dun1Δ* derivatives of 1B-D770 and E134 were crossed to produce a homozygous diploid OK46 (*MATa//MATα ade5-1//ade5-1 lys2-Tn5-13// lys2::InsE$_{A14}$ trp1-289//trp1-289 his7-2//his7-2 leu2-3,112//leu2-3,112 ura3-4//ura3-52 dun1Δ::KanMX4//dun1Δ::KanMX4*). The heterozygous *POL3*/*pol3-Y708A* derivative of OK46 was constructed by replacing one copy of the wild-type chromosomal *POL3* gene with a mutant copy by transformation with HpaI-cut p170 plasmid (Pavlov et al, 2001b). The wild-type diploid strain was obtained by crossing E134 to 1B-D770. Its heterozygous *POL3*/*pol3-Y708A* derivative was constructed as described above. The presence of the *pol3-Y708A* allele was confirmed by DNA sequencing. Next, diploid strains were sporulated on potassium acetate medium, and the haploid progeny of diploid strains were analyzed by tetrad dissection.

The E134 strain and its isogenic derivative PS446 (same, but *rev3*Δ*::LEU2*) (Northam et al, 2006) were used to study the effects of dNTP pools expansion on mutagenesis *in vivo*. To obtain the *pol3-Y708A* mutants, E134 and PS446 strains were transformed with *Hpa*I-cut p170 plasmid, and the mutation was introduced through integration/excision gene replacement as described earlier (Pavlov et al, 2001b). The presence of mutation was confirmed by sensitivity to 100 mM HU (Sigma-Aldrich).

The pRS315-*URA3* OR2 plasmid (Lada et al, 2011) containing the *URA3* gene cloned into the *HindIII* site of pRS315 (Sikorski & Hieter, 1989) was kindly provided by Dr. Youri Pavlov (University of Nebraska Medical Center, Omaha, U.S.A). In addition to the *URA3* gene, it carries the following elements: a *LEU2* selectable marker, the yeast origin of replication *ARS4*, a yeast centromere sequence, and the f1 phage origin of replication. The single-stranded DNA (ssDNA) form of pRS315-*URA3* OR2 contains the transcribed *URA3* strand. *Escherichia coli* F' strain DH12S (Invitrogen) and M13KO7 helper phage (New England Biolabs) were used for isolation of the pRS315-*URA3* OR2 ssDNA. The *E. coli* strains XL10-Blue and MC1061 (Invitrogen) were used for plasmid rescue from yeast cells and for propagation of plasmid DNA.

MC1061 electrocompetent cells and CSH50^{+} strains were used to yield M13mp2 plaques in the *lacZ* polymerase assay as described previously (Bebenek & Kunkel, 1995).

2.2 Proteins

Purifications of yeast PCNA and RPA used in this work were performed by T. M. Mertz in the Dr. Shcherbakova laboratory and have been described earlier (Mertz et al, 2015). Preparations of Polζ_4, Polζ_5 and RFC were provided by Dr. Peter M. J. Burgers (Washington University School of Medicine, St. Louis, MO).

2.3 Construction of the double-stranded plasmid with a site-specific AP lesion

The single-stranded pRS315-*URA3* OR2 phagemid was purified as described in (Banerjee et al, 1990) with some modifications. The DH12S strain transformed with pRS315-*URA3* OR2 was grown in LB medium and infected with M13KO7 (final

concentration of 1 x 10^8 pfu/ml) at OD600 of 0.05. The next day, the bacteriophage particles were collected from the culture supernatant by PEG precipitation. First, *E. coli* cells were pelleted by centrifugation at 4,000 x g for 15 min. Approximately 90% of supernatant was transferred to a new tube. The centrifugation was repeated at least two times. Next, bacteriophage particles were recovered from the cell-free supernatant by stirring it with 4% PEG - 0.5 M NaCl at 4°C for 1 h and subsequent centrifugation at 4,000 x g for 30 min. The pellets were washed with 10 mM Tris-HCl and re-suspended in 10 mM Tris-HCl pH 8.0. The residual cell debris was then removed by centrifugation at 60,000 x g for 15 min at 4°C. To recover the phage particles, a subsequent overnight centrifugation was performed under the same conditions. The pelleted bacteriophage particles were re-suspended in 2 ml of 10 mM TE buffer. To remove residual fragments of bacterial DNA or RNA that could anneal to the pRS315-*URA3* OR2 ssDNA, the bacteriophage particles were incubated with 120 U/ml T4 DNA polymerase (New England Biolabs) and 5 µg/ml RNAse A (USB) in NEB2 buffer (New England Biolabs) at 37 °C for 2 h. To stimulate the 3'-exonuclease rather than the DNA polymerase activity of T4 DNA polymerase, the incubation with the polymerase was performed in the absence of dNTPs. The enzymes were then removed by incubation with 5 µg/ml Proteinase K (Sigma-Aldrich) at 55°C for 30 min, and the pRS315-*URA3* OR2 ssDNA was purified from pre-cooled bacteriophage particles by three sequential extractions with phenol, two extractions with phenol-chloroform, and one extraction with chloroform, followed by ethanol precipitation. Samples were shaken gently to prevent shearing of the DNA. Purified ssDNA was stored in 10 mM TE buffer at -80°C.

The double-stranded plasmid containing a site-specific tetrahydrofuran lesion and a control undamaged plasmid were constructed by annealing oligonucleotides 5'-AGGTTACGATTGGTTGATTATGACAC**THF**CGGTGTGGGTTTAGATGACA-3', where

"THF" is an AP site analog, tetrahydrofuran, (Oligos etc) and 5'-AGGTTACGATTGGTTGATTATGACACGGCGTGTGGGTTTAGATGACA-3' (IDT), respectively, to the pRS315-*URA3* OR2 ssDNA and synthesizing the complementary strand by T7 DNA polymerase. The oligonucleotides are complementary to the *URA3* nucleotides 579-625. The control oligonucleotide contains three bases (underlined) that do not match the wild-type *URA3* sequence and produce a triple CCG → GGC substitution (the *ura3-103,104* allele) resulting in a Ura^- phenotype. The oligonucleotides were PAGE-purified and annealed to the pRS315-*URA3* OR2 ssDNA by incubating a two-fold molar excess of the oligonucleotide with the 400 ng of ssDNA at 72°C for 2 min in T4 DNA ligase buffer (New England Biolabs) and then cooling slowly to room temperature. The whole volume of the annealing mix was then incubated with 10 U of T7 DNA polymerase, 200 μM dNTPs, 4 mM ATP and 10 U of T4 DNA ligase (New England Biolabs) in T7 DNA polymerase buffer at 37°C for 1.5 h. The reactions were then treated with Proteinase K (Invitrogen) at 37°C for 20 min. The covalently closed double-stranded plasmids were isolated from 0.8% agarose gel by centrifugation through premade Sephadex-10 columns (Pharmacia Fine Chemicals) as described elsewhere (Wang & Rossman, 1994) and then ethanol precipitated.

2.4 Isolation and analysis of the AP Site bypass products

Ten-fold diluted overnight PS1001/PS1002 cultures were grown to a logarithmic phase at 30 °C in liquid YPDAU medium [1% yeast extract, 2% bacto-peptone, 2% glucose, 0.006% adenine, and 0.0625% uracil] (Northam et al, 2010). PEG-mediated transformation was used to introduce double-stranded tetrahydrofuran-containing and control plasmids into the yeast cells (Amberg et al, 2006). Yeast cells were then plated on synthetic complete (SC) medium without leucine (SC –leu) to allow for selection of transformants. On the third day of growth colonies were replica-plated on synthetic

complete medium without leucine and uracil (SC −leu –ura) to identify individual TLS products by half-sectored phenotype. Genomic yeast DNA was purified from the Ura^- part of the half-sectored colonies using the MasterPure™ Yeast DNA Purification Kit (Epicentre). To isolate plasmids from the total DNA samples, 5-7 µl of each genomic DNA preparation was used for transformation of the XL10-Blue or MC1061 *E.coli* strain, and plasmid DNA was purified from individual bacterial colonies by using the High-Speed Plasmid Mini Kit (IBI Scientific). The region comprising 550 nucleotides upstream and 1.7 kb downstream of the tetrahydrofuran position (in respect to the direction of lesion bypass), as well as the corresponding region in the progeny of the control plasmid, were analyzed by Sanger sequencing.

2.5 Isolation and analysis of UV lesion bypass products

To select for the independent UV-induced Ura^+ revertants or canavanine-resistant (Can^r) mutants of the OK29 and OK30 strains or their *rev3*Δ, *rev3-L979F*, *rad30*Δ or *msh2*Δ derivatives, the strains were streaked to single colonies on YPDAU plates and grown for three days at 30°C. Single colonies were inoculated into 5 ml of liquid YPDAU and grown overnight at 30°C. The next day, cells were washed with and resuspended in 2.5 ml of water. Next, 200-µl aliquots were spread on a SC –ura plate or SC supplemented with 60 mg/L L-canavanine but lacking arginine (SC –arg +CAN), and irradiated immediately with 60 J/m^2 of 254 nm UV light. The plates were incubated for seven days (for Ura^+ revertants) or five days (for Can^r mutants) to allow for colony formation. One revertant or Can^r mutant was randomly picked from each plate for DNA isolation. Genomic yeast DNA was purified from the revertants and Can^r mutants using the MasterPure™ Yeast DNA Purification Kit (Epicentre). A 5-kb region comprising 2.5 kb upstream and 2.5 kb downstream of the *ura3-G764A* mutation site was amplified by

PCR using Pfu DNA polymerase kindly provided by Dr. Farid Kadyrov (Southern Illinois University School of Medicine, Carbondale, U.S.A.) and analyzed by DNA sequencing.

2.6 Measurement of the mutation frequency

The frequency of UV-induced *ura3-G764A* reversion was determined as follows. Appropriately diluted overnight cultures of the *ura3-G764A* mutants were plated on SC and SC –ura media and irradiated with 254 nm UV light at doses indicated in Figure 4.2 within 30 min after plating. The plates were then incubated for five to seven days at 30 °C. The *ura3-G764A* reversion frequencies were calculated by dividing the number of revertants on selective plates by the number of colonies on SC plates multiplied by the dilution factor.

The effect of HU treatment on DRIM was determined by using a fluctuation test. At least nine independent cultures of each strain (wild-type, *pol3-Y708A* and *pol3-Y708A rev3*Δ) were started from single colonies and grown overnight at 30 °C in liquid YPDAU medium containing HU at concentrations indicated in Figure 5.6. Appropriate dilutions of the overnight cultures were plated onto SC –arg +CAN for selection of Can^r colonies and onto SC medium for viability count. To calculate the Can^r mutant frequency, the number of Can^r mutants was divided by the number of colonies on SC medium and multiplied by the dilution factor. The median frequency of Can^r mutants was used to compare mutagenesis in different strains and at different HU doses. The significance of differences between mutation frequencies was determined by using the Wilcoxon-Mann-Whitney nonparametric criterion.

To determine the effect of HU treatment on UV-induced mutagenesis, appropriate dilutions of overnight cultures of E134 and PS446 strains were plated onto SC and SC –arg +CAN media supplemented with HU at concentrations indicated in

Figure 5.7 and Figure 5.8. The plates were then immediately irradiated with 10 J/m^2 of UV light and incubated at 30 °C. The mutant frequency was calculated as described above. The effect of HU pre-treatment on UV-induced mutagenesis was determined by growing ten-fold diluted overnight cultures of E134 strain for 4 h in the presence of 100 mM HU prior to UV irradiation. Appropriate dilutions of the logarithmic cultures were then plated onto SC and SC –arg +CAN media containing 100 mM HU and irradiated with UV light at doses indicated in Figure 5.8. The mutant frequency was calculated as described above.

2.7 DNA polymerase activity assay

To generate an oligonucleotide substrate for the polymerase reactions, a Cy5-labeled primer (5′-Cy5-CAGCACCACAAACCATACAAAAACA-3′) was annealed to a template strand (5′-GCCATTATCGGGTTTCTAATATACTGTTTTTGTATGGTTTGTGGTGCTG-3′) by incubation at 85°C for 2 min in the presence of 150 mM NaAc. The annealing reactions were then allowed to cool down slowly to room temperature. DNA polymerase reactions contained 40 mM Tris-HCl (pH 7.8), 60 mM NaCl, 8 mM MgAc2, 1 mM dithiothreitol, 0.2 mg/ml bovine serum albumin, 25 nM DNA substrate, and 10 nM Polζ_4 or Polζ_5. The reactions were performed at either S-phase (39 μM dCTP, 66 μM dTTP, 22 μM dATP, and 11 μM dGTP) or damage-response (195 μM dCTP, 383 μM dTTP, 194 μM dATP, and 49.5 μM dGTP) dNTP concentrations (Chabes et al, 2003, Sabouri et al, 2008). Reactions were incubated for 3 or 10 min at 30 °C and stopped by placing the tubes on ice and adding formamide loading dye. The reactions were then analyzed by electrophoresis in a 12% denaturing polyacrylamide gel. Products of polymerase reactions were detected and quantified using the Typhoon imaging system and ImageQuant software (GE Healthcare).

2.8 Measurement of DNA polymerase fidelity *in vitro*

M13mp2 gapped substrate was prepared as described previously (Bebenek & Kunkel, 1995). Briefly, M13mp2 ssDNA and dsDNA were purified from the NR9099 strain as described in (Bebenek & Kunkel, 1995). Double-stranded form of the M13mp2 was digested with *Pvu*II to produce four blunt-ended fragments of 6789, 268, 93, and 46 bp in size. Next, 6789-bp fragment was purified by precipitation with 6% polyethylene glycol (PEG) and 0.55 M NaCl. To produce the gapped substrate, 6789-bp fragment was first denaturated at 70 °C and then hybridized to M13mp2 ssDNA by incubating the mixture at 60 °C for 5 min in the presence of 300 mM NaCl and 30 mM sodium citrate. Following the cooling down of the hybridization mixture on ice, the gapped substrate was gel-purified as described in (Mertz et al, 2015).

Gap filling reactions (25 µl) contained 40 mM Tris-HCl (pH 7.8), 60 mM NaCl, 8 mM $MgAc_2$, 0.5 mM ATP, 1 mM dithiothrietol, 0.2 mg/ml bovine serum albumin, 20 nM PCNA, 8 nM replication factor C (RFC), 200 nM replication protein A (RPA), 1 nM gapped substrate, and 40 nM Polζ_4 or 50 nM Polζ_5. The reactions were performed at either equimolar dNTP concentrations (100 µM each) or at the intracellular concentrations (39 µM dCTP, 66 µM dTTP, 22 µM dATP, and 11 µM dGTP for S-phase, or 195 µM dCTP, 383 µM dTTP, 194 µM dATP, and 49.5 µM dGTP for damage-response concentrations; (Chabes et al, 2003, Sabouri et al, 2008)). The reactions were carried out at 30 °C for 60 min and stopped by placing the reactions on ice and adding 1.5 µl of 0.5 M EDTA. The efficiency of gap filling was determined by separating the reaction products in 0.8% tris-acetate-EDTA agarose gels at 4 °C for 20 h. Aliquots of the reactions were used for transformation of *E. coli* to determine the frequency of mutant plaques. The purification of mutant M13mp2 plaques and isolation of ssDNA were performed as described previously (Bebenek & Kunkel, 1995). Error rates for

individual types of mutations were calculated by using the following formula: ER = [(N_i/N) × MF]/(D × 0.6) where N_i – the number of mutations of a certain type, N – the total number of analyzed mutant plaques, MF – frequency of mutant plaques, D – the number of detectable sites in the *lacZ* reporter gene for that type of nucleotide change, and 0.6 is the probability that a mutant allele of the *lacZ* gene will be expressed in *E. coli* (Bebenek & Kunkel, 1995). Multiple mutations in a single mutant *lacZ* sequence were considered independent events and included separately in the error rate calculations if the distance between mutations was greater than ten nucleotides. Multiple mutations separated by ten or fewer nucleotides were classified as complex mutations and excluded from the calculation of error rates for individual mispairs. The frequency of complex mutations, deletions of more than one nucleotide and large rearrangements were calculated by dividing total number of these types of mutations by the total number of detectable mutations. All data are based on analysis of *lacZ* mutants from at least two independent gap-filling reactions.

Chapter 3. The length of DNA fragments synthesized in an error-prone manner during the bypass of a plasmid-borne abasic site

Material presented in this chapter was published in the following article:

Kochenova OV, Daee DL, Mertz TM, Shcherbakova PV (2015). DNA Polymerase ζ-Dependent Lesion Bypass in *Saccharomyces cerevisiae* Is Accompanied by Error-Prone Copying of Long Stretches of Adjacent DNA. *PLoS Genet* 11(3): e1005110.

3.1 Introduction and rationale

Numerous biochemical and genetic studies of TLS in *E. coli*, yeast and mammalian cells resulted in two models for lesion bypass (reviewed in (Lehmann & Fuchs, 2006, Waters et al, 2009)). In the polymerase-switching model, also known as "TLS at the fork" (Figure 1.4 (k)), TLS polymerases act in the context of active DNA replication providing for continuous synthesis of the nascent DNA strand. Upon DNA damage, monoubiquitylation of PCNA stimulates a temporary exchange of replicative and TLS polymerases at the primer terminus to allow TLS polymerases to bypass a lesion and extend past the resulted aberrant primer terminus. A further polymerase switch restores accurate DNA replication. In contrast, the gap-filling model postulates that TLS polymerases bypass lesions outside of the S-phase of cell cycle. In this scenario, replication fork stalling at the damage site is followed by a quick re-priming downstream of the blocking lesion, leaving ssDNA between the site of the lesion and the site of the replication restart (Figure 1.4 (l)). TLS polymerases are then recruited post-replicatively, in the late S-phase or G2/M, to bypass lesions and facilitate filling of these gaps. While the direct switching from a replicative to a TLS polymerase and back was observed in biochemical studies of lesion bypass *in vitro* (Fujii & Fuchs, 2004, McCulloch et al, 2004), multiple genetic studies provide evidence that TLS *in vivo* might predominantly occur post-replicatively (reviewed in (Lehmann & Fuchs, 2006, Ulrich, 2011, Waters et al, 2009)). Specifically, the unaffected rate of fork progression in TLS-deficient mutants (Callegari et al, 2010, Elvers et al, 2011, Lopes et al, 2006) and the accumulation of gaps in the nascent DNA, observed in multiple studies of UV-irradiated *E. coli*, yeast and mammalian cells (Iyer & Rupp, 1971, Lehmann, 1972, Lopes et al, 2006, Meneghini, 1976, Prakash, 1981, Rupp & Howard-Flanders, 1968), strongly favor the gap-filling model of TLS. Electron microscopy revealed that UV irradiation of yeast

cells leads to uncoupling of leading and lagging strand replication producing gaps of up to 1,000 nucleotides and that TLS polymerases prevent persistence of ssDNA gaps (Lopes et al, 2006). Nevertheless, these *in vivo* data cannot exclude that some lesions can be bypassed in S-phase via polymerase switching at the fork, and, therefore, two described TLS models are not necessarily mutually exclusive. Importantly, the mode of TLS could determine the extent of the error-prone synthesis by TLS polymerases. The "TLS at the fork" model proposes that the switch back to the replicative polymerase occurs as soon as the lesion no longer blocks its activity. *In vitro*, the eukaryotic replicative polymerases Polδ and Polε can continue DNA synthesis once the primer-template terminus is elongated by two to five nucleotides past the lesion (McCulloch et al, 2004). This parallels nicely the fact that replicative DNA polymerases can sense mismatches in the duplex DNA up to six base pairs from the primer terminus (Fujii & Fuchs, 2004, McCulloch et al, 2004, Zhang et al, 2002), and suggests that the size of TLS patch should be long enough to prevent its degradation by the exonuclease activity of a replicative polymerase and not much longer to prevent the accumulation additional mutations in the vicinity of a lesion (Fujii & Fuchs, 2004). In contrast, in the gap-filling model of TLS, the switch to replicative DNA polymerase may not be required. A recent finding of a DNA damage-induced proteasomal degradation of the catalytic subunit of Polδ in yeast suggests that replicative polymerases may not be immediately available to replace TLS polymerase once the lesion bypass is completed (Daraba et al, 2014). Therefore, it is likely that TLS polymerases could be capable of filling of a large portion of the gap or even closing it completely. A model where error-prone TLS could proceed well beyond the lesion and generate "untargeted", or "hitchhiking", mutations downstream of the lesion site has been discussed previously in (Maor-Shoshani et al, 2000, Ruiz-Rubio & Bridges, 1987), but has never been tested. The involvement of the

error-prone Polζ in the extension step during TLS makes it a possible candidate for performing DNA synthesis and generating “hitchhiking” mutations past the lesion site.

The experiments described in this chapter examine if the Polζ-dependent bypass of a single plasmid-born lesion is accompanied by the error-prone synthesis in the adjacent region and define the size of DNA copied in an error-prone manner. The genetic system for identification of individual lesion bypass products described here provides a basis for future investigations of the late steps of TLS *in vivo*.

3.2 A Genetic System to Identify the Products of Mutagenic AP Site Bypass

Earlier studies in yeast showed that Polζ is required for mutagenic bypass of both endogenously generated and artificial AP sites in yeast (Gibbs & Lawrence, 1995, Haracska et al, 2001) and, thus, AP site bypass can be used to study Polζ-dependent TLS. To select for individual products of AP site bypass in yeast, we constructed a double-stranded plasmid containing an artificial analog of AP site, tetrahydrofuran, at a specific position in the *URA3* gene. The plasmid also contained a yeast replication origin *ARS4,* centromere sequence, and the *LEU2* gene for selection of cells bearing the plasmid (Figure 3.1 (A)). Replication of this plasmid was studied in *apn1Δ apn2Δ* strains to prevent repair of the lesion by BER system. The lesion bypass in yeast can be accomplished through several pathways, including TLS and HR-mediated template switching. To distinguish between the products of these two branches of post-replicative repair, we took advantage of the earlier observations that mutagenic lesion bypass through AP sites predominantly results in a dATP or dCTP incorporation opposite the lesion (Auerbach et al, 2005, Chan et al, 2013, Gibbs & Lawrence, 1995, Kim et al, 2011, Kow et al, 2005, Pages et al, 2008, Zhao et al, 2004). A C at position 605 in the

wild-type *URA3* sequence was replaced with an artificial AP site, such that a dATP or dCTP incorporation opposite it would result in a Ura^- phenotype. Accurate bypass by template switching or infrequent repair of the lesion by AP lyases prior to replication (Torres-Ramos et al, 2000) would result in a restoration of the wild-type sequence at this position and a Ura^+ phenotype (Figure 3.1 (B)). While non-TLS events produce Ura^+ colonies, TLS events result in the formation of half-sectored colonies, where the Ura^- and Ura^+ halves result from the replication of the AP site-containing and the complementary undamaged strands, respectively (Figure 3.1 (C)). During replication of a double-stranded AP site-containing plasmid in yeast, mutagenic TLS through AP sites may result in a small percentage of dTTP or dGTP incorporation as well (e.g. approximately 1% and 8% of all TLS products contained a T and G, respectively, at the lesion site in the study by (Pages et al, 2008)). In addition to dATP or dCTP incorporation opposite AP sites, our assay is able to identify dTTP insertions as TLS events, since it produces a Ura^- phenotype as well. However, the dGTP insertions cannot be distinguished from non-TLS events in our system and, therefore, were not included in the analysis.

Only a small fraction of transformants with the AP site-containing plasmids (approximately 1%, e.g. 394 out of ~ 40,000 transformants analyzed) had the half-sectored phenotype indicating that the mutagenic TLS is a minor pathway responsible for AP sites bypass in yeast. While this is in agreement with previous studies (Pages et al, 2008), we cannot exclude the possibility that non-sectored colonies in our assay could be a progeny of the undamaged strand only, as a result of replication fork uncoupling at the lesion site (Lopes et al, 2006). To detect possible “hitchhiking” mutations, we isolated the plasmids from the Ura^- part of the half-sectored colonies and

sequenced a 1.7-kb region downstream of the lesion site extending in the direction of lesion bypass, as well as a 550-bp region upstream of the lesion site.

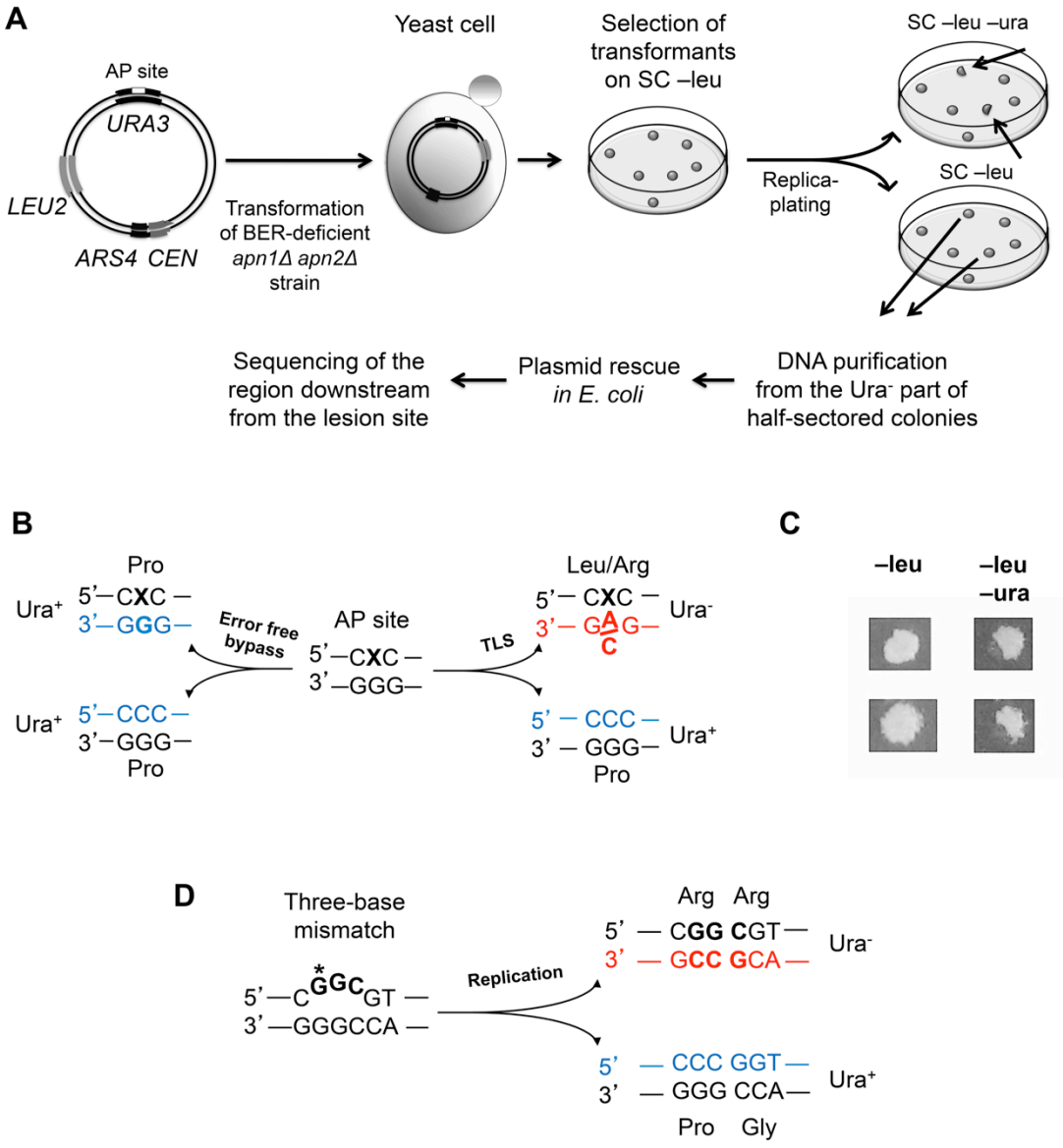

Figure 3.1 A genetic system to analyze the products of TLS through an artificial AP site.

(A) Sequential steps of the AP site bypass assay. A double-stranded centromeric (*CEN*) plasmid containing an AP site at position 605 of the *URA3* gene (white rectangle), a selectable marker (*LEU2*) and the yeast replication origin (*ARS4*) is introduced into the *apn1Δ apn2Δ* yeast strain. Transformants are selected by leucine prototrophy and then replica-plated on the medium lacking uracil to identify half-sectored colonies (shown by the arrows). The Ura- parts of the half-sectored colonies originate from cells that underwent error-prone TLS through the AP site (see text for details). **(B)** Possible phenotypic outcomes of the AP site bypass at position 605. The lesion is indicated with an "X". The newly synthesized strands are in blue (correct incorporation) or in red (incorrect incorporation), with nucleotides across from the lesions highlighted in bold. The amino acids at the corresponding position of the protein and the resulting

phenotypes (Ura+ or Ura-) are listed next to the triplet sequences. **(C)** Identification of TLS events by the half-sectored colony phenotype. Images of two colonies exhibiting full-growth on medium lacking leucine (SC—leu) and half-growth on medium lacking uracil (SC—leu–ura) are shown. **(D)** A schematic showing the “bubble”-type mismatch in the control plasmid and phenotypes associated with copying of each strand. Nucleotides that differ from the wild-type *URA3* sequence are in bold. The position 605 of the *URA3* gene is marked with an asterisk. Other symbols are as in **(B)** (adapted from (Kochenova et al, 2015)).

The region corresponding to the primer used to construct the AP site-containing plasmid (20 nt before and 26 nt after the lesion) was removed from the analysis due to a high probability of errors resulting from *in vitro* oligonucleotide synthesis. All of the plasmids isolated from the Ura^- parts of the half-sectored colonies (a total of 394) had a nucleotide substitution at the AP site position, confirming the mutagenic lesion bypass. The distance from the lesion site at which "hitchhiking" mutations were found was used as an estimate for the length of the error-prone synthesis.

The multistep process used to construct the AP-containing plasmid is expected to result in an accumulation of spontaneous DNA damage in the vector sequence and, thus, give rise to mutations not related to the bypass of AP site. To evaluate the level of these "background" mutations to the overall mutagenesis in the 1.7-kb region past the lesion site, we constructed a control plasmid via the same procedure as the AP site-containing plasmid but without introducing a site-specific lesion. To be able to isolate and analyze the progeny of the same strand that is replicated in an error-prone manner during lesion bypass, we engineered the control substrate so that the two strands of the control plasmid confer different phenotypes. We substituted three nucleotides at the position equivalent to that of the AP site (the *ura3-103,104* mutation) in one strand of a double-stranded plasmid, while another strand contained the wild-type *URA3* sequence (Figure 3.1 (D)). Transformation of yeast cells with a double-stranded plasmid bearing the *ura3-103,104* mutation in one strand resulted in approximately 21% of half-sectored colonies. This is consistent with the segregation of the wild-type copy of the *URA3* gene and *ura3-103,104* allele into the daughter cells. Inactivation of MMR by disruption of the *MSH2* gene only slightly increased the proportion of the half-sectored colonies (by approximately 12%) indicating that MMR is not efficient in recognizing and correcting multiple neighboring mismatches. The Ura^+ colonies could possibly result from the

presence of several plasmid copies in some cells, loss of a fraction of daughter plasmids and/or repair of the three-nucleotide mismatch by an unknown mechanism. For the purpose of this study, only half-sectored colonies were used for the analysis of control replication products. DNA sequence analysis of the regions upstream and downstream of the mismatch provided an estimate of the frequency of background mutations.

3.3 Determination of the Length of TLS Tracts During AP Site Bypass

We selected for and analyzed a total of 394 AP site bypass products and 456 products of the control plasmid replication by DNA sequencing. The majority of bypass events led to a dATP (243/394; 62%) or dCTP (80/394; 20%) insertion opposite the lesion. Incorporation of dTTP was observed in 18% of all cases (71/394). A total of 18 mutations were found in the downstream region at distances between 34 and 1529 nucleotides from the lesion site (Figure 3.2 (A); Table 3.1). These untargeted mutations were noticeably concentrated within an approximately 220-nucleotide region in the vicinity to the AP site. In contrast, 11 mutations found among the 456 control plasmids downstream of the three-base mismatch were randomly scattered throughout the analyzed region. Moreover, no mutations were observed within the first 220 nucleotides in control plasmids, in contrast to ~40% in the TLS products ($p = 0.0045$, Fisher's exact test). The rate of mutation in the 220-bp region downstream of the AP site was 8.1×10^{-5} (Table 3.2) and exceeded the genome-wide mutation rate in yeast by approximately 300,000-fold. Interestingly, the rate of untargeted mutations in this region is similar to the rate of errors estimated for purified Polζ *in vitro* (5.6×10^{-4}, (Zhong et al, 2006)). Notably, the rate of untargeted mutations upstream of the AP site did not differ from that in the control plasmids (Figure 3.2 (A)). This further supports the idea that the hypermutated

patch downstream of the lesion site is a consequence of the error-prone TLS initiated at the lesion site. The rate of mutations downstream of the AP site was reduced to the background level at distances greater than 220 nucleotides. Consequently, the types of nucleotide changes in these distant regions resembled those in the control plasmids (predominantly C→T transitions and -1 deletions). On the contrary, only one C→T transition and no -1 frameshifts were found in the 220-bp region in the vicinity of the AP site (Figure 3.2 (B); Table 3.1). This led us to conclude that untargeted mutations observed in the AP bypass products beyond the 220-bp segment must have originated from damage of ssDNA during the plasmid construction, and only those present within the 220-bp segment resulted from the error-prone DNA synthesis associated with the AP site bypass. We also analyzed the 220-bp segment in 47 TLS products and 57 control plasmids recovered from *msh2*Δ strains to determine whether errors made during AP bypass-associated replication are removed by MMR. MMR deficiency did not increase the frequency of untargeted mutations over that in $Msh2^{+}$ strains (Table 3.2), indicating that MMR does not correct errors in TLS tracts. This idea is also supported by the previous studies showing that MMR does not efficiently correct Polζ-dependent errors (Lehner & Jinks-Robertson, 2009).

Table 3.1 Mutations found in AP site bypass products and in the control plasmids.

Substrate	Nucleotide inserted opposite the AP site	Additional mutations downstream of the AP site position			
		Type of mutation[a]	Distance from the lesion site (nt)	Position in the *URA3* gene[b]	Position in the vector[c]
AP site	C	A → G	- 444		4516
	A	C → T	- 378		4450
	A	G → C	- 368		4440
	A	C ins	- 367		4439
	A	TC → AA	- 24	629	4096
	C	T → A	+ 34	571	4038
	T	A → C	+ 46	559	4030
	A	A → C	+ 92	513	3984
	A	GAT del	+ 108	497	3968
	A	A → C	+ 168	437	3908
	C	C → T	+ 193	412	3883
	A	G → T	+ 213	392	3863
	A	G del	+ 338	267	3738
	T	G del	+ 341	264	3735
	T	A del	+ 498	107	3578
	C	G → C	+ 626		3450
	A	A del	+ 799		3277
	T	A del	+ 799		3277
	C	C → T	+ 980		3096
	C	G → C	+ 1064		3021
	A	A → T	+ 1397		2688
	T	C → T	+ 1405		2680
	A	C → T	+ 1529		2556
Control	NA	A del	- 498		4575
	NA	C → T	- 460		4537
	NA	C ins	- 368		4445
	NA	T del	- 325		4402
	NA	C → G	- 221	826	4298
	NA	C → T	- 34	639	4111
	NA	A → G	+ 236	369	3840
	NA	G del	+ 376	229	3700
	NA	A del	+ 498	107	3578
	NA	T → C	+ 610		3466
	NA	T del	+ 784		3292
	NA	C → T	+ 907		3178
	NA	C → T	+ 1012		3073
	NA	G → T	+ 1209		2876
	NA	C → T	+ 1242		2843
	NA	A → C	+ 1447		2638
	NA	C → T	+ 1621		2812

[a]Nucleotide changes in the strand complementary to the AP-site-containing strand are shown.
[b]Numbering for the *URA3* gene is from the first nucleotide of the open reading frame.
[c]Numbering for the vector is from the first nucleotide following the *ARS4* sequence.
nt, nucleotide; *del*, deletion; *ins*, insertion; *NA*, not applicable. Data shown in this table were previously published in (Kochenova et al, 2015).

Table 3.2 The rate of mutation downstream of the lesion site in the AP site bypass products.

Region	Mutation rate per nucleotide	
	MMR-proficient	MMR-deficient
Within 220 bp	8.1×10^{-5}	$< 9.7 \times 10^{-5}$
Genome-wide	2.2×10^{-10} [a]	ND

The rate of mutation downstream of the lesion site in the AP site experiment was calculated as follows: $\mu = m/(L*n)$, where m is the number of mutations, L is the length of the DNA region analyzed by sequencing (in nucleotides), and n is the number of TLS products examined.
The rate of TLS-associated mutation in MMR-deficient strains was estimated similarly taking into account the rate of background mutation in the corresponding control experiments.
[a]Spontaneous genome-wide mutation rate as calculated in (Drake et al, 1998).
ND, not determined.
Data presented in this table are adapted from (Kochenova et al, 2015).

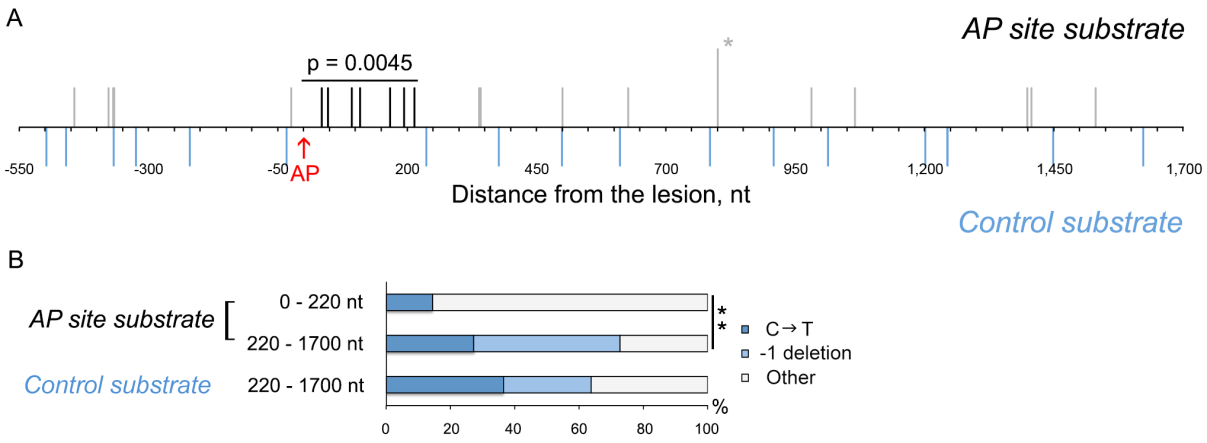

Figure 3.2 AP site bypass is associated with increased mutagenesis downstream of the lesion.

(A) Distribution of mutations found in the products of TLS through the AP site. The AP site position is indicated in red. Each vertical line represents a single mutation; the mutation found twice is marked with the asterisk. Mutations in the TLS products within 220 bp from the lesion are in black, other mutations in TLS products are in grey. Blue lines below the horizontal scale bar represent mutations found in the control substrates without the AP site. The data are based on DNA sequence analysis of 394 AP site bypass products and 456 products of the control plasmid replication. P-value (Fisher's exact test) indicates the significance of differences in the frequency of mutation in the 220-nucleotide region between TLS products and control plasmids. **(B)** Types of mutations observed in the AP site bypass products and control plasmids. C → T changes are shown for the transcribed strand that is exposed as ssDNA during the plasmid construction. The double asterisk indicates a statistically significant difference ($p = 0.0347$, Fisher's exact test). Figure is adapted from (Kochenova et al, 2015).

3.4 Discussion

In this chapter, we described a genetic system that could be efficiently used for analysis of the mutagenic TLS through a site-specific artificial AP site in the context of replication of dsDNA. Consistent with the earlier study of the artificial AP site in yeast (Pages et al, 2008), the bypass of a tetrahydrofuran in our assay results mostly in dATP incorporation opposite the lesion. This supports the hypothesis that the bypass of AP sites follows “A rule” during bidirectional replication in yeast. According to the previous studies (Haracska et al, 2001), Incorporation of dATP implies the predominant role of Polδ in the insertion step of TLS in our system. The second most common type of nucleotide incorporation, dCTP insertion, suggests that Rev1 (Gibbs et al, 2005, Haracska et al, 2001) can be frequently used as an inserter polymerase during the bypass of artificial AP site on a double-stranded plasmid as well.

Importantly, unlike previous studies, the experiments described in this chapter characterized not only the mutagenic potential of the AP site itself, but also aimed to determine the extent of the error-prone synthesis past the lesion site. Until now the best model for studying the bypass of a site-specific AP site in the context of the bidirectional replication was the plasmid-based assay described in (Pages et al, 2008). However, this system does not allow detection of the untargeted mutagenesis past the lesion site, because TLS across from AP site in this assay resulted in the formation of Ura^+ yeast colonies. Therefore, non-synonymous untargeted mutations resulting from a processive error-prone synthesis are likely to be overlooked, as they would inactivate the *URA3* gene. On the contrary, identification of the mutagenic bypass products by the Ura^- phenotype in our system allowed the detection of any additional mutations in the TLS products. The sequencing of the regions adjacent to the AP site in our system revealed that the error-prone synthesis is not limited to the lesion site, but spans a much greater

region than was previously appreciated. We observed that the error-prone synthesis in the described assay continued for approximately 200 nucleotides after the AP site bypass was completed. While a potential source of these untargeted mutations and the importance of this observation for the field will be thoroughly discussed in Chapter 6, this subsection will focus on the directions for future research in which this study can be expanded.

First, the results presented in this chapter pose a question of whether the untargeted mutagenesis is a common trait of the TLS across from various types of lesions or whether this phenomenon is unique for the AP site bypass. The extent of the error-prone synthesis can be determined by the type of the "inserter-extender" pair of DNA polymerases used during the bypass of a certain lesion. Although Polζ is the predominant extender polymerase in yeast, *in vitro* studies show that Polη is also capable of extending from distorted primer termini (Zhao et al, 2004). Because of its low processivity (Washington et al, 1999), if Polη acts as an extender during the bypass of some lesions (e.g. UV photolesions), it is expected to dissociate from the primer termini at a shorter distance from the lesion site than Polζ. Because our genetic system allows us to analyze only the events where Polζ participates in the extension step of lesion bypass, a separate study is required to test this hypothesis. Specifically, the analysis of the length of TLS tracts during the bypass of other types of lesions, e.g. TT CPDs, where Polη acts as both inserter and extender polymerases would help to clarify this point.

The experiments described in this chapter also raise a question of whether the bypass of chromosomal lesions is associated with error-prone synthesis beyond the lesion site. Although yeast vectors containing chromosomal replication origins and centromeres are maintained and replicated as chromosomal DNA (discussed in (Newlon, 1988)), we cannot exclude the possibility that the error-prone synthesis is more

tightly controlled on a chromosome. Thus, one of the probable explanations for the occurrence of untargeted mutations past the lesion site could be a lack of the regulatory mechanism that allows immediate replacement of the TLS polymerases with an accurate replicative polymerase after the completion of the bypass on a chromosome. To exclude this possibility, it would be important to determine the extent of error-prone synthesis during the bypass of chromosomal lesions.

Although the AP site bypass assay described in this chapter provides an opportunity to study late steps of TLS in the context of replication of a double-stranded plasmid, we recognize several limitations of this system. The first limitation is related to a high level of spontaneous damage to ssDNA used for the plasmid construction. The high level of background mutagenesis precluded analysis of a fraction of error-prone synthesis that could have spanned a distance greater than 200 nucleotides. The second limitation is related to mutations in the primer sequence that result from errors during the oligonucleotide synthesis *in vitro*. This prevented detection of untargeted mutations within 26 nt after the lesion. Finally, because of the low frequency of mutagenic AP site bypass in our system, it is challenging to determine which TLS polymerase is responsible for generating untargeted mutations. Inactivation of genes encoding for TLS polymerases is expected to dramatically decrease the frequency of mutagenic AP site bypass and, as a result, the frequency of sector colonies. Conversely, the system described in the following chapter allowed us to overcome these limitations and, in addition, to address some the questions discussed above.

Chapter 4. The length of DNA fragments synthesized in an error-prone manner during the bypass of a chromosomal UV lesion

Most of the material presented in this chapter was published in the following article:

Kochenova OV, Daee DL, Mertz TM, Shcherbakova PV (2015). DNA Polymerase ζ-Dependent Lesion Bypass in *Saccharomyces cerevisiae* Is Accompanied by Error-Prone Copying of Long Stretches of Adjacent DNA. *PLoS Genet* 11(3): e1005110.

4.1 Introduction and Rationale

As described in the previous chapter, sensitivity of the plasmid TLS assay is limited due to the high level of mutagenesis resulting from spontaneous DNA damage in the plasmid backbone. The high level of background mutagenesis results from the multiple *in vitro* procedures used for substrate constructions. To overcome this limitation, we set out to develop an approach to study the extent of the error-prone synthesis during bypass of a lesion at a specific location on a chromosome. One of the advantages of a system with chromosomal lesion is eliminating multiple *in vitro* manipulations with ssDNA.

Because introducing a single site-specific AP site in a yeast chromosome appeared to be challenging, we decided to use UV light as a source of DNA damage. As described in Subsection 1.1.2., UV light induces formation of UV photolesions at any of the four dipyrimidine sites: TT, TC, CT and CC. Similar to the AP site bypass, TLS through cytosine-containing CPDs and (6-4)PPs is highly mutagenic and requires Polζ/Rev1 (Gibbs et al, 2005, Kozmin et al, 2003, Yu et al, 2001). The genetic system described in this chapter allows selection of individual products of mutagenic Polζ-dependent UV lesion bypass at a specific TC site in the chromosome. Similar to the AP site assay, we then use DNA sequence analysis of the regions upstream and downstream of the TC site to identify untargeted mutations in these TLS products. We present data demonstrating that untargeted mutagenesis accompanies the error-prone bypass of a chromosomal UV-induced lesion as well. However, a comparison of the distribution of untargeted mutations in the AP site and UV lesion bypass products revealed that the error-prone synthesis through the chromosomal lesion could span a greater distance than was observed in the plasmid-based assay. We determined that the

bypass of a single chromosomal lesion could be associated with an error-prone copying of undamaged DNA for a distance up to 1000 bp downstream from the TC site. Furthermore, the UV lesion bypass assay allowed us to test which TLS polymerase is responsible for generating the untargeted mutations in this region. Unlike the AP site bypass assay, the genetic system described in this chapter is based on the positive selection for the mutagenic TLS events and allowed us to investigate the extent of the error-prone synthesis in different genetic backgrounds, including mutants with severely decreased rate of bypass. Sequencing of the UV lesion bypass products obtained from Polζ-, Polη- deficient strains and a strain bearing a mutator allele of Polζ, *rev3-L979F,* suggested a role for Polζ in generating untargeted mutations downstream of the lesion site.

4.2 A Genetic System to Identify the Products of TLS through a UV-Induced Chromosomal Lesion

To select for individual products of TLS through a chromosomal UV lesion, we introduced a single base substitution, G to A, at the 764 nucleotide of the chromosomal *URA3* gene. G to A substitution at this location results in a mutant allele, *ura3-G764A,* and creates a TC dipyrimidine site for a possible UV-induced lesion formation (Figure 4.1 (A)). The occurrence of either substitution upon UV treatment of yeast cells manifests the UV photolesion formation at this site and its subsequent mutagenic bypass.

In yeast, there are two known TLS polymerases that are capable of accomplishing the mutagenic bypass of UV-induced lesions at TC sites, Polζ and Polη.

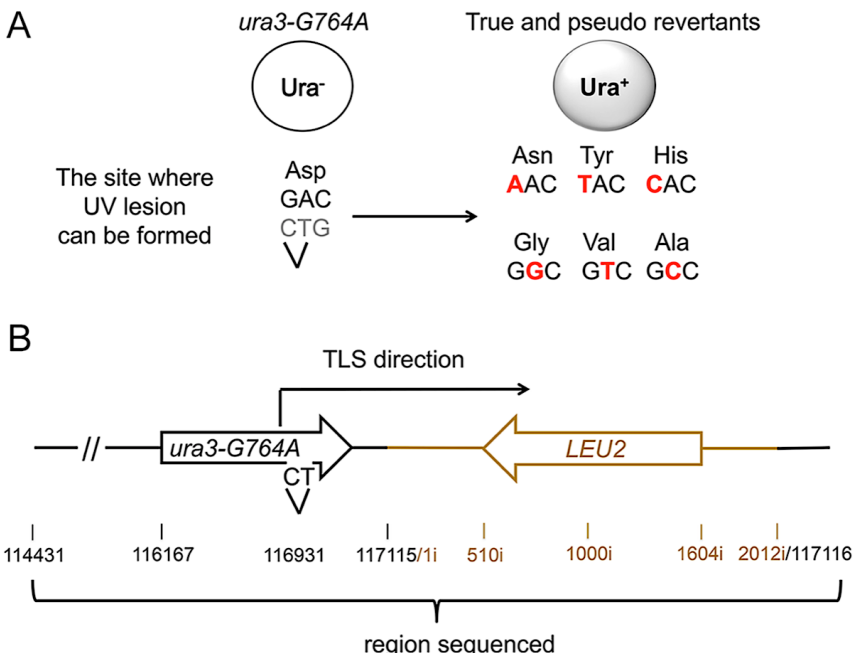

Figure 4.1 A genetic system to analyze the products of TLS through a chromosomal UV lesion.

(A) The *ura3-G764A* allele and the most common UV-induced single nucleotide substitutions that lead to a Ura$^+$ phenotype (marked in red). The sequence of the non-transcribed DNA strand is in black, and the transcribed strand is in grey. The site of potential UV lesion formation is indicated with a "V". **(B)** A schematic showing the structure of the *ura3-G764A-LEU2* cassette in chromosome *V*, the direction of the UV lesion bypass, and the region that was analyzed by DNA sequencing. The 2-kb *Hpa*I *LEU2* fragment used as a selectable marker for introducing the *ura3-G764A* allele into the chromosome is in dark yellow. Open arrows indicate open reading frames. Black numbers show chromosomal nucleotide position in respect to the left telomere; dark yellow numbers with the "i" index show nucleotide position within the *LEU2* insert in respect to the end of the *Hpa*I fragment (previously published in (Kochenova et al, 2015)).

To confirm that the mutagenic TLS at the TC site in our system is dependent on Polζ and not Polη, we first determined the frequency of the *ura3-G764A* reversion in the wild-type, *rev3Δ, rad30Δ* strains, and in the strain bearing a mutator allele of Polζ, *rev3-L979F*. The mutator allele *rev3-L979F* results in a single amino acid substitution in the active site of Polζ that significantly reduces the fidelity of DNA synthesis by Polζ on undamaged DNA (Sakamoto et al, 2007) and can be used to provide additional support for the proposed role of Polζ in generating of mutations past the lesion site, as it is expected to elevate the level of untargeted mutagenesis in this region. First, we demonstrated that the frequency of the *ura3-G764A* reversion showed a significant dose-dependent increase in the wild-type, Polη-deficient and *rev3-L979F* strains in comparison to the spontaneous reversion frequency in these strains (Figure 4.2). On the contrary, Polζ deficiency led to a lack of the robust increase in the reversion frequency, and only three-fold increase was observed at the highest dose of UV light used in this study. These results indicate that Polζ is required for the mutagenic bypass of UV lesions at this site. Polη-deficient strains showed a slight decrease in the reversion rate in comparison to the wild-type strain at all doses. This observation indicates that Polη is only rarely involved in the mutagenic bypass of the UV-induced lesion at the TC site in our system and is in agreement with preferential participation of Polη in the non-mutagenic bypass of CPDs and (6-4)PPs ((Abdulovic & Jinks-Robertson, 2006, Gibbs et al, 2005, Kozmin et al, 2003, Yagi et al, 2005)). Conversely, the reversion frequency was increased three-fold in the strains bearing the *rev3-L979F* allele in comparison to the wild-type strain at all doses (Figure 4.2). Altogether these data indicated that UV irradiation readily induces DNA damage at position 764 of the *URA3* gene that is bypassed by Polζ-dependent TLS to produce the Ura^+ revertants.

Previous *in vitro* studies showed that Polζ has a limited capacity to incorporate a nucleotide across from 3' base of UV lesions (Guo et al, 2001, Nelson et al, 1996b), but is able to efficiently extend from a nucleotide inserted opposite 3' T of the TT (6-4)PP by Polη (Johnson et al, 2001). To determine that the mechanism of TLS across from UV lesion in our *in vivo* system is consistent with the previously proposed model where Polζ participates in the completion rather than initiation of the bypass, we analyzed the frequencies of nucleotide substitutions induced by UV irradiation at the 5' T and 3' C bases of the dipyrimidine site in the wild-type, *rev3*Δ, *rad30*Δ and *rev3-L979F* strains. DNA sequence analysis of the *URA3* gene in 165 independent revertants obtained in the wild-type strain after irradiation with 60 J/m^2 UV light confirmed that all of the revertants had nucleotide substitutions at 3' C, 5' T or multiple nucleotide changes (Table 4.1, Table 4.2). Most of the reversion in the wild-type strain occurred via nucleotide substitutions at the 3' C position of the dipyrimidine site (95/165) (Table 4.1, Table 4.2). Deletion of the *RAD30* gene led to a two-fold decrease in the frequency of nucleotide substitutions at the 3' C, but not at the 5' T of the TC site, in comparison to the wild-type strain (Table 4.2). This is in agreement with the role of Polη in generating mutations at the 3' base of the TC (6-4)PP (Kozmin et al, 2003). Conversely, Polζ deficiency decreased the frequency of nucleotide substitutions at both positions (Table 4.2). Although we are not able to determine whether Polζ can also act as an inserter polymerase in our assay, the requirement of Polζ for mutagenesis at both of the positions of the TC site is consistent with its proposed participation in extension from both 3' and 5' bases of the TC site. Interestingly, we observed the complete absence and a significant decrease in the frequency of multiple nucleotide changes at the *GAC* codon in the *rev3*Δ and *rad30*Δ strains, respectively (Table 4.2). This suggests that Polζ and Polη may cooperate to generate these types of reversions. Additionally, we

observed that the L979F change in the Rev3p elevated the frequency of nucleotide substitutions at both positions of the TC site and substantially increased the frequency of multiple nucleotide changes at the GAC codon, which frequently involved mutations in the 5' T and the next +1 nucleotide, in comparison to the wild-type strain (Table 4.1, Table 4.2). In summary, our results support the role of Polζ in the extension step of the UV lesion bypass and a smaller role of Polη in the mutagenic bypass of UV photolesions in our genetic assay.

Next, we set out to determine the extent of the error-prone synthesis past the UV lesion by sequencing the 2.5-kb regions upstream and downstream from the reversion site (Figure 4.1 (B)).

Table 4.1 Nucleotide changes at the site of the presumed UV lesion at positions 763-765 of the *URA3* gene in UV-induced revertants of the *ura3-G764A* strain.

Reversion type	Number of occurrences in the strain			
	wild-type	***rad30*Δ**	***rev3*Δ**	***rev3-L979F***
GAC → **A**AC	62	45	124	28
GAC → **T**AC	28	28	53	4
GAC → **C**AC	6	2	3	4
GAC → G**G**C	31	42	39	13
GAC → G**T**C	15	19	10	14
GAC → G**C**C	8	26	2	3
GAC → **TT**C	2	1		
GAC → **AT**C	1			1
GAC → **A**A**T**	1			
GAC → G**TT**	9			12
GAC → G**GT**	1			2
GAC → G**CT**	1			5
GAC → **CCT**				1
GAC → **AGT**				1
GAC → **CTT**				1
AGAC → **TA**AC	1	1		
AGAC → **GA**AC				1
AGAC → **CC**AC		1		
AGAC → **TT**AC				1

The location of the potential photolesion site and the true and pseudo reversion pathways are explained in detail in Figure 4.1 (adapted from (Kochenova et al, 2015).

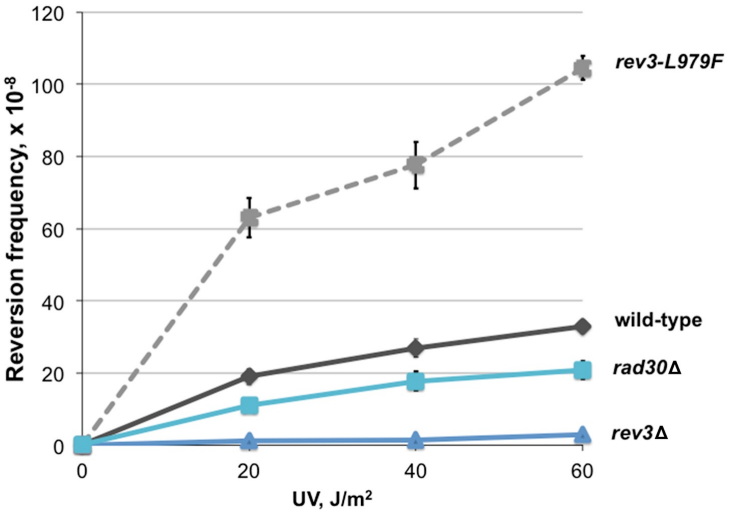

Figure 4.2 Frequency of UV-induced reversion of the *ura3-G764A* allele in the wild-type, *rev3*Δ, *rad30*Δ, *and rev3-L979F* strains.

The data are mean frequencies for at least six determinations. Error bars are shown unless they are smaller than the plot symbol and represent standard errors.

Table 4.2 The frequencies of mutations at 3' C, 5' T or multiple nucleotide changes at the 5'TC3' dipyrimidine site.

Strain	Frequency of nucleotide changes, x 10^{-8}		
	3' C	5' T	Multiple changes
wild-type	19	11	3.2
*rev3*Δ	2.3	0.64	< 0.01
rev3-L979F	43	35	26
*rad30*Δ	9.5	11	0.38

The data are based on the sequencing of 165 revertants for the wild-type strain, 231 revertants for the *rev3*Δ, 164 for the *rad30*Δ, and 91 for the *rev3-L979F* strains. The frequency of nucleotide substitutions was calculated as follows: the proportion of mutations at a specific position of the 5'TC3' site was multiplied by the overall frequency of UV-induced reversion of the *ura3-G764A* allele for each particular strain at the UV dose of 60 J/m^2.

4.3 Determination of the Length of TLS Tracts During the Bypass of a Chromosomal UV Lesion

Like in the case of the AP site bypass, mutagenic bypass of the chromosomal UV lesion was frequently associated with increased mutagenesis in the 2.5-kb region downstream of the lesion site. In addition to a mutation at the 3' or 5' nucleotide of the TC doublet, 12 out of 165 revertants had a base substitution at the next G presumably not involved in the formation of UV photolesion (+1 position; Table 4.1). Because the fidelity of nucleotide insertion at this position is likely profoundly affected by the distortions in DNA structure at the damaged site, these mutations were excluded from the calculation of mutation rate in the downstream region.

A total of 15 additional mutations were found in the 165 TLS products at distances between 16 to 2155 nucleotides downstream of the reversion site (Figure 4.3; Table 4.3). Similar to the AP site bypass, the "hitchhiking" mutations noticeably concentrated in the region in the vicinity of the lesion, but the hypermutated patch spanned a substantially larger distance – up to 1 kb from the presumed lesion position (Figure 4.3). The mutation rate in this 1-kb region constituted 6.7×10^{-5} (Table 4.4) and was similar to the level of mutagenesis observed in the products of TLS through the AP site.

To confirm that these mutations were indeed associated with TLS at the TC site in the *ura3-G764A* reporter and were not a result of additional UV damage to this region, we irradiated cells with the same dose of UV light but selected for mutations at a distant locus, the *CAN1* gene, rather than Ura^+ reversion. The *CAN1* gene is located approximately 83 kb away from the *ura3-G764A* reporter gene in the same chromosome *V*. Only one out of 161 sequenced independent Can^r mutants contained a nucleotide

change in the 1000-nt region downstream of the *ura3-G764A* (Figure 4.3). Also, no nucleotide substitutions were observed at the TC site in the *ura3-G764A* allele in the sequenced Can^r mutants. This confirms that the additional mutations in the Ura$^+$ revertants were, indeed, related to the mutagenic bypass of nearby DNA damage and were not the result of a high level of genome-wide mutagenesis in irradiated cells. Furthermore, the frequency of mutations upstream of the *ura3-G764A* site was did not exceed the level of background mutagenesis observed in the Can^r controls, consistent with the idea that the error-prone synthesis initiated at the site of *ura3-G764A* mutation.

The rare mutations we observed in the Can^r controls and in the Ura$^+$ revertants outside the hypermutated 1000-nt region likely resulted from additional UV damage. It has been estimated that the dose of 60 J/m^2 is expected to generate approximately one lesion per 1-2 kb (Budd & Campbell, 1995, Unrau et al, 1973). The rate of mutagenesis we observed in the Can^r controls is about 100-fold lower. This is consistent with the assumption that the majority of lesions are removed by NER, and only a fraction of the remaining lesions are converted to mutations.

Polζ was shown to be required for the extension step during the TLS through AP sites and UV-induced photolesions (see (Gibbs et al, 2005, Haracska et al, 2001, Kozmin et al, 2003, Lawrence, 2004, Yu et al, 2001)) and could, thus, be responsible for generating untargeted mutations in the downstream region. To exclude the involvement of another low-fidelity yeast polymerase, Polη, in the error-prone synthesis in this region, we analyzed the 1000 nt region downstream of the TC site in 165 Ura$^+$ revertants obtained in Polη-deficient background (Table 4.1) after irradiation with 60 J/m^2. As mentioned in the previous section, the reversion frequency was only marginally affected by the inactivation of *RAD30* (Figure 4.2).

Table 4.3 Mutations found in UV-induced Ura$^+$ revertants of the *ura3-G764A* strain and Can^r controls.

	Nucleotide change at positions 763-765 of the *URA3* gene[a]	Additional mutations downstream of the presumed UV lesion		
		Mutation type[a]	Distance from the lesion site (nt)	Chromosomal position[b]
Ura$^+$ revertants (TLS at the site of *ura3-G764A* mutation)	GAC→G**C**C	A → T	- 635	116294
	GAC→G**T**C	G → A	- 23	116906
	GAC→**A**AC	G → A	+ 16	116946
	GAC→**A**AC	A → G	+ 34	116964
	GAC→**A**AC	A → G	+ 40	116970
	GAC→**A**AC	A ins	+ 177	117107
	GAC→**A**AC	C ins	+ 190	5i
	GAC→G**G**C	A ins	+ 262	77i
	GAC→**A**A**T**	T ins	+ 414	229i
	GAC→G**G**C	A → T	+ 631	446i
	GAC→**C**AC	A ins	+ 636	451i
	GAC→**A**AC	C → T	+ 772	587i
	GAC→G**TT**	G → A	+ 886	701i
	GAC→**A**AC	G → A	+ 968	783i
	GAC→G**T**C	G → A	+ 1654	1469i
	GAC→**A**AC	G → T	+ 2015	1830i
	GAC→G**C**C	C → T	+ 2155	1970i
Can^r controls (no TLS at the site of *ura3-G764A* mutation)	NA	A → T	- 1774	115155
	NA	T → C	- 181	116748
	NA	C → T	+ 621	436i

[a]Nucleotide changes (bold) are shown for the coding DNA strand complementary to the strand containing the dipyrimidine sequence at positions 763-764.
[b]Numbers with the "i" index indicate the position of the mutation in the inserted LEU2 gene fragment (see Figure 4.1 (B) for a more detailed explanation of the numbering system). Abbreviations are as in

Table 3.1 (previously published in (Kochenova et al, 2015).

Table 4.4 The rate of mutation downstream of the lesion site in the products of UV lesion bypass.

Region	Mutation rate per nucleotide	
	MMR-proficient	MMR-deficient
Within 1000 bp	6.7×10^{-5}	$< 7.7 \times 10^{-5}$
Genome-wide	0.4×10^{-5} [a]	ND

The rate of mutation downstream of the lesion site in the UV lesion bypass experiment was calculated as described in the Table 3.2 legend, except the background mutation rate (0.6×10^{-5}; calculated from sequencing of the 1-kb region next to the *ura3-G764A* site in UV-induced Can^r mutants) was subtracted from the observed rate of TLS-associated mutation.

[a]Genome-wide mutation rate in cells undergoing UV-induced mutagenesis was estimated based on the observance of three mutations within the sequenced 5-kb region in the UV-induced Can^r mutants.

ND, not detected (adapted from (Kochenova et al, 2015)).

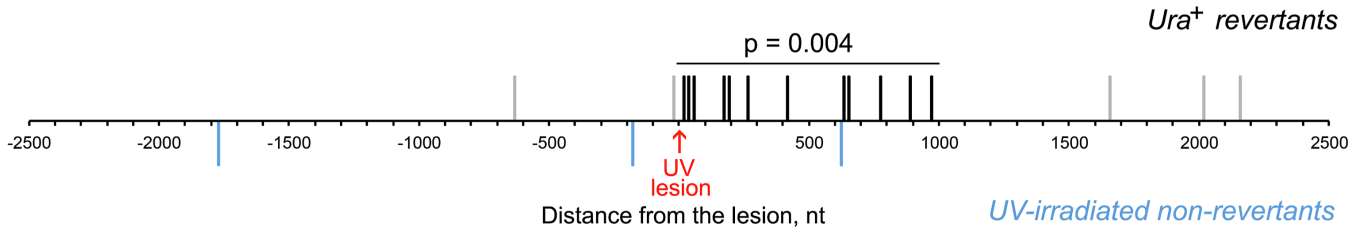

Figure 4.3 UV lesion bypass is associated with increased mutagenesis downstream of the lesion

The position of the presumed UV lesion at the *ura3-G764A* mutation site is indicated in red. Distribution of untargeted mutations in UV-induced Ura$^+$ revertants is shown above the horizontal scale bar. Each vertical line represents a single mutation. Mutations found within 1000 bp downstream from the lesion are in black, those in other regions are in grey. Blue lines below the horizontal scale bar represent mutations found in UV-induced Can^r mutants of the *ura3-G764A* strain. The data are based on DNA sequence analysis of 165 independent Ura$^+$ revertants and 161 independent Can^r mutants. P-value (Fisher's exact test) indicates the significance of differences in the frequency of mutation in the 1-kb region between Ura$^+$ revertants and Can^r controls (previously published in (Kochenova et al, 2015)).

A total of five mutations were observed at distances of 505-1026 nucleotides from the reversion site, which corresponds to a mutation rate of 3 x 10^{-5}. This is similar to what we observed in the Polη-proficient strain and argues against a major role of Polη in generating untargeted mutations. In contrast, Polζ appeared to be essential for the mutagenesis downstream the lesion site. Although very little induced mutagenesis could be seen in Polζ-deficient strain (Figure 4.2), irradiation with 60 J/m^2 of UV light led to approximately three-fold increase in the reversion frequency. This let us recover the rare revertants resulting from Polζ-independent bypass. Sequencing of the 1000-nt segment downstream of the *ura3-G764A* reversion site in 231 Ura^+ revertants obtained in Polζ-deficient background (Table 4.1) detected no additional mutations. This suggested that the long stretches of hypermutation downstream of the DNA damage site are specifically associated with Polζ-dependent lesion bypass. This result strongly implicates Polζ in generating untargeted mutations. Sequencing of a 300-bp region downstream from the lesion site in the revertants obtained in the *rev3-L979F* background showed a two-fold increase in the level of untargeted mutagenesis in this region in comparison to the level of mutagenesis in the wild-type strain in the same region (26 x 10^{-5} in the *rev3-L979F* strains and 12 x 10^{-5} in the wild-type strain) (Table 4.5). No mutations were observed in the 48 sequenced Can^r controls obtained from the *rev3-L979F* strain at the same dose of UV irradiation, which corresponds to an error rate of < 7 x 10^{-5} in this region. The two-fold increase in the frequency of untargeted mutations in this region correlates with the effect of L979F substitution on the overall Polζ fidelity observed in our strains (approximately a three-fold decrease; Figure 4.2). This result provides a further support for the role of Polζ in replication of undamaged DNA past the lesion site. Interestingly, two complex mutations, the hallmark of Polζ mutagenesis, were observed in the

immediate vicinity upstream of the lesion site (-3 and -4 positions) in the revertants obtained in the *rev3-L979F* background (Table 4.5).

As in the case of the AP site bypass assay, sequencing of the 1-kb region from UV-induced Ura^+ revertants obtained in the MMR-deficient background showed that the rate of untargeted mutations was not elevated in the *msh2*Δ strain (Table 4.4). This result indicates that the MMR does not efficiently correct errors in TLS tracts during the bypass of chromosomal lesions either.

Table 4.5 Mutations found in UV-induced Ura$^+$ revertants of the *rad30Δ and rev3-L979F* strains.

	Nucleotide change at positions 763-765 of the *URA3* gene[a]	Additional mutations downstream of the presumed UV lesion		
		Mutation type[a]	Distance from the lesion site (nt)	Chromosomal position[b]
Ura$^+$ revertants obtained from the *rad30*Δ strain	GAC→G**T**C	C → G	+ 505	320i
	GAC→**A**AC	G → A	+ 928	743i
	GAC→**A**AC	C ins	+ 994	809i
	GAC→G**G**C	C ins	+ 994	809i
	GAC→**A**AC	G → A	+1026	841i
Ura$^+$ revertants obtained from the *rev3-L979F* strain	GAC→G**G**C	GC → AG	- 4	116926
	GAC→G**GT**	CA → GA	- 3	116927
	GAC→**A**AC	A → G	+ 59	116989
	GAC→G**T**C	A → T	+ 99	117029
	GAC→G**TT**	A → T	+ 99	117029
	GAC→**A**AC	A → G	+ 108	117038
	GAC→**C**AC	C → T	+ 116	117046
	GAC→G**TT**	C → T	+ 125	117053
	GAC→**A**AC	G → A	+ 276	91i

[a]Nucleotide changes (bold) are shown for the coding DNA strand complementary to the strand containing the dipyrimidine sequence at positions 763-764.
[b]Numbers with the "i" index indicate the position of the mutation in the inserted *LEU2* gene fragment (see Figure 3.1 for a more detailed explanation of the numbering system). The data shown in this table are partially published in (Kochenova et al, 2015).

4.4 Discussion

In this chapter, we described a genetic system that allows us to select for products of mutagenic bypass of individual UV-induced chromosomal lesions. The results presented in this chapter demonstrate that the bypass of chromosomal lesions is also accompanied by an increased untargeted mutagenesis in the adjacent downstream region. Similar to the AP site bypass assay, the rate of mutagenesis in the hypermutated patch exceeded the genome-wide mutation rate by more than 300,000-fold. This indicates that untargeted mutagenesis is not limited to the bypass of AP sites, but is a common characteristic of mutagenic Polζ-dependent TLS through various types of lesions. In addition, the results presented in this chapter demonstrate that the bypass of lesions on the double-stranded plasmid and on a chromosome is controlled in a similar way and provide an important insight into the late steps of TLS. Our findings suggest that TLS polymerases are not always immediately replaced by accurate replicative polymerases, as it was proposed in the “TLS at the fork” model. On the contrary, our results argue that, upon DNA damage, TLS polymerases can contribute to replication of a substantial portion of the genome, supporting the “gap-filling” model of TLS.

The genetic approach described in this chapter helped us to overcome the limitations that we faced in the earlier plasmid-based assay. First, by eliminating the unwanted background mutagenesis associated with *in vitro* manipulations, we were able to detect untargeted mutations at greater distances from the lesion site and to compare the extent of the error-prone synthesis in the two assays. Although the rate of untargeted mutagenesis was similar in both assays, the length of TLS tracts was substantially greater in the case of UV-induced lesion bypass. We speculate that the difference in the length of TLS tracts in the two assays may reflect a possible regulatory mechanism of TLS that will be thoroughly discussed in Chapter 6.

In addition, by using the genetic system described in this chapter, we were able to analyze the extent of the error-prone synthesis in the various TLS mutants. This allowed us to provide support for the involvement of Polζ in generating the untargeted mutations past the lesion site. Interestingly, similar to the AP site bypass, the MMR deficiency did not elevate the rate of untargeted mutagenesis past the UV lesion. These results further confirm that MMR does not efficiently correct Polζ-dependent errors in TLS tracts. However, the rate of untargeted mutagenesis in these regions was still approximately ten-fold lower than expected if Polζ were continuously copying undamaged DNA (*in vitro* studies in Chapter 5 and (Zhong et al, 2006)). This intriguing observation suggests a possibility that another process operates in the TLS tracts that corrects Polζ errors. Arguments supporting the role of Polζ in generating untargeted mutations, as well as the possible mechanism contributing to the removal of Polζ errors in TLS tracts will be discussed in Chapter 6.

Furthermore, the experiments described in this chapter provide additional support for the distinct roles of Polζ and Polη in the mutagenic bypass of the UV photolesion. Our results are consistent with the previously proposed model where the mutagenic bypass of UV lesions involves incorporation of a nucleotide across from 3' base of the UV lesion by Polη or another polymerase and extension from the resulting primer terminus by Polζ. Interestingly, we observed that the mutator variant of Polζ generates more multiple nucleotide substitutions at the UV lesion site suggesting that sometimes Polζ can also act as an inserter polymerase during the bypass of UV photolesions. This is further supported by the occurrence of two complex mutations in the adjacent upstream region in the revertants obtained from the strains with the mutator variant of Polζ. This observation suggests that the switch to Polζ can sometimes occur a few nucleotides upstream of the lesion, when the replicative polymerase, unable to

extend the abnormal primer terminus, utilizes its exonucleolytic activity. However, separate studies are required to confirm this hypothesis.

In summary, the genetic assay described in this chapter is efficient for studies of the late steps of TLS and can be used to identify factors that regulate the length of TLS tracts.

Chapter 5. The role of dNTP pools in Polζ-dependent mutagenesis

5.1 Introduction and Rationale

Despite being a member of the B family DNA polymerases (Braithwaite & Ito, 1993, Ito & Braithwaite, 1991), Polζ that lacks exonuclease activity is at least 10-fold less accurate than replicative polymerases Polε and Polδ (Fortune et al, 2005, Shcherbakova et al, 2003). Therefore, while the unique ability to extend mismatched and aberrant primer termini makes Polζ essential for rescuing stalled replication forks, participation of Polζ in genome replication is mutagenic and, as we showed in the previous chapter, can lead to accumulation of mutation not only at the lesion sites but in the adjacent region as well. Therefore, identifying factors that can alter Polζ fidelity is important to understand the mechanisms that contribute to or attenuate accumulation of Polζ-dependent errors in DNA.

The study described in this chapter was inspired by the recent finding that the mutagenic potential of many replicative DNA polymerase variants is greatly affected by changes in intracellular dNTP levels (Mertz et al, 2015, Williams et al, 2015). For many years balanced deoxynucleotide triphosphate (dNTP) pools were thought to be critical for maintaining the fidelity of DNA replication in yeast. The size of dNTP pools is strictly controlled during cell cycle and expands only two- to three-fold during S-phase to allow efficient DNA replication (Chabes et al, 2003, Labib & De Piccoli, 2011). Imbalanced, constantly high or low dNTP concentrations induce genome instability during normal S-phase either by affecting the fidelity of DNA polymerases or by slowing down fork progression (Kumar et al, 2011, Kumar et al, 2010, Watt et al, 2016, Zhao et al, 2001). On the other hand, dramatic expansion of dNTP pools (up to eight-fold) during DNA damage and replication stress is essential for cell survival (Chabes et al, 2003, Poli et al, 2012). This chapter addresses the question of how natural increases in dNTP levels,

such as those occurring during DNA damage response, affect the mutagenic properties of Polζ.

To study the effect of dNTP changes on Polζ-dependent mutagenesis, we first mimicked the physiological S-phase and damage-response dNTP concentrations in reactions with four-subunit Polζ (Polζ$_4$) and five-subunit Polζ$_4$–Rev1 (Polζ$_5$) *in vitro*. We demonstrated that activity, fidelity and error specificity of purified Polζ$_4$ and Polζ$_5$ complexes *in vitro* were not greatly affected by the switch from "normal S-phase" to "damage-response" dNTP concentrations *in vitro*. Furthermore, we provide evidence that Polζ-dependent lesion bypass and Polζ-dependent mutagenesis during copying of undamaged DNA *in vivo* do not require high dNTP levels. These results argue that Polζ is less sensitive to fluctuations in the size of dNTP pools than the replicative DNA polymerases and, thus, Polζ may be uniquely capable of bypassing lesions or other impediments when dNTP pools are low.

5.2 The effect of dNTP levels on the catalytic activity of Polζ$_4$ and Polζ$_5$

In vivo studies of DRIM and DNA damage-induced mutagenesis suggest that Polζ-dependent mutagenesis is observed when dNTP pools are dramatically elevated (Figure 8.1 and (Chabes et al, 2003)). To study the effect of dNTP pools on Polζ function, we first determined how dNTP levels affect the catalytic activity of Polζ$_4$ and Polζ$_5$ complexes *in vitro*. We performed a primer extension assay with Cy5-labeled primer at either normal S-phase (39 μM dCTP, 66 μM dTTP, 22 μM dATP, and 11 μM dGTP) or at damage-response (195 μM dCTP, 383 μM dTTP, 194 μM dATP, and 49.5 μM dGTP) dNTP concentrations described elsewhere (Sabouri et al, 2008). These concentrations were calculated based on the reported amount of dNTPs per cell in

logarithmically growing yeast cultures or in cultures treated with 0.2 mg/l 4-nitroquinoline 1-oxide for 150 min (Chabes et al, 2003) using a haploid yeast cell volume estimate of 45 μm^3.

In a primer extension assay using an oligonucleotide template, we observed that the percentage of the extended primer was the same at both dNTP concentrations at 3 and 10 min (Figure 5.1). However, high dNTP levels slightly increased the percentage of the full-length product by approximately two-fold in comparison to the reactions with normal S-phase dNTPs. Altogether these data suggest that increased dNTP levels do not greatly stimulate Polζ catalytic activity during copying of undamaged DNA *in vitro*.

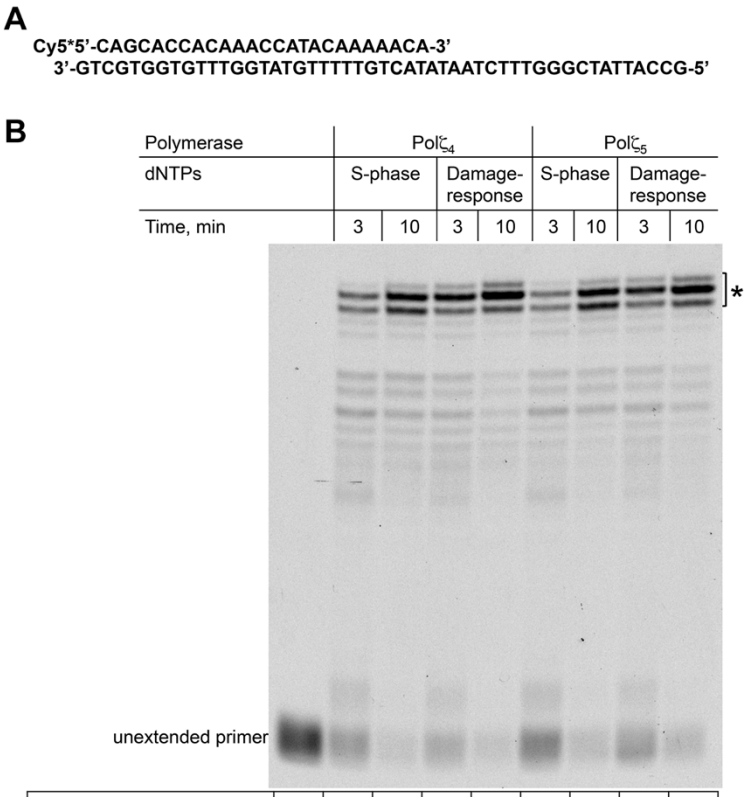

% primer extended	0	73	92	84	93	61	89	77	91
% of full-length product		23	52	46	73	19	56	42	70

Figure 5.1 Polζ-dependent DNA synthesis at S-phase and damage-state dNTP concentrations.

(A) Cy5-labeled DNA substrate used in reactions with Polζ4 and Polζ5. **(B)** Reactions were carried out at 30 °C and contained 10 nM Polζ4 and Polζ5, 24 nM DNA substrate, 40 mM Tris·HCl (pH7.8), 60 mM NaCl, 8 mM MgAc, 1 mM dithiothrietol, 0.2 mg/mL bovine serum albumin, and the indicated dNTPs. The percentage of primer extended (+1 products and longer) and the percentage of nearly full-length product (≥22) are shown below each lane.

5.3 The fidelity and error specificity of Polζ$_4$ and Polζ$_5$ at S-phase and damage-response dNTP levels

We next aimed to understand the effects of DNA damage-induced expansion of dNTP pools on the fidelity and error specificity of Polζ. To this end, we performed the M13mp2 *lacZ* forward mutation assay (Bebenek & Kunkel, 1995) with purified Polζ$_4$ and Polζ$_5$ using dNTP concentrations that mimic intracellular S-phase and damage-response levels.

In the M13mp2 assay, a 407-nt single-stranded gap in a double-stranded M13mp2 DNA is filled by the polymerases *in vitro*, and nucleotide changes introduced during the gap-filling synthesis are detected by genetic selection in *E. coli*. All reactions were performed in the presence of the polymerase accessory proteins PCNA, RFC and RPA. Analysis of the reaction products by agarose gel electrophoresis showed that, under the conditions used (see Chapter 2.8), the 407-nucleotide gap was filled completely by Polζ$_4$ (Figure 5.2). Consistent with the inhibitory effect of Rev1 on Polζ activity described previously (Makarova et al, 2014), synthesis by Polζ$_5$ was less efficient. Nevertheless, using a higher concentration of the five-subunit complex (50 nM instead of 40 nM), we were able to achieve nearly complete gap-filling (Figure 5.2). The average frequency of *lacZ* mutants obtained upon transfecting *E. coli* with Polζ$_4$ gap-filling reactions at S-phase dNTPs was 0.015 (Table 5.1), and it was only slightly elevated when damage-response dNTP concentrations were used (approximately 1.3-fold; Table 5.1). The types and rate of individual errors made by Polζ$_4$ at the intracellular dNTP levels were determined by DNA sequence analysis of 280 mutants for S-phase and 220 mutants for damage-response levels. We found that, as suggested by the

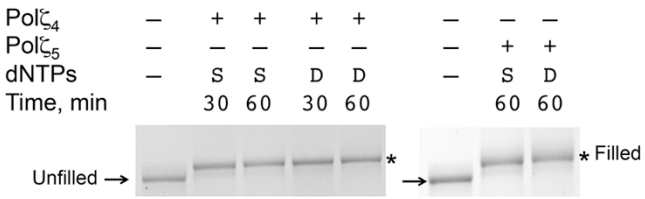

Figure 5.2 Analysis of the gap-filling reactions by agarose gel electrophoresis.

Reactions were treated with Proteinase K and then subjected to electrophoresis in 0.8% agarose gel in tris-acetate-EDTA buffer containing 0.5 μg/mL ethidium bromide. Electrophoresis was carried out at 4 °C at 70 V for 20 h. Gap-filing reactions incubated for 30 and 60 min are shown for Polζ$_4$, however, only 60-min reactions showing complete or nearly complete gap-filling products, were used to determine the fidelity and error specificity of Polζ complexes. Arrows and asterisks indicate the unfilled and filled gapped DNA substrate, respectively. *S*, S-phase dNTPs; *D*, damage-response dNTPs.

minimal change in the *lacZ* mutant frequency, the increase in dNTP concentrations did not greatly affect the error rate of Polζ$_4$. The overall rate of single-base changes was 77 x 10^{-5} at S-phase dNTPs and 95 x 10^{-5} at damage-response dNTPs. The mutational spectra of Polζ$_4$ at both dNTP levels were dominated by single-base substitutions, while the rate of single-base insertions/deletions (indels) was relatively low (1.7 x 10^{-5} and 2.9 x 10^{-5} for S-phase and damage-response dNTPs, respectively; Table 5.1). The shift from S-phase to damage-response dNTP concentrations had no major effect on Polζ$_4$ error spectrum either. Polζ$_4$ was predominantly promiscuous at G template nucleotides at both dNTP levels (Table 5.1, Figure 5.3 (A)). Interestingly, Polζ$_4$ was very inefficient at generating all three types of X-dCTP mismatches, with the C-dCTP mismatch being the least frequent among all twelve possible mispairs (<0.54 x 10^{-5} at S-phase dNTPs and 0.89 x 10^{-5} at damage-response dNTPs; Table 5.1 and Figure 5.3 (A)). At both dNTP levels, Polζ$_4$ showed notable propensity to create multiple sequence changes (Table 5.1 and Table 8.1). Their frequency was unaffected by the increase in dNTP concentrations. Approximately 5% of *lacZ* mutants contained multiple changes within short (≤10 nucleotides) stretches of DNA, which we classified as complex mutations and which Polζ is notorious for generating during TLS and copying of undamaged DNA *in vivo* (Harfe & Jinks-Robertson, 2000, Northam et al, 2010). An additional 10% of *lacZ* mutants contained multiple mutations separated by larger distances (Table 8.1).

Because Rev1 is indispensable for Polζ-dependent mutagenesis *in vivo*, we examined how the presence of Rev1 modulates the fidelity of Polζ. We found that the five-subunit complex was slightly more error-prone than Polζ$_4$. The frequencies of *lacZ* mutants determined upon transfecting *E. coli* with the products of Polζ$_5$ gap-filling reactions were increased approximately 1.5-fold at both S-phase and damage-response dNTP concentrations in comparison to reactions with Polζ$_4$ (Table 5.1).

Table 5.1 Fidelity of *in vitro* DNA synthesis by Polζ$_4$ and Polζ$_5$ at cellular dNTP concentrations

	Polζ$_4$[a]						Polζ$_5$[a]					
	S–phase dNTPs			Damage-response dNTPs			S-phase dNTPs			Damage-response dNTPs		
	Detectable	Non-detectable	ER (x10^{-5})[b]	Detectable	Non-detectable	ER (x10^{-5})[b]	Detectable	Non-detectable	ER (x10^{-5})[b]	Detectable	Non-detectable	ER (x10^{-5})[b]
Base substitutions (mispair)	237	18	75	182	9	92	166	9	125	147	24	135
A → G (A·dCTP)	10	1	2.9	2	1	0.97	10		6.6	9	2	7.5
A → T (A·dATP)	8	2	2.0	12		4.9	13		7.4	13	2	9.1
A → C (A·dGTP)	10		3.8	4		2.5	7		6.1	8	1	8.6
T → C (T·dGTP)	20	1	5.2	16		6.9	10		6.0	6		4.4
T → A (T·dTTP)	23	5	10.5	10		7.5	6		6.3	7	1	9.1
T → G (T·dCTP)	12		4.4	2		1.2	10		8.4	9	1	9.3
G → A (G·dTTP)	20	1	6.3	29	3	15	12	1	8.7	10	1	9.8
G → C (G·dGTP)	39	3	12	31		16	19		14	16	2	14
G → T (G·dATP)	46	3	14	44	4	22	36	4	25	37	5	32
C → T (C·dATP)	20		5.7	18	1	8.5	11	1	7.2	13	4	11
C → G (C·dCTP)			<0.54	1		0.89	14	1	17	7	4	11
C → A (C·dTTP)	29	2	8.2	13		6.1	18	2	12	11	1	8.9
Single-base indels	38		1.7	39		2.9	33		3.5	27	1	3.4
-1 run	12		0.54	17		1.3	18		1.9	8		1.0
+1 run	6		0.27	9		0.67	2		0.21	8	1	1.0
-1 non-run	20		0.90	12		0.89	13		1.3	8		1.0
+1 non-run			<0.04	1		0.074	1		0.10	3		0.38
Complex[c]	13		4.5%	12		5.2%	19		8.6%	34		15%
Other[d]	3		1.0%			<0.4%	3		1.4%	14		6.3%
Total[e]	291			233			221			222		
lacZ mutant frequency		0.015			0.02			0.025			0.027	

[a] All reactions were performed in the presence of PCNA, RFC and RPA.
[b] Error rates (ER) for individual mutation types were calculated as described in Materials and Methods. Only detectable mutations were included in the error rate calculation. Percent of the total number of detectable mutations is shown for complex and “other” types of mutations.

[c] Complex mutations are multiple changes within short DNA stretches (≤10 nucleotides; see Table 8.1).
[d] "Other" mutations include deletions of more than one nucleotide and large rearrangements (see Figure 5.4 and Table 8.1).
[e] Data for Polζ$_4$ at S-phase and damage-response dNTPs are based on the analysis of 280 and 220 mutant plaques, respectively. Data for Polζ$_5$ at S-phase and damage-response dNTPs are based on the analysis of 210 and 207 mutant plaques, respectively. Some of the plaques contained multiple detectable mutations. The numbers show the total number of detectable mutations found in the plaques analyzed.
The background mutation frequency for unfilled M13mp2 gapped substrate was 0.0009.

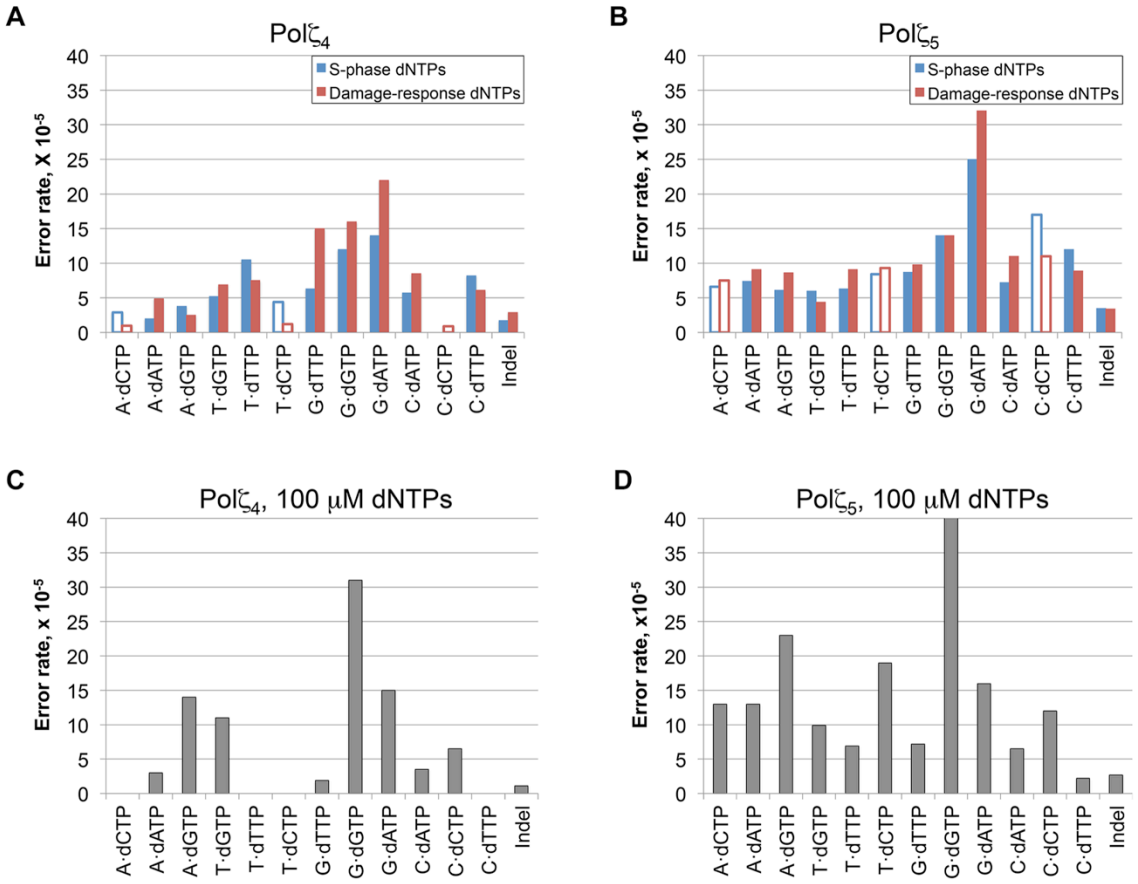

Figure 5.3 Rates of individual single-base errors generated by Polζ *in vitro* at intracellular and equimolar dNTP concentrations.

The graphs show rates of single-base mispairs and insertion/deletion mismatches observed in reactions with Polζ$_4$ **(A and C)** and Polζ$_5$ **(B and D)** at S-phase and damage-response dNTP concentrations **(A and B)** and at standard 100 μM dNTPs **(C and D)**. Data for Polζ$_4$ and Polζ$_5$ at 100 μM dNTP are based on the analysis of 53 and 80 mutant plaques, respectively. "X·dCTP" mispairs in the Polζ$_4$ and Polζ$_5$ mutational spectra are shown as open bars.

As in the case of Polζ$_4$, the switch from S-phase to damage-response dNTP concentrations did not greatly affect the *lacZ* mutant frequency or the overall error rate of Polζ$_5$ complex (Table 5.1). The rate of single-base changes made by Polζ$_5$ was 130 x 10^{-5} and 140 x 10^{-5} at S-phase and damage-response dNTP concentrations, respectively. The error specificity of the five-subunit complex was determined by sequencing 210 mutants from reactions with S-phase dNTPs and 207 mutants from reactions with damage-response dNTPs. Similar to reactions with Polζ$_4$, the switch from S-phase to damage-response dNTP concentrations did not change the error specificity of Polζ$_5$ either (Figure 5.3 (B)). Like Polζ$_4$, the five-subunit complex was the most promiscuous at G nucleotides, with G-dATP being the most frequently generated mispair. Generally, the error spectra produced by Polζ$_5$ were remarkably similar to those of Polζ$_4$, with one important exception: the presence of Rev1 significantly increased the rates of all three X-dCTP mispairs (Table 5.1, Figure 5.3 (B)). This increase accounted for most of the difference in the overall error rate between Polζ$_4$ and Polζ$_5$. The dCTP misincorporation is likely due to the deoxycytidyl transferase activity of Rev1, and it indicates that Polζ and Rev1 can freely exchange at the primer terminus during DNA synthesis *in vitro*. In comparison to Polζ$_4$, a somewhat higher proportion of *lacZ* mutations from Polζ$_5$ reactions constituted complex changes (approximately 9% and 15% at S-phase and damage-response dNTP concentrations, respectively). This is consistent with the important role of Rev1 in the generation of Polζ-dependent complex mutations *in vivo* (Northam et al, 2014). An additional 7% and 15% of *lacZ* mutants from reactions with S-phase and damage-response dNTPs, respectively, contained multiple mutations separated by more than ten nucleotides (Table 8.1). Interestingly, Polζ$_5$ reactions produced a new class of large rearrangements, which involved substitutions of a large stretch of DNA (>30 nucleotides) with a different, typically much shorter, sequence (Table 8.1). At damage-response dNTP concentrations, these large rearrangements

were observed in approximately 5% of *lacZ* mutants. Unlike complex mutations affecting short stretches of DNA, such large rearrangements are not usually seen in spectra of Polζ-dependent mutations *in vivo*. It is possible that they result from the inhibitory effect of Rev1 on Polζ-dependent synthesis *in vitro* and may not be relevant to *in vivo* situations.

Prior to this work, the error specificity of Polζ has been studied using equimolar (100 μM) dNTP concentrations and enzyme preparations containing mostly Rev3-Rev7 subassembly (Zhong et al, 2006). Although the mutational spectrum observed in that earlier study similarly showed a predominance of base substitutions and a high frequency of complex mutations, the spectrum of base substitutions was drastically different from the one shown in Figure 5.3 (A). To determine if the proper dNTP balance was the key in shaping the error signature of Polζ, we performed gap-filling reactions with $Pol\zeta_4$ and $Pol\zeta_5$ using 100 μM concentration of each dNTP. The average *lacZ* mutant frequency for $Pol\zeta_4$ reactions (0.018) and the overall error rate for single-nucleotide changes (87×10^{-5}) were similar to those observed at the intracellular dNTP levels. However, the error specificity of $Pol\zeta_4$ in reactions with equimolar dNTPs was profoundly different (Figure 5.3 (C)). The dGTP misincorporation became the predominant source of mutations, with the G-dGTP mispair being the single most frequent error (Figure 5.3 (C)). The use of equimolar dNTP concentrations also elevated the rate of C-dCTP mispair more than seven-fold in comparison to reactions with intracellular dNTPs (Figure 5.3 (A, B)). At the same time, the use of 100 μM dNTPs significantly lowered the ability of $Pol\zeta_4$ to misincorporate dTTP: the rates of all three possible X-dTTP mispairs were drastically decreased (Figure 5.3 (A, C)). The changes in the base substitution pattern were consistent with the dNTP imbalance introduced by the use of equimolar concentrations (relatively higher dGTP and dCTP levels, and a lower

dTTP level). Interestingly, the percentage of *lacZ* mutants resulting from complex mutations was greater at 100 uM dNTPs and constituted 13% (compared to 5% with intracellular dNTPs). Similar results were observed with Polζ$_5$: its overall error rate at 100 μM dNTPs was comparable to that at intracellular dNTPs (with the *lacZ* mutant frequency of 0.032, the error rate for single-base changes of 170 x 10^{-5}, the frequency of complex mutations of 11%, and the frequency of large rearrangements or deletions of 3%), but the spectrum of single-base changes was dramatically different (Figure 5.3 (B, D)). Like in the case of Polζ$_4$, the majority of mutations produced by Polζ$_5$ at 100 μM dNTPs resulted from dGTP and dCTP incorporation, with the G-dGTP being the single most frequent error (Figure 5.3 (D)). This is, again, consistent with the non-physiological high levels of dGTP and dCTP in the reactions with equimolar dNTPs. Taken together, these data provide evidence that, although the shift from S-phase to damage-response dNTP concentrations does not affect the fidelity and error specificity of Polζ$_4$ or Polζ$_5$, severely imbalanced dNTP levels, as in the case of 100 μM dNTPs, can dramatically change the error signature of these polymerases.

Figure 5.4 shows the distribution in the *lacZ* sequence of single-nucleotide changes made by Polζ$_4$ and Polζ$_5$ at the intracellular dNTP concentrations. The overall distribution of mutations appears to be quite uniform in all four spectra, with the exception of several mild hotspots. The strongest hotspot was observed in the Polζ$_4$ spectra for a +1 frameshift in the TTT homonucleotide run at position 137-139 where almost all +1 frameshifts occurred (Figure 5.4 (A, B)). Although we could not discern any specific nucleotide context for generating particular types of mutations by Polζ$_4$, it could be noted that most of the sites with frequent G misincorporation are followed by a template C, such as at positions -36, 121, 169, 171, 178 in the “S-phase” mutational spectrum and 79, 121, 141 in the “damage-response” mutational spectrum. This might

point to primer-template misalignment as a possible mechanism for generating these types of mutations at these particular sites. The presence of Rev1 in the complex with Polζ_4 did not change the distribution of mutations, suggesting that Rev1 does not stimulate misincorporation of nucleotides at any particular sequence context.

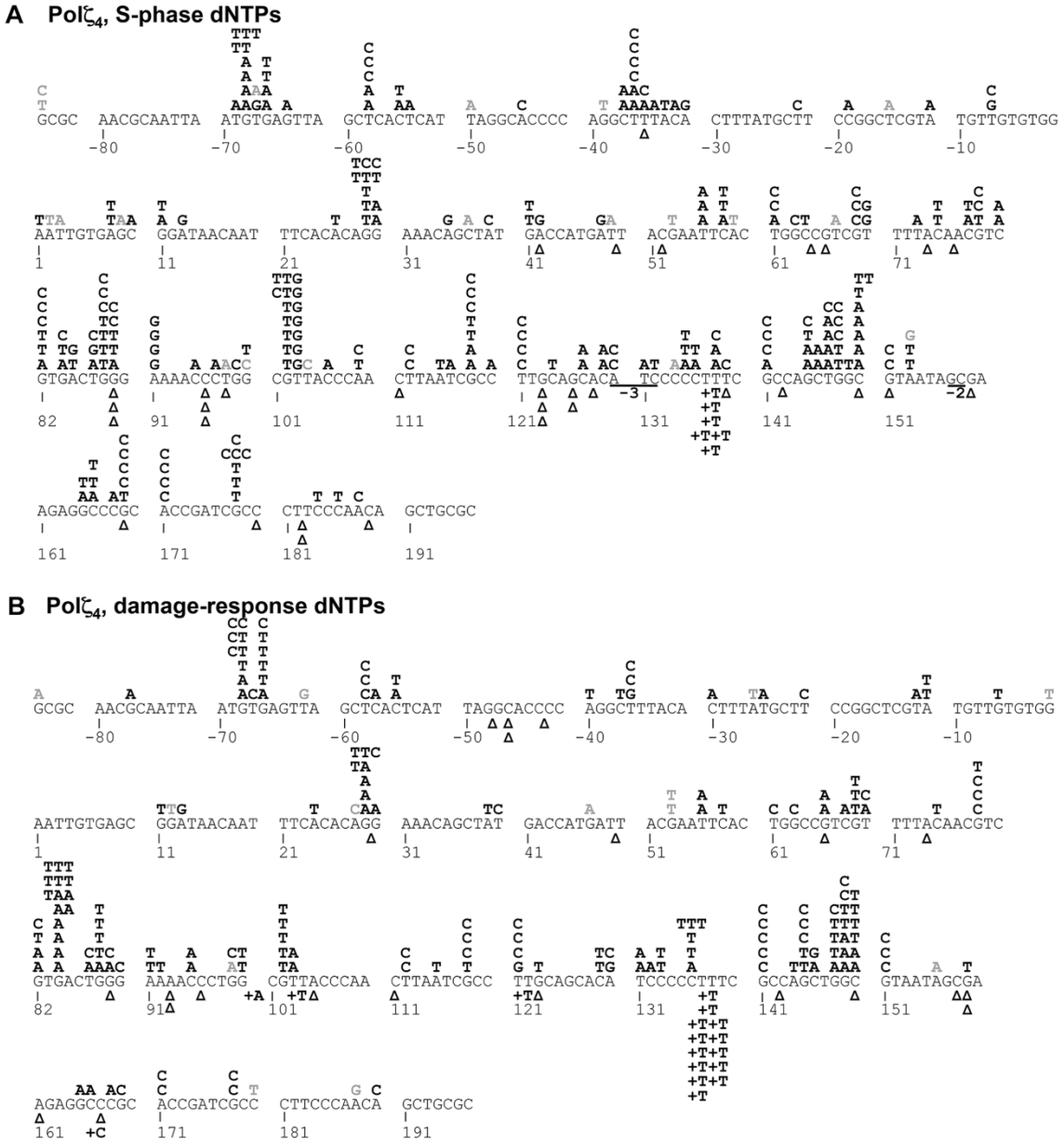

Figure 5.4 Spectra of single-base substitutions and insertion/deletion mutations generated by Polζ complexes in the *lacZ* gene at cellular dNTP concentrations.

(A) Polζ$_4$, S-phase dNTPs. **(B)** Polζ$_4$, damage-response dNTPs. **(C)** Polζ$_5$, S-phase dNTPs. **(D)** Polζ$_5$, damage-response dNTPs. In addition to the mutations shown, one *lacZ* mutant contained a large deletion spanning nucleotides -119 – 150. Base substitutions are displayed above the *lacZ* sequence, insertions and deletions are below the *lacZ* sequence. Single-base deletions and insertions are shown as triangles and letters with a "+" symbol, respectively. Deletions of more than one nucleotide are indicated by a line below the sequence with a number of deleted nucleotides next to it. Detectable mutations are in black, bold text. Silent mutations are in gray. Data are summarized in Table 5.1 and Figure 5.3.

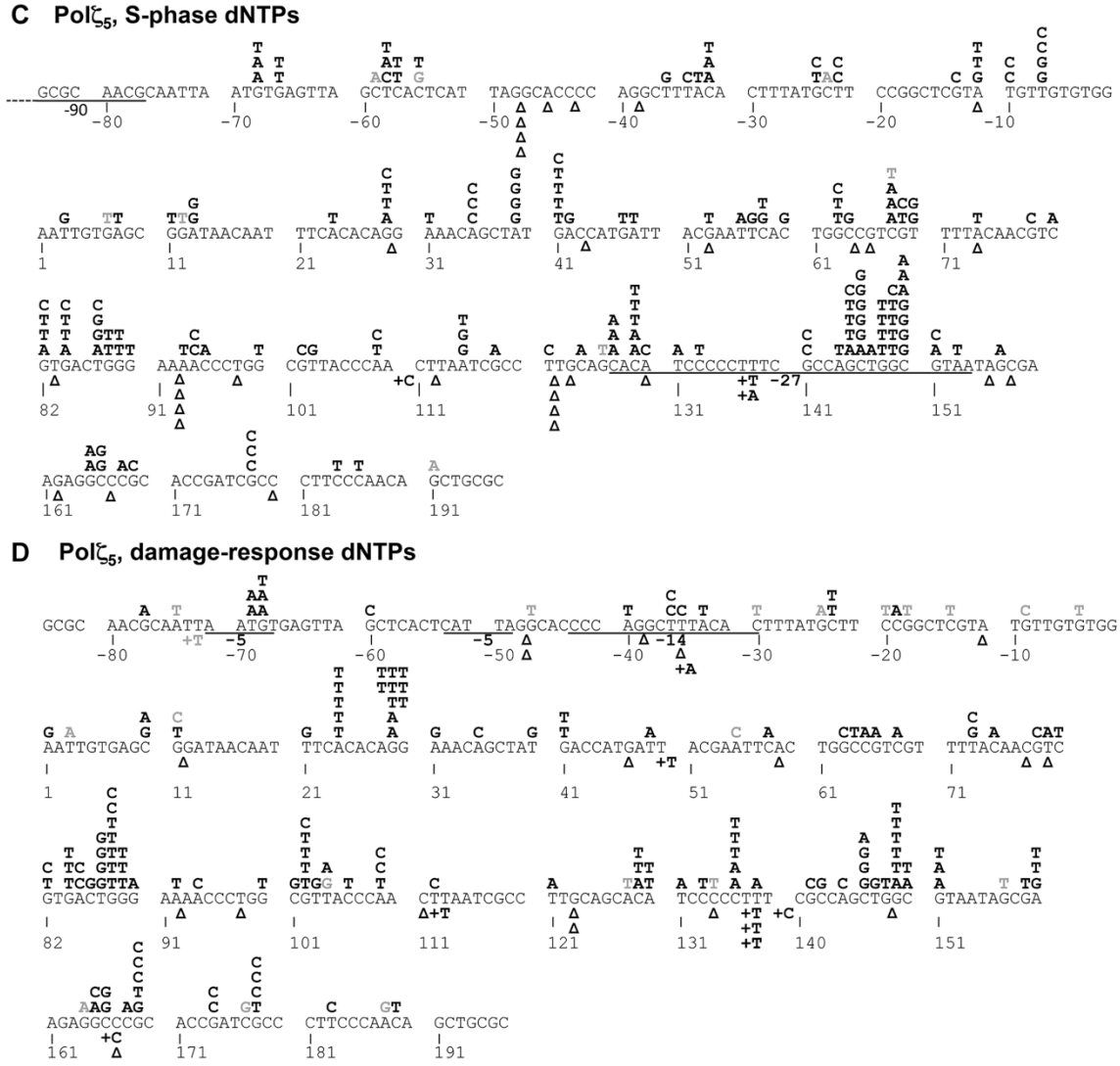

Figure 5.4 Continuation

5.4 Polζ-dependent mutagenesis *in vivo* does not require high dNTP levels

The *in vitro* data described in the previous subsections indicate that the activity, fidelity and error specificity of Polζ is only minimally affected by the switch from the S-phase to damage-response dNTP concentrations. In yeast cells, however, Polζ-dependent mutagenesis is mostly observed when dNTP pools are expanded. We therefore aimed to determine whether high dNTP levels are essential for Polζ function *in vivo*.

First, we set out to determine whether the expansion of dNTP pools is required for Polζ-dependent DRIM. As described in the Section 1.4, various defects in the catalytic and accessory subunits of yeast replicative DNA polymerases impede the progression of the replication fork and cause DRIM (Aksenova et al, 2010, Garbacz et al, 2015, Kraszewska et al, 2012, Northam et al, 2006, Pavlov et al, 2001b, Shcherbakova et al, 1996, Stodola et al, 2016). Among these defects, the *pol3-Y708A* mutation has been used most commonly for the mechanistic studies of DRIM (Northam et al, 2006, Northam et al, 2014, Northam et al, 2010) because of its rather strong mutator phenotype that is almost entirely Polζ-dependent. Importantly, the *pol3-Y708A* strain exhibits elevated dNTP pools and abnormal cell cycle distribution, with a large proportion of cells in the G2/M phase (Figure 8.1). The prolonged G2/M phase may be a sign of checkpoint activation, which is likely responsible for the expansion of dNTP pools. To investigate the significance of increased dNTP pools for Polζ function in DRIM, we first set out to inhibit RNR activation by deleting the *DUN1* gene in the *pol3-Y708A* strain. To do so, we constructed the *POL3/pol3-Y708A dun1*Δ*/dun1*Δ diploid and analyzed the

products of its sporulation by tetrad dissection. Tetrad analysis of the *POL3/pol3-Y708A dun1*Δ*/dun1*Δ diploid showed reduced spore viability in comparison to the single *POL3/pol3-Y708A* and *dun1*Δ*/dun1*Δ mutants (Figure 5.5). Subsequent phenotypic analysis of the surviving spores confirmed that combination of the *pol3-Y708A* allele with Dun1 deficiency is lethal in haploids. This finding suggests that the *pol3-Y708A* mutant requires checkpoint response activation and Dun1-dependent dNTP pools expansion for efficient DNA replication and survival.

Since we were unable to bring dNTP levels down in the *pol3-Y708A* mutants by deleting the *DUN1* gene, we set out to inhibit RNR by treatment of these strains with HU, (Krakoff et al, 1968). Because the *pol3-Y708A* mutants require expansion of dNTP pools for survival (Figure 5.5) and cannot tolerate high HU concentrations (Pavlov et al, 2001b), we used a range of lower concentrations (10-20 mM) that did not cause growth arrest in this strain. At 20 mM HU, dNTP pools in the *pol3-Y708A* mutant were reproducibly decreased by ~25% within 2 h after the addition of the drug to logarithmically growing cultures, as was measured by our collaborators Andrei Chabes and Phong Tran (Figure 8.2 (A)). Remarkably, the frequency of mutation to canavanine resistance (Can^r) in the *pol3-Y708A* strain was not reduced in the presence of HU, but was in fact slightly elevated (up to two-fold at 20 mM HU; Figure 5.6 (A)). The mutator effect of *pol3-Y708A* in the presence of HU remained completely dependent on Polζ: the mutant frequency in the *pol3-Y708A rev3*Δ strain was similar to that in the wild-type strain. These data indicate that the participation of Polζ in replication of undamaged DNA *in vivo* does not depend on high dNTP levels, and that it is stimulated rather than suppressed by the decrease in dNTP pools. It is therefore likely that the high dNTP pools in the *pol3-Y708A* strain are required for efficient replication by Polδ rather than Polζ. In support of this idea, we found that the moderate decrease in

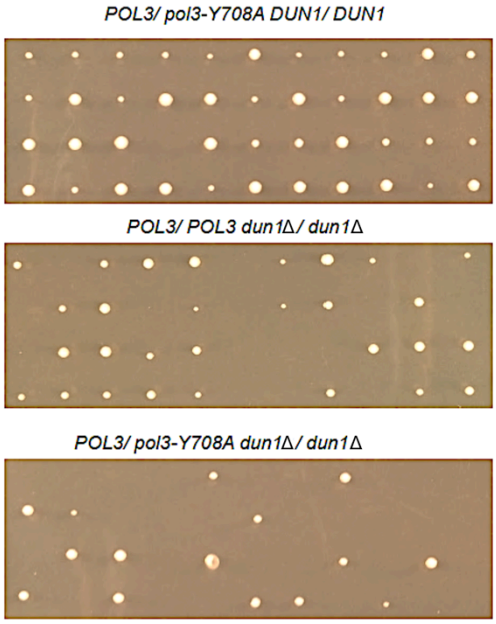

Figure 5.5 Tetrad analysis of the heterozygous diploid strains *POL3/pol3-Y708A DUN1/DUN1*, *POL3/pol3*-Y708A *dun1Δ/dun1Δ*, and the homozygous *POL3/POL3 dun1Δ/dun1Δ* strain.

Spores were dissected on YPDAU medium.

dNTP concentrations induced by low doses of HU in our experiments led to a dramatic reduction in survival of the *pol3-Y708A* strain (Figure 5.6 (B)). Replication problems caused by the Polδ defect are likely exacerbated by dNTP depletion, increasing the need for the recruitment Polζ, whose function is unaffected by the reduced dNTP levels.

Next, we examined whether high dNTP pools are required for Polζ-dependent mutagenesis during lesion bypass. While Polζ is predominately an extender polymerase during TLS across from most DNA lesions, previous studies showed that it might be a major polymerase involved in the bypass of UV-induced lesions at low doses of UVC light (Abdulovic & Jinks-Robertson, 2006, Sharma et al, 2011). To study if Polζ-dependent mutagenesis at low UV doses is affected by changes in dNTP pools, we measured UV-induced Can^r mutant frequency in the presence of HU, such that the bypass of UV lesions would happen in cells with reduced dNTP levels. Overnight cultures were plated on complete and selective media containing HU at concentrations indicated in Figure 5.7 and irradiated with 10 J/m^2 of 254 nm UV light within 15 min. These experiments were done with wild-type yeast strains, so we could use higher HU concentrations (up to 100 mM), which are expected to deplete dNTP pools efficiently. UV-induced mutagenesis was only marginally decreased (~1.5-fold) at the highest dose of HU, while still remaining an order of magnitude higher than the level of spontaneous mutagenesis (Figure 5.7). Notably, UV-induced mutagenesis observed in the presence of HU was completely dependent on Polζ: no induced mutagenesis was seen in the *rev3*Δ strain with or without HU (Figure 5.7). These data indicate that, like copying of undamaged DNA, lesion bypass by Polζ *in vivo* does not require high dNTP pools. Mutagenesis at higher UV doses, however, was significantly suppressed by the HU treatment (Figure 5.8 (A)), consistent with the idea that high dNTP levels are required for the activity of other DNA polymerases that become important for TLS at these doses.

To strengthen the conclusion that Polζ function in TLS and damage-induced mutagenesis does not require high dNTP pools, we also measured UV-induced Can^r mutant frequency in cells that were pre-treated with 100 mM HU for 4 h before UV irradiation. We reasoned that dNTP pools in this case could be more severely reduced by the time DNA replication machinery encounters lesions. We found that the frequency of mutation induced by lower doses of UV (up to 30 J/m^2) was, in fact, significantly elevated in HU-treated cells in comparison to cells not treated with HU (Figure 5.8 (B)). Similar to the experiment shown in Figure 5.8 (A), mutagenesis at higher UV doses was reduced in cells pre-treated with HU. The increase in Polζ mutagenesis at lower UV doses could potentially result from the inhibition of error-free mechanisms of lesion bypass under conditions of severely reduced dNTP pools, or from altered fidelity of nucleotide incorporation opposite lesions by Polζ. In either case, the results clearly demonstrate that the capacity of Polζ to bypass lesions *in vivo* does not require expanded dNTP pools. High dNTP levels, however, might be essential for lesion bypass by other DNA polymerases and for repair under DNA-damaging conditions.

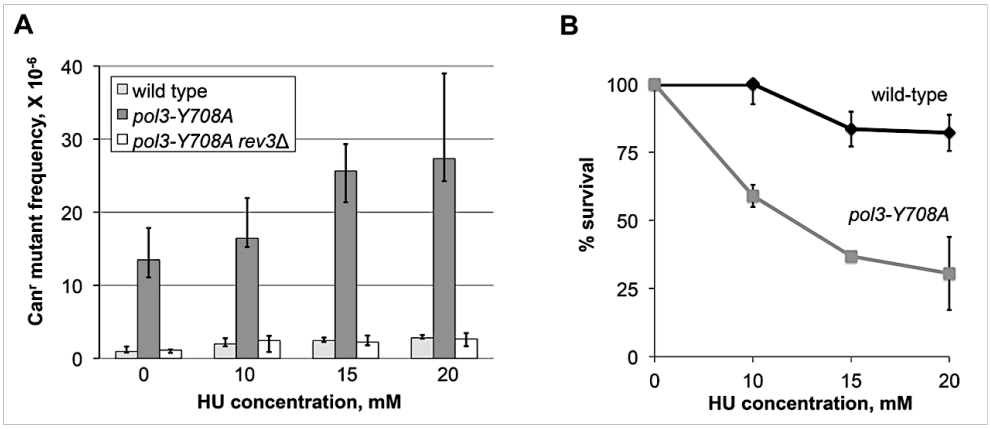

Figure 5.6 Polζ-dependent mutagenesis during replication of undamaged DNA *in vivo* does not require high dNTP levels.

(A) Effect of hydroxyurea (HU) treatment on Polζ-dependent mutator phenotype of the *pol3-Y708A* yeast strain. Wild-type, *pol3-Y708A* and *pol3-Y708A rev3*Δ strains were grown overnight in the presence of indicated HU concentrations and then plated onto selective and complete media. Mutant frequencies are medians and 95% confidence intervals for at least 18 independent cultures. **(B)** Effect of HU treatment on survival of the *pol3-Y708A* and wild-type strains. Viability data were collected from the same experiment shown in (A). Survival was determined by dividing the number of colonies from HU-treated cultures by the number of colonies from untreated cultures. Data are means for 18 independent cultures. Standard errors are shown unless the size of the error bar is smaller than the size of the plot symbol.

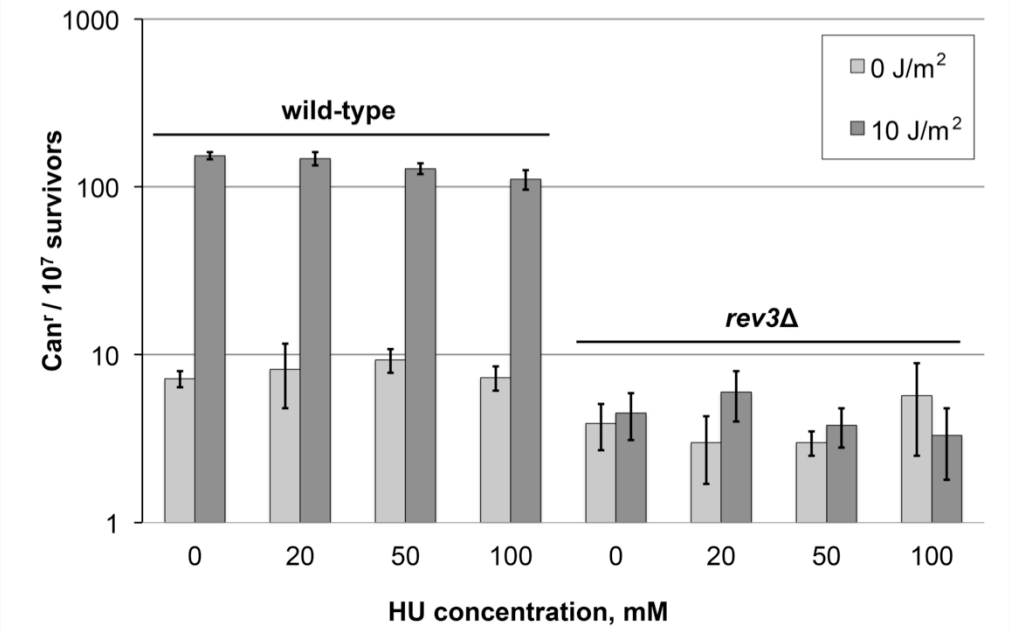

Figure 5.7 Effect of HU treatment on Polζ-dependent mutagenesis induced by 10 J/m^2 UV irradiation.

Overnight cultures of the wild-type and *rev3*Δ strains were plated onto selective and complete media with indicated HU concentrations and then irradiated with 10 J/m^2 of UV light. Data are average frequencies and standard errors for three independent determinations.

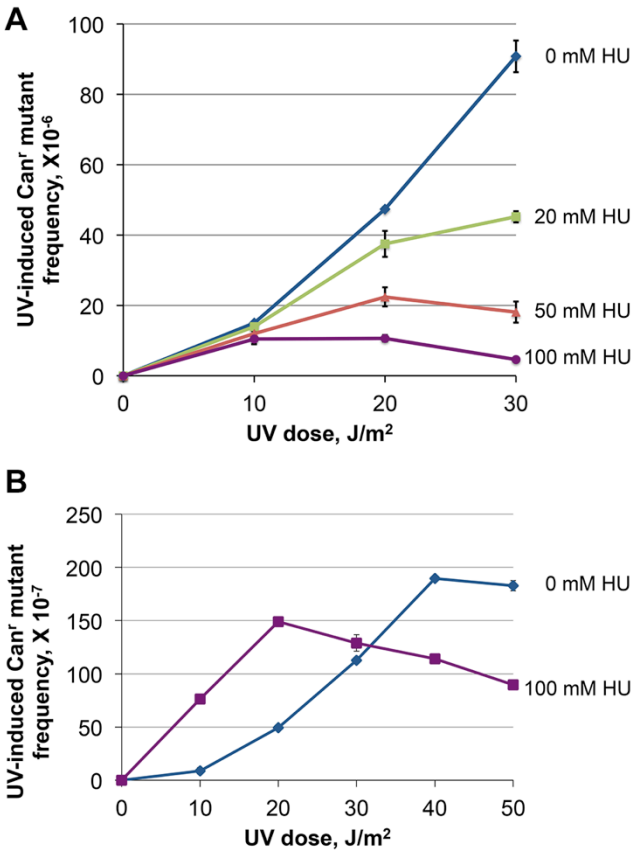

Figure 5.8 Effect of HU treatment on the mutagenicity of high doses of UV light in the wild-type yeast strain.

(A) Effect of various doses of HU on UV-induced mutagenesis. Overnight cultures of the wild-type strain were plated onto selective and complete media with indicated HU concentrations and then irradiated with UV light. Each data point is an average frequency of UV-induced Can^r mutants for three independent determinations. Standard errors are shown where the size of the error bar exceeds the size of the plot symbol. **(B)** Effect of HU pre-treatment on UV-induced mutagenesis. Overnight cultures of the wild-type strain were diluted ten-fold and grown to the logarithmic stage in the presence or absence of 100 mM HU and then plated onto selective and complete media with or without 100 mM HU, respectively. Each data point is an average frequency of UV-induced Can^r mutants for three independent determinations. Standard errors are shown where the size of the error bar exceeds the size of the plot symbol.

5.5 Discussion

While the expansion of cellular dNTP pools is an integral part of DNA damage and replication stress response, the effects of dNTP levels on the function of TLS polymerases are poorly understood. This is the first study to determine the fidelity and error specificity of four-subunit Polζ and Polζ$_4$-Rev1 complex at physiological dNTP concentrations observed during normal S-phase and DNA damage response in yeast. Results presented in this chapter provide evidence that, unlike replicative DNA polymerases, Polζ is remarkably resistant to proportional increases in dNTP levels and does not require high dNTP levels for its *in vivo* functions.

One of the important insights from this work is that the error signature of Polζ at the physiological dNTP levels (Figure 5.3) is drastically different from its previously reported signature observed at equimolar (100 μM) dNTP concentrations (Zhong et al, 2006). This finding emphasizes the need to mimic absolute and relative *in vivo* dNTP levels in order to deduce DNA polymerase signatures from *in vitro* studies. It is also interesting that, in addition to using a non-physiological dNTP ratio, the study by Zhong et al was performed at a time when Polζ was thought to be a two-subunit enzyme. Although low levels of four-subunit enzyme in those Polζ preparations are now thought to be predominately responsible for the observed polymerase activity (Makarova et al, 2012), the abundance of two-subunit Rev3-Rev7 complex and the variable content of Pol31-Pol32 subunits in the preparations could have additionally contributed to the differences in error signature. Curiously, while we could not recapitulate the error spectrum reported by Zhong et al even when we used 100 μM dNTPs with Polζ$_4$, we saw a rather close similarity when we used Polζ$_5$ and 100 μM dNTPs (Figure 5.3 and (Zhong et al, 2006)). The only major difference was a higher rate of A-dCTP errors in the study by Zhong et al, which might have resulted from a bias introduced by strong

hotspots that we did not observe. This profound spectra similarity suggests that the error spectrum reported by Zhong et al might have, in fact, resulted from the activity of Polζ$_5$.

Results described in this chapter also shed light onto the interplay between Polζ and Rev1 during active DNA replication. We demonstrated that in reactions with intracellular dNTPs, Polζ$_4$ is extremely inefficient in misincorporation of dCTP. Interestingly, Rev1 catalytic activity nicely complements Polζ$_4$ in producing all three types of X-dCTP mispairs. This suggests that Rev1 can freely exchange with Polζ at the primer terminus not only at the lesion sites, but during copying of undamaged DNA as well. This idea is further supported by the fact that in the absence of catalytic activity of Rev1, mutational spectrum in strains experiencing DRIM showed a dramatic reduction in base substitutions resulting from misinsertion of dCTP (Northam et al, 2014). In addition to producing X-dCTP mispairs, physical interaction of Rev1 with Polζ slightly elevates the error rates for G-dATP, C-dATP, C-dTTP, A-dTTP, A-dGTP, and T-dATP mispairs. This observation parallels nicely with earlier kinetic studies proposing that interaction of Rev1 with the polymerase domain of Rev3 can alter the structure of Polζ active site to enhance its TLS activity (Acharya et al, 2006). This alteration could promote more efficient binding of Polζ to the aberrant primer termini and/or provide an optimal conformation of the active site for the nucleophilic attack by the primer terminus on the incoming dNTP. Our findings indicate that the presence of Rev1 can also stimulate the mismatch extension by Polζ during active DNA replication.

While the expansion of dNTP pools does not seem to be important for the function of Polζ, we provide evidence that expansion of dNTP pools is essential for survival of the *pol3-Y708A* strain experiencing severe replication stress. It is likely that the impaired DNA replication in the *pol3-Y708A* mutants results in frequent replication fork stalling and may lead to accumulation of single-stranded regions in the genome that

serve as a signal for the checkpoint activation. Activation of Mec1/Rad53/Dun1 checkpoint likely promotes survival of these mutants by stabilization of the stalled replication forks and induction of HR-mediated post-replicative repair (Andreson et al, 2010, Branzei & Foiani, 2010, Chabes et al, 2003, Gangavarapu et al, 2011, Reichard, 1988). Synthetic lethality of the *pol3-Y708A dun1*Δ double mutants and severe sensitivity of the *pol3-Y708A* single mutant to the HU treatment suggest that lower dNTP pools in these strains can cause cell death by the following means. First, it is possible that lower dNTP pools further impair DNA replication by defective Polδ. Second, HR-mediated post-replicative repair that plays a role in rescuing stalled replication forks can be inhibited by low dNTP supply since it requires replicative polymerases as well. Altogether this will lead to accumulation of more single-stranded gaps in these mutants. Although Polζ can be recruited to fill these gaps even when dNTP supply is low, the amount of the ssDNA is likely to be above the threshold that cells can tolerate. However, further studies are required to determine whether HU treatment leads to accumulation of more single-stranded gaps in the *pol3-Y708A* mutants.

The remarkable resistance of Polζ to fluctuations in dNTP levels occurring in response to DNA damage and replication stress, as well as its possible implication in the maintenance of genome stability in yeast, will be discussed in more detail in Chapter 6.

Chapter 6. Discussion, Conclusions and Future Directions

6.1 Discussion

6.1.1 Continuous synthesis by Polζ as a source of mutations downstream of the lesion.

We demonstrated that the bypass of an AP site and the UV-induced lesion in yeast is associated with an untargeted mutagenesis in the adjacent region. The following observations argue that this mutagenesis likely results from continuous replication of long DNA stretches by Polζ. First, the requirement of Polζ for the extension step during TLS puts this polymerase in a perfect position to proceed with DNA synthesis beyond the damage site. Second, the mutation rate in the region downstream of the lesion (~10^{-4} per bp) is similar to the rate of errors produced by purified Polζ *in vitro* (Chapter 5 and (Zhong et al, 2006)). Third, Polζ-deficient *rev3*Δ strains exhibit no untargeted mutagenesis. Forth, while the rate of untargeted mutagenesis remained high in Polη-deficient strain, it was elevated in the strains bearing a mutator allele *rev3-L979F*. The results presented in this dissertation also argue against a genome-wide elevation of the mutation rate as the cause of untargeted mutagenesis, as only rare mutations were observed outside the hypermutated patch.

Another possible source of untargeted mutations is ssDNA formed due to re-priming of replication downstream of the lesion site and the recruitment of Polζ to sites of secondary lesions in the single-stranded gaps. However, the frequency and specificity of mutations in the hypermutated patch argue against the major role of ssDNA in elevated mutagenesis in this region. First, the frequency of mutation induced by spontaneous DNA damage in ssDNA is at least an order of magnitude lower than that observed past the lesion site during TLS (Yang et al, 2008). The distinctive signature of ssDNA-

associated mutagenesis is the abundance of C→T substitutions in the exposed strand (~43% of all base substitutions; (Yang et al, 2008)), which were not detected in the 200-bp segment adjacent to the AP site in our study (Table 3.1). While the TLS products through UV lesions contained C→T transitions (Table 4.3), the rate of untargeted mutations downstream of the lesion site still greatly exceeded that expected from spontaneous damage in ssDNA gaps (Table 4.4 and (Yang et al, 2008)). Altogether these arguments led to a conclusion that the TLS-associated untargeted mutagenesis (Figure 3.2 and Figure 4.3) directly reflects the extent of continuous synthesis by Polζ. Therefore, we estimate that, *in vivo*, Polζ can synthesize up to 1,000 nucleotides upon completing the lesion bypass. This correlates well with electron microscopy studies showing that uncoupling of replication at UV-induced lesions in yeast leads to the formation of single-stranded gaps with an average size of 400 nucleotides, but longer gaps (up to 3000 nt) could be formed sometimes as well (Lopes et al, 2006). If TLS, as it is widely accepted, occurs predominantly in these gaps, Polζ must be responsible for filling a substantial portion of the gaps. However, further studies are required to determine whether a switch to the replicative polymerase occurs later during the gap filling.

6.1.2 Replication restart as a possible determinant of the length of TLS tracts.

We observed that the bypass of the chromosomal UV lesion is associated with longer TLS tracts in comparison to the AP site bypass on a plasmid. It seems likely that the extent of Polζ-dependent synthesis may be regulated by the size of the single-stranded gap formed after re-priming of replication downstream of the lesion. The size of the gap could vary depending on the lesion position in the leading or lagging strand

template. The stalled replication forks on the lagging strand do not require a special mechanism for re-priming downstream of the lesion sites, as it can be restarted with the priming of the next Okazaki fragment. In this case, the size of single-stranded gaps on the lagging strand would correspond to the size of Okazaki fragments (140-175 nucleotides (Smith & Whitehouse, 2012, Waisertreiger et al, 2012)). In contrast, due to continuous nature of replication on the leading strand, replication re-priming is likely to require additional regulation, and the re-priming might occur at a greater distance from the damage site. Although whether the lesion is located in the lagging or leading strand in the AP site assays is unknown, we believe the lesion is mostly encountered by the lagging strand machinery. The AP site is located at similar distances from the centromere-proximal and centromere-distal sides of the replication origin *ARS4* in the plasmid (Figure 3.1 (A)). However, the inhibitory effect of the repetitive centromeric region on the fork progression (Greenfeder & Newlon, 1992) will likely slow down the progression of the left-ward replication fork and, thus, the lesion-containing region is likely to be replicated by the rightward replication fork. In this case, the AP site will be in the lagging strand template. Conversely, the UV photolesions in chromosome *V* are likely to be approached by the leading strand machinery. The end of the *URA3* gene in a genetically unmanipulated chromosome *V* corresponds to the beginning of the replication termination zone (the region between 117 and 123 kb in Figure 4.1 (B) ((Fachinetti et al, 2010, McGuffee et al, 2013)). The *LEU2* insertion to the right of the *URA3* gene (Figure 4.1 (B)) presumably moves the *URA3* gene away from the termination zone by at least 1 kb, placing the TC site into the leading strand template. The lesion position in the opposite DNA strands in the two TLS assays could potentially explain the differences in the length of the TLS tracts.

6.1.3 Clustered mutagenesis as a consequence of TLS.

The occurrence of untargeted mutagenesis beyond the lesion site increases the probability of inactivating a nearby gene. Approximately 2 to 7% of TLS tracts contain an additional mutation in the adjacent region (Chapter 3 and 4). Considering that ~1/3 of base substitutions and almost all frameshifts in coding regions affect the gene function (Drake, 1991), we estimate that approximately 1 to 4% of TLS tracts spanning a coding region will inactivate the gene. Such extended tracts of TLS can lead to accumulation of multiple mutations in a localized area leading to a phenomenon called clustered mutagenesis. The localized hypermutability serves as a mechanism for rapid genome changes without overloading it with mutations and is believed to significantly contribute to biological processes such as tumorigenesis, immunity and adaptation (discussed in (Camps et al, 2007, Drake et al, 2005, Nik-Zainal et al, 2012, Roberts et al, 2012, Stone et al, 2012, Taylor et al, 2013)). While a major cause of clustered mutagenesis was shown to be the enzymatic deamination of cytosines in ssDNA, untargeted mutagenesis associated with TLS may also contribute to this phenomenon. Given that the excision of uracil resulting from cytosine deamination by uracil DNA glycosylases produces AP sites (Crosby et al, 1981), the subsequent bypass of unrepaired AP sites by TLS can potentially contribute to formation of the deaminase-induced clusters as well (Chan et al, 2013, Taylor et al, 2013). Therefore, we propose that TLS-associated untargeted mutagenesis may also contribute to promoting adaptation, evolution or cancer development through generating clustered mutations. For example, Polζ/Rev1-dependent TLS is believed to be responsible for the acquiring of chemoresistance and the development of secondary tumors in patients undergoing chemotherapy with DNA-damaging agents (Doles et al, 2010, Okuda et al, 2005, Sharma et al, 2012, Xie et al, 2010). Considering the emerging role of Polζ-dependent mutagenesis in accumulation of

clustered mutations in genome, it appears to be important to identify factors that modulate fidelity of Polζ *in vivo*.

6.1.4 What makes Polζ resistant to fluctuations in dNTP levels occurring in vivo?

It has been proposed that high or imbalanced dNTP pools induce genome instability by several possible mechanisms, including increasing the probability of nucleotide misinsertion, mismatched primer extension, and strand misalignment (Buckland et al, 2014, Gon et al, 2011, Kumar et al, 2010, Mertz et al, 2015, Williams et al, 2015). For example, mutations in the yeast *RNR1* gene encoding a subunit of RNR lead to alterations in dNTP pools and, as a result, to a dramatic increase in genome instability (Kumar et al, 2011). The mutational specificity observed in these strains correlates well with misincorporation of nucleotides that are in excess. In addition, higher dNTP concentrations may facilitate more efficient extension of mismatched primer termini by reducing proofreading activity of replicative DNA polymerases and by stimulating elongation mode (Buckland et al, 2014, Gon et al, 2011, Kumar et al, 2011, Watt et al, 2016). It would be rational to assume that the low sensitivity of TLS DNA polymerase ζ to increasing dNTP concentrations is due to its exonuclease deficiency. However, a recent study by Stodola and Burgers showed that catalytic activity of exonuclease-deficient variant of Polδ *in vitro* is strongly stimulated when dNTP concentrations are increased above physiological dNTPs levels (Stodola & Burgers, 2016). In addition, earlier studies of exonuclease-deficient Polε showed that increasing dNTP concentrations in the M13mp2 assay decreases the polymerase fidelity by promoting more frequent generation of frameshifts and alters the specificity of nucleotide misincorporation (Shcherbakova et al, 2003). These studies suggest that high dNTP

levels may affect activity and fidelity of Exo$^-$ variants of replicative DNA polymerases, presumably by changing their nucleotide selectivity (Watt et al, 2016). Therefore, it seems likely that intrinsic selectivity of Polζ is less dependent on dNTP concentrations in comparison to that of replicative DNA polymerases. Resistance of Polζ to physiological fluctuations in dNTP levels may reflect a unique trait in the structure of its active site. This idea is further supported by the fact that amino acid substitution L979F in the active site of Polζ makes it more sensitive to dNTP levels, as could be seen from significant improvement of the bypass of certain DNA lesions at damage-state dNTPs in comparison to the normal S-phase dNTPs by L979F, but not the wild-type Polζ, *in vitro* (Stone et al, 2011). However, future studies are required to determine whether high dNTP levels also affect fidelity and error-specificity of L979F Polζ.

6.1.5 Polζ as a unique tool for rescuing stalled replication forks at low dNTP levels.

This study also reveals that Polζ does not require high dNTP pools for replication of undamaged DNA or the bypass of DNA lesions *in vivo*. DRIM was not decreased in the *pol3-Y708A* strain, but on the contrary, was even further elevated when dNTP pools were brought down by treatment with HU (Figure 5.6). Similarly, mutagenesis induced by low doses of UV light was increased rather than decreased when cells were treated with HU prior to UV irradiation (Figure 5.8). In line with these observations, using damage-response dNTP concentrations for TLS by the wild-type Polζ *in vitro* only slightly improved nucleotide incorporation opposite *cis-syn* cyclobutane pyrimidine dimer and (6-4)-photoproduct and the bypass of these lesions (Stone et al, 2011). Furthermore, we observed only a minor difference in the activity, fidelity and error specificity of Polζ$_4$ and

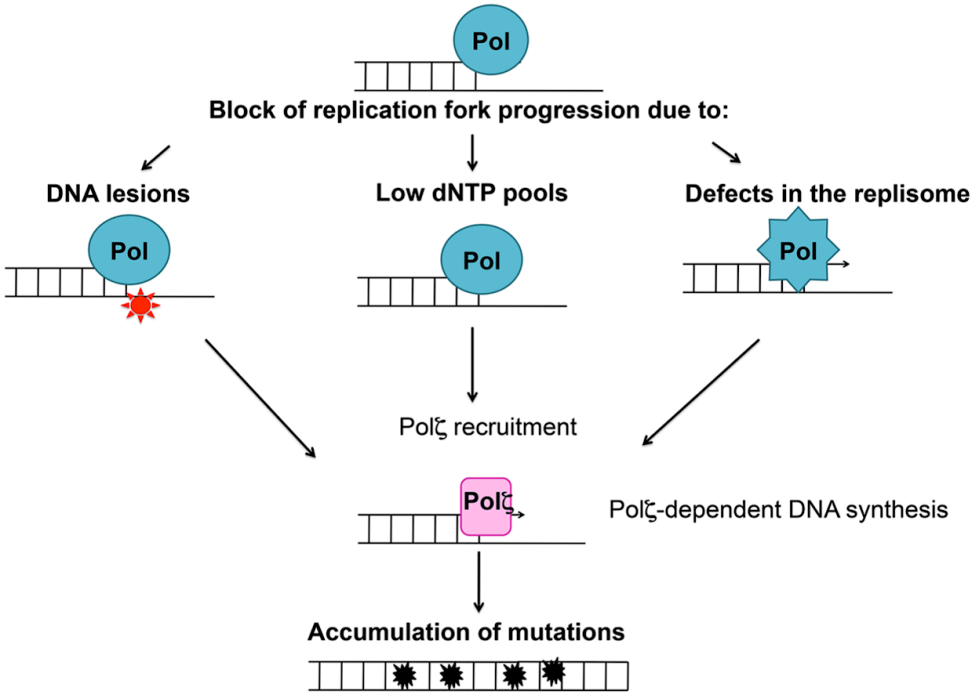

Figure 6.1 Circumstances under which Polζ is permitted to replicate DNA *in vivo*.

Polζ can be recruited to rescue stalled replication forks due to replisome stalling at a lesion (left), perturbed DNA replication at low dNTP pools (middle), and defects in replisome components (right). In all situations, participation of Polζ in DNA replication is expected to induce accumulation of mutations.

Polζ$_5$ when damage response dNTP concentrations were used instead of S-phase concentrations (Figure 5.1, Table 5.1, Figure 5.3 (A, B)). These findings suggest that the rise in dNTP levels in response to DNA damage or replication perturbations may be primarily needed to facilitate other, non-mutagenic tolerance mechanisms. High dNTP levels could improve the activity of replicative DNA polymerases, as well as the TLS capacity of Polη, which, at least in the case of UV-induced lesions, would contribute to mutation avoidance. Expanded dNTP pools could also potentially promote DNA repair and high-fidelity template-switching mechanisms of damage tolerance, where synthesis by replicative DNA polymerases might be required. Indeed, up-regulation of the RNR activity has been shown to increase the rate of fork progression during normal replication and under conditions of replication stress (Poli et al, 2012). Moreover, the rate of DNA synthesis by Polδ is not optimal at physiological dNTP concentrations and can be substantially improved by increasing dNTP levels (Stodola & Burgers, 2016). Finally, increased dNTP concentrations are also known to facilitate the bypass of certain lesions by replicative DNA polymerases *in vitro* and *in vivo* (Lis et al, 2008, Sabouri et al, 2008).

Additional support for the role of dNTP pools expansion in facilitating the function of replicative polymerases, but not Polζ, upon DNA damage comes from the studies of regulation of mutagenesis at high and low doses of UV irradiation. Previous studies of UV sensitivity of yeast strains deficient in TLS revealed a differential involvement of TLS polymerases in the bypass of UV lesions at low and high doses of irradiation. Polζ-deficient strains show higher sensitivity to low doses of UV light than Polη mutants, while Polη-deficient strains are more sensitive to higher doses (greater than 30 J/m^2; (Abdulovic & Jinks-Robertson, 2006)). These data imply that the bypass of UV-induced lesions at lower doses relies predominantly on Polζ, while other polymerases become important at higher doses. The lack of effect of HU treatment on UV-induced

mutagenesis at the low UV dose and the clear inhibition of mutagenesis by HU at higher UV doses (Figure 5.7, Figure 5.8 (A)) further proves that, unlike other DNA polymerases, Polζ does not require high dNTP levels for TLS *in vivo*. On the contrary, expanded dNTP pools become vital for lesion bypass at higher doses of UV irradiation when other DNA polymerases must be involved, such as Polη or replicative polymerases. The importance of high dNTP concentrations for the damage tolerance at high doses of UV light has been noted previously (Lis et al, 2008, Sabouri et al, 2008).

It appears possible that Polζ evolved toward decreasing the dependence of its DNA synthesis activity on the levels of intracellular dNTPs, providing cells with a rescue tool when normal DNA replication is perturbed due to low dNTP supply (Figure 6.1). This hypothesis is further reinforced by our earlier finding that treatment of wild-type yeast strains with HU causes a Polζ-dependent increase in mutagenesis (Northam et al, 2010). Interestingly, it has been reported that depletion of dNTP pools can contribute to early stages of tumorigenesis by promoting replication stress and genome instability (Bester et al, 2011, Gorrini et al, 2007, Niida et al, 2010). If human Polζ is similarly insensitive to decreases in dNTP levels, it is likely this genome instability results, at least in part, from error-prone DNA synthesis by Polζ recruited to the stalled replication forks and accumulation of mutations in these regions (Figure 6.1).

6.2 Conclusions

The results presented in Chapter 3 of this dissertation demonstrate that the bypass of a single plasmid-borne AP site is associated with error-prone synthesis downstream of the lesion. The error-prone synthesis typically continues for approximately 200 nucleotides after the lesion bypass is completed in our assay. The mutation rate in this region exceeds the genome-wide mutation rate in yeast by

approximately 300,000-fold and is similar to rate of errors produced by purified Polζ during copying of undamaged DNA *in vitro* (10^{-4} -10^{-3}) (Chapter 5 and (Zhong et al, 2006)). The genetic system described in Chapter 3 can be used as a tool to investigate error-prone bypass of a single lesion and define the factors that modulate the length of the TLS tracts.

The results presented in Chapter 4 of this dissertation demonstrate that the mutagenic bypass of a UV-induced chromosomal lesion is also accompanied by the untargeted mutagenesis downstream of the lesion site. In contrast to the AP site bypass, the error-prone synthesis past the site-specific UV lesion we investigated spans approximately 1000 nucleotides. This suggests an existence of a potential regulatory mechanism that can determine the length of the TLS tracts. The results in Chapter 4 also provide arguments in support of the role of Polζ in generating untargeted mutations: 1. Polζ serves as an extender polymerase during the bypass of most lesions, including the ones analyzed in this work; 2. No untargeted mutations were observed in the Polζ-deficient strain; 3. The mutation rate in the region downstream of the lesion (~10^{-4} per bp) is comparable to the rate of errors observed during Polζ-dependent copying of undamaged DNA *in vitro*. 4. The rate of mutations in this region remains unaffected in Polη-deficient strain. In addition, results in both Chapter 3 and 4 demonstrate that MMR is not efficient in the removal of replication errors in TLS tracts.

The results in Chapter 5 of this dissertation demonstrate that Polζ activity, fidelity and error specificity are not affected by increases in dNTP levels occurring during DNA damage response. We demonstrated that Polζ_4 and Polζ_5 are predominantly promiscuous at G nucleotides at both S-phase and damage-response dNTP concentrations. Polζ_5 showed reduced fidelity in comparison to Polζ_4 and generated all three X·dCTP mispairs (particularly, C·dCTP) and complex mutations at higher rates in

comparison to Polζ$_4$. The results in Chapter 5 also demonstrate that the replication mutant *pol3-Y708A* experiencing DRIM requires activation of checkpoint response and expansion of dNTP pools for survival. However, the results argue against the importance of high dNTP pools for Polζ-dependent mutagenesis *in vivo*. These findings support a model where expansion of dNTP pools facilitates the function of replicative DNA polymerases and HR-mediated post-replicative repair upon DNA damage or replication stress. On the contrary, Polζ appears to be uniquely capable of rescuing stalled replication when dNTP supply is limited.

6.3 Future Directions

6.3.1 How are lesion bypass and the extent of error-prone synthesis affected by replication timing?

Previous studies proposed that the damaged bases in the late-replicating regions are more likely bypassed by a mutagenic TLS than the lesions in the early-replicating regions (Lang & Murray, 2011). The support for this hypothesis comes from the following observations. First, UV irradiation induces accumulation of single-stranded regions behind the replication fork in TLS-deficient strains only in the late S phase (Lopes et al, 2006). Second, *REV1* expression is cell cycle dependent with a maximum level in the G2/M phase (Waters & Walker, 2006). Finally, late-replicating regions exhibit higher rates of spontaneous mutagenesis in comparison to early-replicating regions. Importantly, these variations in mutation rates are dependent on Rev1 (Lang & Murray, 2011). Curiously, in both genetic systems where we detected TLS-associated hypermutated patches (Chapters 3 and 4), the lesions were located close to the

replication termination zone and presumably in the late replicating regions. Therefore, it is not known whether the observed hypermutated patch is specific to the lesion bypass in the late-replicating regions. To test this, we could place a lesion in the early replicating template near a defined strong origin of replication. First, this will allow us to test whether the mutagenic bypass of a site-specific lesion occurs with similar efficiencies in the early and late-replicating regions. Second, we will be able to determine whether the mutagenic bypass of a lesion in the early-replicating region also leads to an increase in the rate of untargeted mutagenesis beyond the lesion site. If the length of the hypermutated patch is shorter in the early-replicating regions, this will suggest that the extent of TLS tracts is more tightly regulated in these regions and is dependent on replication timing.

6.3.2 How does the lesion position in the leading vs. lagging strands affect the length of TLS tracts?

According to the gap-filling model of TLS, TLS polymerases are recruited to the gaps formed between the lesion sites and re-priming of replication downstream of the lesion. We hypothesize that the size of the gaps and, as a result, the extent of the error-prone synthesis, might vary depending on the lesion location in the leading or lagging strands. To test this hypothesis, we could place a site-specific lesion in the leading and lagging strands and analyze the regions downstream of the lesion site in TLS products. If we observe shorter stretches of error-prone synthesis in the lagging strand and longer in the leading strand, this would suggest that the length of TLS tracts is controlled differently on the leading and lagging strands.

6.3.3 Does the efficiency of re-priming downstream of the lesion regulate the extent of error-prone synthesis?

We proposed that re-priming of replication downstream of the lesion site might physically limit the extent of Polζ synthesis during lesion bypass. To test this hypothesis, we could determine the length of TLS tracts in Polα mutants that show inefficient priming of replication. Such inefficient priming is expected to increase the distance between the lesion and the site of replication restart. If replication re-priming does regulate the size of the hypermutated patch, we would expect to detect untargeted mutations at greater distances from the lesion site than in the wild-type strain.

6.3.4 Can Polδ correct Polζ errors in TLS tracts?

We demonstrated that MMR is not efficient in removal of errors in TLS tracts. However, the rate of mutagenesis observed downstream from the lesion site is ten-fold lower than the fidelity of purified Polζ observed *in vitro*. This suggests the existence of another mechanism that is able to correct Polζ errors *in vivo*. We propose that some of the errors produced by Polζ can be corrected by the exonucleolytic activity of replicative DNA polymerase δ, when it replaces Polζ to fill the gap after lesion bypass is completed. To test this hypothesis, we could determine the rate of untargeted mutations downstream from the lesion site in strains with exonuclease-deficient Polδ. If Polδ does correct Polζ errors, we would expect to see an increase in the rate of mutations in TLS tracts.

6.3.5 Do defects in non-catalytic components of replisome inducing DRIM activate checkpoint response?

DRIM can be induced by various defects in the catalytic and accessory subunits of yeast replicative DNA polymerases, replication factor Mcm10 and chromatin factors (Aksenova et al, 2010, Becker et al, 2014, Garbacz et al, 2015, Kadyrova et al, 2013, Kraszewska et al, 2012, Northam et al, 2006, Pavlov et al, 2001b, Shcherbakova et al, 1996, Stodola et al, 2016). The level of Polζ-dependent mutagenesis greatly varies in these mutants and, probably, reflects the severity of replication defect. Results in Chapter 5 describe the importance of checkpoint activation and elevated dNTP pools for survival of the *pol3-Y708A* mutant. However, it is not known whether defects in non-catalytic replisome components and replication factors resulting in DRIM phenotype also require checkpoint activation for cell survival. To study this, we could test the synthetic lethality of mutations in genes encoding various components of the replisome, which are known to induce DRIM, and Dun1 deficiency. Candidates for this analysis could be *pol2-100* mutant affecting binding of Polε to the GINS complex and mutant *mcm10-1* allele impairing the function of essential component of replisome Mcm10 (Becker et al, 2014, Kraszewska et al, 2012). Given the fact that these mutations affect regulation of the essential steps of replication initiation, it is tempting to speculate that these mutants would also require checkpoint activation for resolving replication stress. On the contrary, lack of a non-essential subunit of Polε, Dpb3, does not result in a slow growth phenotype suggesting that Dpb3 deficiency causes only minor replication stress and does not require checkpoint activation. Considering that 90% of mutagenesis in this strain is dependent on Polζ function (Northam et al, 2006), this study would provide further

support for the hypothesis that Polζ can function under conditions when DNA replication checkpoint is not activated.

6.3.6 Does Polζ play a role in rescuing stalled replication forks due to insufficient dNTP supply in human cells?

Insufficient dNTP supply was proposed to contribute to replication stress and genome instability required for overcoming the apoptosis/senescence barrier in the human papillomavirus (HPV)-infected cells (Bester et al, 2011). Interestingly, such cells proliferated normally, suggesting that there is a potential mechanism allowing them to complete chromosomal replication even when dNTP pools are low. If human Polζ is also insensitive to decreases in dNTP levels, it is likely that it can, at least in part, release the replication stress in the newly transformed HPV-infected cells. Importantly, error-prone DNA synthesis by Polζ recruited to the stalled replication forks can contribute to mutagenesis in these cells and promote malignant transformation.

To test this hypothesis, we propose to determine how the expression of HPV oncoproteins affects REV3L protein levels in the newly transformed cells with insufficient dNTP levels. If REV3L levels are increased, this would indicate a requirement of Polζ for overcoming replication stress in these cells. This can be further proved by the knockdown of the *REV3L* gene in the HPV-infected cells. If Polζ is required for proliferation of HPV-infected cells at early stages of malignant transformation, *REV3L* knockdown would significantly reduce viability of the newly transformed cells.

Additionally, comparing HU-induced mutagenesis in human cells with or without knockdown of the *REV3L* gene would allow us to test whether Polζ contributes to genome instability induced by low dNTP levels in human cells as well.

References

Abdulovic AL, Jinks-Robertson S (2006) The *in vivo* characterization of translesion synthesis across UV-induced lesions in *Saccharomyces cerevisiae*: insights into Pol ζ- and Pol η-dependent frameshift mutagenesis. *Genetics* **172**:1487-98.

Acharya N, Haracska L, Johnson RE, Unk I, Prakash S, Prakash L (2005) Complex formation of yeast Rev1 and Rev7 proteins: a novel role for the polymerase-associated domain. *Mol Cell Biol* **25**:9734-40.

Acharya N, Johnson RE, Pages V, Prakash L, Prakash S (2009) Yeast Rev1 protein promotes complex formation of DNA polymerase ζ with Pol32 subunit of DNA polymerase δ. *Proc Natl Acad Sci USA* **106**:9631-6.

Acharya N, Johnson RE, Prakash S, Prakash L (2006) Complex formation with Rev1 enhances the proficiency of *Saccharomyces cerevisiae* DNA polymerase ζ for mismatch extension and for extension opposite from DNA lesions. *Mol Cell Biol* **26**:9555-63.

Ahluwalia D, Schaaper RM (2013) Hypermutability and error catastrophe due to defects in ribonucleotide reductase. *Proc Natl Acad Sci USA* **110**:18596-601.

Aksenova A, Volkov K, Maceluch J, Pursell ZF, Rogozin IB, Kunkel TA, Pavlov YI, Johansson E (2010) Mismatch repair-independent increase in spontaneous mutagenesis in yeast lacking non-essential subunits of DNA polymerase ε. *PLoS Genet* **6**:e1001209.

Amberg DC, Burke DJ, Strathern JN (2006) High-efficiency transformation of yeast. *CSH Protoc* **2006**

Andreson BL, Gupta A, Georgieva BP, Rothstein R (2010) The ribonucleotide reductase inhibitor, Sml1, is sequentially phosphorylated, ubiquitylated and degraded in response to DNA damage. *Nucleic Acids Res* **38**:6490-501.

Auerbach P, Bennett RA, Bailey EA, Krokan HE, Demple B (2005) Mutagenic specificity of endogenously generated abasic sites in *Saccharomyces cerevisiae* chromosomal DNA. *Proc Natl Acad Sci USA* **102**:17711-6.

Avkin S, Adar S, Blander G, Livneh Z (2002) Quantitative measurement of translesion replication in human cells: evidence for bypass of abasic sites by a replicative DNA polymerase. *Proc Natl Acad Sci U S A* **99**:3764-9.

Baldo V, Liang J, Wang G, Zhou H (2012) Preserving Yeast Genetic Heritage through DNA Damage Checkpoint Regulation and Telomere Maintenance. *Biomolecules* **2**:505-23.

Banerjee SK, Borden A, Christensen RB, LeClerc JE, Lawrence CW (1990) SOS-dependent replication past a single *trans-syn* T-T cyclobutane dimer gives a different mutation spectrum and increased error rate compared with replication past this lesion in uninduced cells. *J Bacteriol* **172**:2105-12.

Bebenek K, Kunkel TA (1995) Analyzing fidelity of DNA polymerases. *Methods Enzymol* **262**:217-32.

Becker JR, Nguyen HD, Wang X, Bielinsky AK (2014) Mcm10 deficiency causes defective-replisome-induced mutagenesis and a dependency on error-free postreplicative repair. *Cell Cycle* **13**:1737-48.

Bester AC, Roniger M, Oren YS, Im MM, Sarni D, Chaoat M, Bensimon A, Zamir G, Shewach DS, Kerem B (2011) Nucleotide deficiency promotes genomic instability in early stages of cancer development. *Cell* **145**:435-46.

Boiteux S, Guillet M (2004) Abasic sites in DNA: repair and biological consequences in *Saccharomyces cerevisiae*. *DNA Repair* **3**:1-12.

Boiteux S, Jinks-Robertson S (2013) DNA repair mechanisms and the bypass of DNA damage in *Saccharomyces cerevisiae*. *Genetics* **193**:1025-64.

Braithwaite DK, Ito J (1993) Compilation, alignment, and phylogenetic relationships of DNA polymerases. *Nucleic Acids Res* **21**:787-802.

Branzei D, Foiani M (2010) Maintaining genome stability at the replication fork. *Nat Rev Mol Cell Biol* **11**:208-19.

Branzei D, Szakal B (2016) DNA damage tolerance by recombination: Molecular pathways and DNA structures. *DNA Repair*

Brash DE, Haseltine WA (1982) UV-induced mutation hotspots occur at DNA damage hotspots. *Nature* **298**:189-92.

Bresson A, Fuchs RP (2002) Lesion bypass in yeast cells: Pol η participates in a multi-DNA polymerase process. *EMBO J* **21**:3881-7.

Broyde S, Wang L, Rechkoblit O, Geacintov NE, Patel DJ (2008) Lesion processing: high-fidelity versus lesion-bypass DNA polymerases. *Trends Biochem Sci* **33**:209-19.

Buckland RJ, Watt DL, Chittoor B, Nilsson AK, Kunkel TA, Chabes A (2014) Increased and imbalanced dNTP pools symmetrically promote both leading and lagging strand replication infidelity. *PLoS Genet* **10**:e1004846.

Budd ME, Campbell JL (1995) DNA polymerases required for repair of UV-induced damage in *Saccharomyces cerevisiae*. *Mol Cell Biol* **15**:2173-9.

Budzowska M, Kanaar R (2009) Mechanisms of dealing with DNA damage-induced replication problems. *Cell Biochem Biophys* **53**:17-31.

Cabral Neto JB, Cabral RE, Margot A, Le Page F, Sarasin A, Gentil A (1994) Coding properties of a unique apurinic/apyrimidinic site replicated in mammalian cells. *J Mol Biol* **240**:416-20.

Callegari AJ, Clark E, Pneuman A, Kelly TJ (2010) Postreplication gaps at UV lesions are signals for checkpoint activation. *Proc Natl Acad Sci USA* **107**:8219-24.

Camps M, Herman A, Loh E, Loeb LA (2007) Genetic constraints on protein evolution. *Crit Rev Biochem Mol Biol* **42**:313-26.

Chabes A, Georgieva B, Domkin V, Zhao X, Rothstein R, Thelander L (2003) Survival of DNA damage in yeast directly depends on increased dNTP levels allowed by relaxed feedback inhibition of ribonucleotide reductase. *Cell* **112**:391-401.

Chan K, Resnick MA, Gordenin DA (2013) The choice of nucleotide inserted opposite abasic sites formed within chromosomal DNA reveals the polymerase activities participating in translesion DNA synthesis. *DNA Repair* **12**:878-89.

Choi K, Szakal B, Chen YH, Branzei D, Zhao X (2010) The Smc5/6 complex and Esc2 influence multiple replication-associated recombination processes in *Saccharomyces cerevisiae*. *Mol Biol Cell* **21**:2306-14.

Crosby B, Prakash L, Davis H, Hinkle DC (1981) Purification and characterization of a uracil-DNA glycosylase from the yeast *Saccharomyces cerevisiae*. *Nucleic Acids Res* **9**:5797-809.

D'Souza S, Walker GC (2006) Novel role for the C terminus of *Saccharomyces cerevisiae* Rev1 in mediating protein-protein interactions. *Mol Cell Biol* **26**:8173-82.

Daraba A, Gali VK, Halmai M, Haracska L, Unk I (2014) Def1 promotes the degradation of Pol3 for polymerase exchange to occur during DNA-damage--induced mutagenesis in *Saccharomyces cerevisiae*. *PLoS Biol* **12**:e1001771.

Doles J, Oliver TG, Cameron ER, Hsu G, Jacks T, Walker GC, Hemann MT (2010) Suppression of Rev3, the catalytic subunit of Polζ, sensitizes drug-resistant lung tumors to chemotherapy. *Proc Natl Acad Sci USA* **107**:20786-91.

Drake JW (1991) A constant rate of spontaneous mutation in DNA-based microbes. *Proc Natl Acad Sci USA* **88**:7160-4.

Drake JW, Bebenek A, Kissling GE, Peddada S (2005) Clusters of mutations from transient hypermutability. *Proc Natl Acad Sci USA* **102**:12849-54.

Drake JW, Charlesworth B, Charlesworth D, Crow JF (1998) Rates of spontaneous mutation. *Genetics* **148**:1667-86.

Duxin JP, Walter JC (2015) What is the DNA repair defect underlying Fanconi anemia? *Curr Opin Cell Biol* **37**:49-60.

Elvers I, Johansson F, Groth P, Erixon K, Helleday T (2011) UV stalled replication forks restart by re-priming in human fibroblasts. *Nucleic Acids Res* **39**:7049-57.

Fachinetti D, Bermejo R, Cocito A, Minardi S, Katou Y, Kanoh Y, Shirahige K, Azvolinsky A, Zakian VA, Foiani M (2010) Replication termination at eukaryotic chromosomes is mediated by Top2 and occurs at genomic loci containing pausing elements. *Mol Cell* **39**:595-605.

Fishel R (2015) Mismatch repair. *J Biol Chem* **290**:26395-403.

Fortune JM, Pavlov YI, Welch CM, Johansson E, Burgers PM, Kunkel TA (2005) Saccharomyces cerevisiae DNA polymerase delta: high fidelity for base substitutions but lower fidelity for single- and multi-base deletions. *J Biol Chem* **280**:29980-7.

Friedberg EC, Walke GC, Siede W, Wood RD, Schultz RA, Ellenberger T (2006) DNA repair and mutagenesis. ASM Press, Washington D. C.

Fujii S, Fuchs RP (2004) Defining the position of the switches between replicative and bypass DNA polymerases. *EMBO J* **23**:4342-52.

Gangavarapu V, Santa Maria SR, Prakash S, Prakash L (2011) Requirement of replication checkpoint protein kinases Mec1/Rad53 for postreplication repair in yeast. *MBio* **2**:e00079-11.

Garbacz M, Araki H, Flis K, Bebenek A, Zawada AE, Jonczyk P, Makiela-Dzbenska K, Fijalkowska IJ (2015) Fidelity consequences of the impaired interaction between DNA polymerase ε and the GINS complex. *DNA Repair* **29**:23-35.

Gentil A, Cabral-Neto JB, Mariage-Samson R, Margot A, Imbach JL, Rayner B, Sarasin A (1992) Mutagenicity of a unique apurinic/apyrimidinic site in mammalian cells. *J Mol Biol* **227**:981-4.

Gibbs PE, Lawrence CW (1995) Novel mutagenic properties of abasic sites in *Saccharomyces cerevisiae*. *J Mol Biol* **251**:229-36.

Gibbs PE, McDonald J, Woodgate R, Lawrence CW (2005) The relative roles in vivo of *Saccharomyces cerevisiae* Pol η, Pol ζ, Rev1 protein and Pol32 in the bypass and mutation induction of an abasic site, T-T (6-4) photoadduct and T-T *cis-syn* cyclobutane dimer. *Genetics* **169**:575-82.

Gon S, Napolitano R, Rocha W, Coulon S, Fuchs RP (2011) Increase in dNTP pool size during the DNA damage response plays a key role in spontaneous and induced-mutagenesis in *Escherichia coli*. *Proc Natl Acad Sci USA* **108**:19311-6.

Gorrini C, Squatrito M, Luise C, Syed N, Perna D, Wark L, Martinato F, Sardella D, Verrecchia A, Bennett S, Confalonieri S, Cesaroni M, Marchesi F, Gasco M, Scanziani E, Capra M, Mai S, Nuciforo P, Crook T, Lough J et al. (2007) Tip60 is a haplo-insufficient tumour suppressor required for an oncogene-induced DNA damage response. *Nature* **448**:1063-7.

Grabowska E, Wronska U, Denkiewicz M, Jaszczur M, Respondek A, Alabrudzinska M, Suski C, Makiela-Dzbenska K, Jonczyk P, Fijalkowska IJ (2014) Proper functioning of the GINS complex is important for the fidelity of DNA replication in yeast. *Mol Microbiol* **92**:659-80.

Greenfeder SA, Newlon CS (1992) Replication forks pause at yeast centromeres. *Mol Cell Biol* **12**:4056-66.

Guldener U, Heck S, Fielder T, Beinhauer J, Hegemann JH (1996) A new efficient gene disruption cassette for repeated use in budding yeast. *Nucleic Acids Res* **24**:2519-24.

Guo C, Fischhaber PL, Luk-Paszyc MJ, Masuda Y, Zhou J, Kamiya K, Kisker C, Friedberg EC (2003) Mouse Rev1 protein interacts with multiple DNA polymerases involved in translesion DNA synthesis. *EMBO J* **22**:6621-30.

Guo D, Wu X, Rajpal DK, Taylor JS, Wang Z (2001) Translesion synthesis by yeast DNA polymerase ζ from templates containing lesions of ultraviolet radiation and acetylaminofluorene. *Nucleic Acids Res* **29**:2875-83.

Haracska L, Prakash S, Prakash L (2000) Replication past O(6)-methylguanine by yeast and human DNA polymerase η. *Mol Cell Biol* **20**:8001-7.

Haracska L, Torres-Ramos CA, Johnson RE, Prakash S, Prakash L (2004) Opposing effects of ubiquitin conjugation and SUMO modification of PCNA on replicational bypass of DNA lesions in Saccharomyces cerevisiae. *Mol Cell Biol* **24**:4267-74.

Haracska L, Unk I, Johnson RE, Johansson E, Burgers PM, Prakash S, Prakash L (2001) Roles of yeast DNA polymerases δ and ζ and of Rev1 in the bypass of abasic sites. *Genes Dev* **15**:945-54.

Harfe BD, Jinks-Robertson S (2000) DNA polymerase ζ introduces multiple mutations when bypassing spontaneous DNA damage in *Saccharomyces cerevisiae*. *Mol Cell* **6**:1491-9.

Helleday T (2013) PrimPol breaks replication barriers. *Nat Struct Mol Biol* **20**:1348-50.

Hoege C, Pfander B, Moldovan GL, Pyrowolakis G, Jentsch S (2002) RAD6-dependent DNA repair is linked to modification of PCNA by ubiquitin and SUMO. *Nature* **419**:135-41.

Hoeijmakers JH (2009) DNA damage, aging, and cancer. *N Engl J Med* **361**:1475-85.

Hogg M, Seki M, Wood RD, Doublie S, Wallace SS (2011) Lesion bypass activity of DNA polymerase θ (POLQ) is an intrinsic property of the pol domain and depends on unique sequence inserts. *J Mol Biol* **405**:642-52.

Huang M, Zhou Z, Elledge SJ (1998) The DNA replication and damage checkpoint pathways induce transcription by inhibition of the Crt1 repressor. *Cell* **94**:595-605.

Ito J, Braithwaite DK (1991) Compilation and alignment of DNA polymerase sequences. *Nucleic Acids Res* **19**:4045-57.

Iyer VN, Rupp WD (1971) Usefulness of benzoylated naphthoylated DEAE-cellulose to distinguish and fractionate double-stranded DNA bearing different extents of single-stranded regions. *Biochim Biophys Acta* **228**:117-26.

Johnson RE, Haracska L, Prakash S, Prakash L (2001) Role of DNA polymerase η in the bypass of a (6-4) TT photoproduct. *Mol Cell Biol* **21**:3558-63.

Johnson RE, Prakash L, Prakash S (2012) Pol31 and Pol32 subunits of yeast DNA polymerase δ are also essential subunits of DNA polymerase ζ. *Proc Natl Acad Sci USA* **109**:12455-60.

Johnson RE, Torres-Ramos CA, Izumi T, Mitra S, Prakash S, Prakash L (1998) Identification of *APN2*, the *Saccharomyces cerevisiae* homolog of the major human AP endonuclease *HAP1*, and its role in the repair of abasic sites. *Genes Dev* **12**:3137-43.

Johnson RE, Washington MT, Haracska L, Prakash S, Prakash L (2000a) Eukaryotic polymerases ι and ζ act sequentially to bypass DNA lesions. *Nature* **406**:1015-9.

Johnson RE, Washington MT, Prakash S, Prakash L (2000b) Fidelity of human DNA polymerase η. *J Biol Chem* **275**:7447-50.

Kadyrova LY, Mertz TM, Zhang Y, Northam MR, Sheng Z, Lobachev KS, Shcherbakova PV, Kadyrov FA (2013) A reversible histone H3 acetylation cooperates with mismatch repair and replicative polymerases in maintaining genome stability. *PLoS Genet* **9(10)**:e1003899.

Kannouche PL, Wing J, Lehmann AR (2004) Interaction of human DNA polymerase η with monoubiquitinated PCNA: a possible mechanism for the polymerase switch in response to DNA damage. *Mol Cell* **14**:491-500.

Kim JK, Choi BS (1995) The solution structure of DNA duplex-decamer containing the (6-4) photoproduct of thymidylyl(3'-->5')thymidine by NMR and relaxation matrix refinement. *Eur J Biochem* **228**:849-54.

Kim N, Mudrak SV, Jinks-Robertson S (2011) The dCMP transferase activity of yeast Rev1 is biologically relevant during the bypass of endogenously generated AP sites. *DNA Repair* **10**:1262-71.

Kochenova OV, Daee DL, Mertz TM, Shcherbakova PV (2015) DNA polymerase ζ-dependent lesion bypass in *Saccharomyces cerevisiae* is accompanied by error-prone copying of long stretches of adjacent DNA. *PLoS Genet* **11**:e1005110.

Kow YW, Bao G, Minesinger B, Jinks-Robertson S, Siede W, Jiang YL, Greenberg MM (2005) Mutagenic effects of abasic and oxidized abasic lesions in *Saccharomyces cerevisiae*. *Nucleic Acids Res* **33**:6196-202.

Kowalczykowski SC (2015) An Overview of the Molecular Mechanisms of Recombinational DNA Repair. *Cold Spring Harb Perspect Biol* **7**

Kozmin SG, Pavlov YI, Kunkel TA, Sage E (2003) Roles of *Saccharomyces cerevisiae* DNA polymerases Polη and Polζ in response to irradiation by simulated sunlight. *Nucleic Acids Res* **31**:4541-52.

Krakoff IH, Brown NC, Reichard P (1968) Inhibition of ribonucleoside diphosphate reductase by hydroxyurea. *Cancer Res* **28**:1559-65.

Kraszewska J, Garbacz M, Jonczyk P, Fijalkowska IJ, Jaszczur M (2012) Defect of Dpb2p, a noncatalytic subunit of DNA polymerase ε, promotes error prone replication of undamaged chromosomal DNA in *Saccharomyces cerevisiae*. *Mutat Res* **737**:34-42.

Kumar D, Abdulovic AL, Viberg J, Nilsson AK, Kunkel TA, Chabes A (2011) Mechanisms of mutagenesis *in vivo* due to imbalanced dNTP pools. *Nucleic Acids Res* **39**:1360-71.

Kumar D, Viberg J, Nilsson AK, Chabes A (2010) Highly mutagenic and severely imbalanced dNTP pools can escape detection by the S-phase checkpoint. *Nucleic Acids Res* **38**:3975-83.

Kunz BA, Henson ES, Roche H, Ramotar D, Nunoshiba T, Demple B (1994) Specificity of the mutator caused by deletion of the yeast structural gene (*APN1*) for the major apurinic endonuclease. *Proc Natl Acad Sci USA* **91**:8165-9.

Labib K, De Piccoli G (2011) Surviving chromosome replication: the many roles of the S-phase checkpoint pathway. *Philos Trans R Soc Lond B Biol Sci* **366**:3554-61.

Lada AG, Waisertreiger IS, Grabow CE, Prakash A, Borgstahl GE, Rogozin IB, Pavlov YI (2011) Replication protein A (RPA) hampers the processive action of APOBEC3G cytosine deaminase on single-stranded DNA. *PLoS One* **6**:e24848.

Lang GI, Murray AW (2011) Mutation rates across budding yeast chromosome *VI* are correlated with replication timing. *Genome Biol Evol* **3**:799-811.

Lawrence CW (2004) Cellular functions of DNA polymerase ζ and Rev1 protein. *Adv Protein Chem* **69**:167-203.

Lawrence CW, Hinkle DC (1996) DNA polymerase ζ and the control of DNA damage induced mutagenesis in eukaryotes. *Cancer Surv* **28**:21-31.

Lee YS, Gao Y, Yang W (2015) How a homolog of high-fidelity replicases conducts mutagenic DNA synthesis. *Nat Struct Mol Biol* **22**:298-303.

Lehmann AR (1972) Postreplication repair of DNA in ultraviolet-irradiated mammalian cells. *J Mol Biol* **66**:319-37.

Lehmann AR, Fuchs RP (2006) Gaps and forks in DNA replication: Rediscovering old models. *DNA Repair* **5**:1495-8.

Lehner K, Jinks-Robertson S (2009) The mismatch repair system promotes DNA polymerase ζ-dependent translesion synthesis in yeast. *Proc Natl Acad Sci USA* **106**:5749-54.

Lindahl T (1974) An *N*-glycosidase from *Escherichia coli* that releases free uracil from DNA containing deaminated cytosine residues. *Proc Natl Acad Sci USA* **71**:3649-53.

Lindahl T (1979) DNA glycosylases, endonucleases for apurinic/apyrimidinic sites, and base excision-repair. *Prog Nucleic Acid Res Mol Biol* **22**:135-92.

Lindahl T (1993) Instability and decay of the primary structure of DNA. *Nature* **362**:709-15.

Lindahl T, Barnes DE (2000) Repair of endogenous DNA damage. *Cold Spring Harb Symp Quant Biol* **65**:127-33.

Lindahl T, Karlstrom O (1973) Heat-induced depyrimidination of deoxyribonucleic acid in neutral solution. *Biochemistry* **12**:5151-4.

Lindahl T, Nyberg B (1972) Rate of depurination of native deoxyribonucleic acid. *Biochemistry* **11**:3610-8.

Lindahl T, Nyberg B (1974) Heat-induced deamination of cytosine residues in deoxyribonucleic acid. *Biochemistry* **13**:3405-10.

Lis ET, O'Neill BM, Gil-Lamaignere C, Chin JK, Romesberg FE (2008) Identification of pathways controlling DNA damage induced mutation in *Saccharomyces cerevisiae*. *DNA Repair* **7**:801-10.

Livneh Z, Ziv O, Shachar S (2010) Multiple two-polymerase mechanisms in mammalian translesion DNA synthesis. *Cell Cycle* **9**:729-35.

Loeb LA, Preston BD (1986) Mutagenesis by apurinic/apyrimidinic sites. *Annu Rev Genet* **20**:201-30.

Lopes M, Foiani M, Sogo JM (2006) Multiple mechanisms control chromosome integrity after replication fork uncoupling and restart at irreparable UV lesions. *Mol Cell* **21**:15-27.

Makarova AV, Burgers PM (2015) Eukaryotic DNA polymerase ζ. *DNA Repair* **29**:47-55.

Makarova AV, Nick McElhinny SA, Watts BE, Kunkel TA, Burgers PM (2014) Ribonucleotide incorporation by yeast DNA polymerase ζ. *DNA Repair* **18**:63-7.

Makarova AV, Stodola JL, Burgers PM (2012) A four-subunit DNA polymerase ζ complex containing Pol δ accessory subunits is essential for PCNA-mediated mutagenesis. *Nucleic Acids Res* **40**:11618-26.

Mann DB, Springer DL, Smerdon MJ (1997) DNA damage can alter the stability of nucleosomes: effects are dependent on damage type. *Proc Natl Acad Sci USA* **94**:2215-20.

Maor-Shoshani A, Reuven NB, Tomer G, Livneh Z (2000) Highly mutagenic replication by DNA polymerase V (UmuC) provides a mechanistic basis for SOS untargeted mutagenesis. *Proc Natl Acad Sci USA* **97**:565-70.

Matsuda T, Bebenek K, Masutani C, Hanaoka F, Kunkel TA (2000) Low fidelity DNA synthesis by human DNA polymerase-eta. *Nature* **404**:1011-3.

McCulloch SD, Kokoska RJ, Chilkova O, Welch CM, Johansson E, Burgers PM, Kunkel TA (2004) Enzymatic switching for efficient and accurate translesion DNA replication. *Nucleic Acids Res* **32**:4665-75.

McCulloch SD, Kunkel TA (2008) The fidelity of DNA synthesis by eukaryotic replicative and translesion synthesis polymerases. *Cell Res* **18**:148-61.

McDonald JP, Levine AS, Woodgate R (1997) The *Saccharomyces cerevisiae RAD30* gene, a homologue of *Escherichia coli dinB* and *umuC*, is DNA damage inducible and functions in a novel error-free postreplication repair mechanism. *Genetics* **147**:1557-68.

McGuffee SR, Smith DJ, Whitehouse I (2013) Quantitative, genome-wide analysis of eukaryotic replication initiation and termination. *Mol Cell* **50**:123-35.

McVey M (2010) Strategies for DNA interstrand crosslink repair: insights from worms, flies, frogs, and slime molds. *Environ Mol Mutagen* **51**:646-58.

Meneghini R (1976) Gaps in DNA synthesized by ultraviolet light-irradiated WI38 human cells. *Biochim Biophys Acta* **425**:419-27.

Mertz TM, Sharma S, Chabes A, Shcherbakova PV (2015) Colon cancer-associated mutator DNA polymerase δ variant causes expansion of dNTP pools increasing its own infidelity. *Proc Natl Acad Sci USA* **112**:E2467-76.

Mitchell DL, Jen J, Cleaver JE (1992) Sequence specificity of cyclobutane pyrimidine dimers in DNA treated with solar (ultraviolet B) radiation. *Nucleic Acids Res* **20**:225-9.

Mitchell DL, Nairn RS (1989) The biology of the (6-4) photoproduct. *Photochem Photobiol* **49**:805-19.

Mitchell DL, Nguyen TD, Cleaver JE (1990) Nonrandom induction of pyrimidine-pyrimidone (6-4) photoproducts in ultraviolet-irradiated human chromatin. *J Biol Chem* **265**:5353-6.

Murakumo Y, Ogura Y, Ishii H, Numata S, Ichihara M, Croce CM, Fishel R, Takahashi M (2001) Interactions in the error-prone postreplication repair proteins hREV1, hREV3, and hREV7. *J Biol Chem* **276**:35644-51.

Nelson JR, Lawrence CW, Hinkle DC (1996a) Deoxycytidyl transferase activity of yeast REV1 protein. *Nature* **382**:729-31.

Nelson JR, Lawrence CW, Hinkle DC (1996b) Thymine-thymine dimer bypass by yeast DNA polymerase ζ. *Science* **272**:1646-9.

Neto JB, Gentil A, Cabral RE, Sarasin A (1992) Mutation spectrum of heat-induced abasic sites on a single-stranded shuttle vector replicated in mammalian cells. *J Biol Chem* **267**:19718-23.

Newlon CS (1988) Yeast chromosome replication and segregation. *Microbiol Rev* **52**:568-601.

Niida H, Shimada M, Murakami H, Nakanishi M (2010) Mechanisms of dNTP supply that play an essential role in maintaining genome integrity in eukaryotic cells. *Cancer Sci* **101**:2505-9.

Nik-Zainal S, Alexandrov LB, Wedge DC, Van Loo P, Greenman CD, Raine K, Jones D, Hinton J, Marshall J, Stebbings LA, Menzies A, Martin S, Leung K, Chen L, Leroy C, Ramakrishna M, Rance R, Lau KW, Mudie LJ, Varela I et al. (2012) Mutational processes molding the genomes of 21 breast cancers. *Cell* **149**:979-93.

Northam MR, Garg P, Baitin DM, Burgers PM, Shcherbakova PV (2006) A novel function of DNA polymerase ζ regulated by PCNA. *EMBO J* **25**:4316-25.

Northam MR, Moore EA, Mertz TM, Binz SK, Stith CM, Stepchenkova EI, Wendt KL, Burgers PM, Shcherbakova PV (2014) DNA polymerases ζ and Rev1 mediate error-prone bypass of non-B DNA structures. *Nucleic Acids Res* **42**:290-306.

Northam MR, Robinson HA, Kochenova OV, Shcherbakova PV (2010) Participation of DNA polymerase ζ in replication of undamaged DNA in *Saccharomyces cerevisiae*. *Genetics* **184**:27-42.

Ohashi E, Murakumo Y, Kanjo N, Akagi J, Masutani C, Hanaoka F, Ohmori H (2004) Interaction of hREV1 with three human Y-family DNA polymerases. *Genes Cells* **9**:523-31.

Okuda T, Lin X, Trang J, Howell SB (2005) Suppression of hREV1 expression reduces the rate at which human ovarian carcinoma cells acquire resistance to cisplatin. *Mol Pharmacol* **67**:1852-60.

Otsuka C, Kunitomi N, Iwai S, Loakes D, Negishi K (2005) Roles of the polymerase and BRCT domains of Rev1 protein in translesion DNA synthesis in yeast *in vivo*. *Mutat Res* **578**:79-87.

Pages V, Johnson RE, Prakash L, Prakash S (2008) Mutational specificity and genetic control of replicative bypass of an abasic site in yeast. *Proc Natl Acad Sci USA* **105**:1170-5.

Pavlov YI, Nguyen D, Kunkel TA (2001a) Mutator effects of overproducing DNA polymerase eta (Rad30) and its catalytically inactive variant in yeast. *Mutat Res* **478**:129-39.

Pavlov YI, Shcherbakova PV, Kunkel TA (2001b) *In vivo* consequences of putative active site mutations in yeast DNA polymerases α, ε, δ, and ζ. *Genetics* **159**:47-64.

Pfeifer GP, Drouin R, Riggs AD, Holmquist GP (1991) *In vivo* mapping of a DNA adduct at nucleotide resolution: detection of pyrimidine (6-4) pyrimidone photoproducts by ligation-mediated polymerase chain reaction. *Proc Natl Acad Sci USA* **88**:1374-8.

Poli J, Tsaponina O, Crabbe L, Keszthelyi A, Pantesco V, Chabes A, Lengronne A, Pasero P (2012) dNTP pools determine fork progression and origin usage under replication stress. *EMBO J* **31**:883-94.

Popoff SC, Spira AI, Johnson AW, Demple B (1990) Yeast structural gene (*APN1*) for the major apurinic endonuclease: homology to *Escherichia coli* endonuclease IV. *Proc Natl Acad Sci USA* **87**:4193-7.

Prakash L (1981) Characterization of postreplication repair in *Saccharomyces cerevisiae* and effects of *rad6*, *rad18*, *rev3* and *rad52* mutations. *Mol Gen Genet* **184**:471-8.

Prakash S, Johnson RE, Prakash L (2005) Eukaryotic translesion synthesis DNA polymerases: specificity of structure and function. *Annu Rev Biochem* **74**:317-53.

Rastogi RP, Richa, Kumar A, Tyagi MB, Sinha RP (2010) Molecular mechanisms of ultraviolet radiation-induced DNA damage and repair. *J Nucleic Acids* **2010**:592980.

Ravanat JL, Douki T, Cadet J (2001) Direct and indirect effects of UV radiation on DNA and its components. *J Photochem Photobiol B* **63**:88-102.

Rebhandl S, Huemer M, Greil R, Geisberger R (2015) AID/APOBEC deaminases and cancer. *Oncoscience* **2**:320-33.

Reichard P (1988) Interactions between deoxyribonucleotide and DNA synthesis. *Annu Rev Biochem* **57**:349-74.

Roberts SA, Sterling J, Thompson C, Harris S, Mav D, Shah R, Klimczak LJ, Kryukov GV, Malc E, Mieczkowski PA, Resnick MA, Gordenin DA (2012) Clustered mutations in yeast and in human cancers can arise from damaged long single-strand DNA regions. *Mol Cell* **46**:424-35.

Ruiz-Rubio M, Bridges BA (1987) Mutagenic DNA repair in *Escherichia coli*. XIV. Influence of two DNA polymerase III mutator alleles on spontaneous and UV mutagenesis. *Mol Gen Genet* **208**:542-8.

Rupp WD, Howard-Flanders P (1968) Discontinuities in the DNA synthesized in an excision-defective strain of *Escherichia coli* following ultraviolet irradiation. *J Mol Biol* **31**:291-304.

Sabouri N, Viberg J, Goyal DK, Johansson E, Chabes A (2008) Evidence for lesion bypass by yeast replicative DNA polymerases during DNA damage. *Nucleic Acids Res* **36**:5660-7.

Sakamoto AN, Stone JE, Kissling GE, McCulloch SD, Pavlov YI, Kunkel TA (2007) Mutator alleles of yeast DNA polymerase ζ. *DNA Repair* **6**:1829-38.

Sale JE (2013) Translesion DNA synthesis and mutagenesis in eukaryotes. *Cold Spring Harb Perspect Biol* **5**:a012708.

Sale JE, Lehmann AR, Woodgate R (2012) Y-family DNA polymerases and their role in tolerance of cellular DNA damage. *Nat Rev Mol Cell Biol* **13**:141-52.

Schaaper RM, Mathews CK (2013) Mutational consequences of dNTP pool imbalances in *E. coli*. *DNA Repair* **12**:73-9.

Scharer OD (2013) Nucleotide excision repair in eukaryotes. *Cold Spring Harb Perspect Biol* **5**:a012609.

Shapiro R (1981) Damage to DNA caused by hydrolysis. In Chromosome damage and repair, Seeberg E, Kleppe K (eds) pp 3-12. New York, NY: Plenum Publishing Corp.

Sharma NM, Kochenova OV, Shcherbakova PV (2011) The non-canonical protein binding site at the monomer-monomer interface of yeast proliferating cell nuclear antigen (PCNA) regulates the Rev1-PCNA interaction and Polzeta/Rev1-dependent translesion DNA synthesis. *J Biol Chem* **286**:33557-66.

Sharma S, Shah NA, Joiner AM, Roberts KH, Canman CE (2012) DNA polymerase ζ is a major determinant of resistance to platinum-based chemotherapeutic agents. *Mol Pharmacol* **81**:778-87.

Shcherbakova PV, Kunkel TA (1999) Mutator phenotypes conferred by *MLH1* overexpression and by heterozygosity for *mlh1* mutations. *Mol Cell Biol* **19**:3177-83.

Shcherbakova PV, Noskov VN, Pshenichnov MR, Pavlov YI (1996) Base analog 6-*N*-hydroxylaminopurine mutagenesis in the yeast *S. cerevisiae* is controlled by replicative DNA polymerases. *Mutat Res* **369**:33-44.

Shcherbakova PV, Pavlov YI (1993) Mutagenic specificity of the base analog 6-*N*-hydroxylaminopurine in the *URA3* gene of the yeast *Saccharomyces cerevisiae*. *Mutagenesis* **8**:417-21.

Shcherbakova PV, Pavlov YI (1996) 3'-->5' exonucleases of DNA polymerases e and d correct base analog induced DNA replication errors on opposite DNA strands in *Saccharomyces cerevisiae*. *Genetics* **142**:717-26.

Shcherbakova PV, Pavlov YI, Chilkova O, Rogozin IB, Johansson E, Kunkel TA (2003) Unique error signature of the four-subunit yeast DNA polymerase ε. *J Biol Chem* **278**:43770-80.

Sikorski RS, Hieter P (1989) A system of shuttle vectors and yeast host strains designed for efficient manipulation of DNA in *Saccharomyces cerevisiae*. *Genetics* **122**:19-27.

Smith DJ, Whitehouse I (2012) Intrinsic coupling of lagging-strand synthesis to chromatin assembly. *Nature* **483**:434-8.

Stelter P, Ulrich HD (2003) Control of spontaneous and damage-induced mutagenesis by SUMO and ubiquitin conjugation. *Nature* **425**:188-91.

Stodola JL, Burgers PM (2016) Resolving individual steps of Okazaki-fragment maturation at a millisecond timescale. *Nat Struct Mol Biol* **23(5)**:402-8.

Stodola JL, Stith CM, Burgers PM (2016) Proficient replication of the yeast genome by a viral DNA polymerase. *J Biol Chem* **291(22)**:11698-705.

Stone JE, Kumar D, Binz SK, Inase A, Iwai S, Chabes A, Burgers PM, Kunkel TA (2011) Lesion bypass by *S. cerevisiae* Pol ζ alone. *DNA Repair* **10**:826-34.

Stone JE, Lujan SA, Kunkel TA, Kunkel TA (2012) DNA polymerase ζ generates clustered mutations during bypass of endogenous DNA lesions in *Saccharomyces cerevisiae*. *Environ Mol Mutagen* **53**:777-86.

Takata K, Tomida J, Reh S, Swanhart LM, Takata M, Hukriede NA, Wood RD (2015) Conserved overlapping gene arrangement, restricted expression, and biochemical activities of DNA polymerase v (*POLN*). *J Biol Chem* **290**:24278-93.

Taylor BJ, Nik-Zainal S, Wu YL, Stebbings LA, Raine K, Campbell PJ, Rada C, Stratton MR, Neuberger MS (2013) DNA deaminases induce break-associated mutation showers with implication of APOBEC3B and 3A in breast cancer kataegis. *Elife* **2**:e00534.

Taylor JS, Garrett DS, Cohrs MP (1988) Solution-state structure of the Dewar pyrimidinone photoproduct of thymidylyl-(3'----5')-thymidine. *Biochemistry* **27**:7206-15.

Tijsterman M, de Pril R, Tasseron-de Jong JG, Brouwer J (1999) RNA polymerase II transcription suppresses nucleosomal modulation of UV-induced (6-4) photoproduct and cyclobutane pyrimidine dimer repair in yeast. *Mol Cell Biol* **19**:934-40.

Tissier A, Kannouche P, Reck MP, Lehmann AR, Fuchs RP, Cordonnier A (2004) Co-localization in replication foci and interaction of human Y-family members, DNA polymerase pol η and REV1 protein. *DNA Repair* **3**:1503-14.

Torres-Ramos CA, Johnson RE, Prakash L, Prakash S (2000) Evidence for the involvement of nucleotide excision repair in the removal of abasic sites in yeast. *Mol Cell Biol* **20**:3522-8.

Tremblay M, Teng Y, Paquette M, Waters R, Conconi A (2008) Complementary roles of yeast Rad4p and Rad34p in nucleotide excision repair of active and inactive rRNA gene chromatin. *Mol Cell Biol* **28**:7504-13.

Tropp BE (2012) Molecular Biology: Genes to Proteins. Sudbury, MA: Jones & Bartlett Learning.

Tse L, Kang TM, Yuan J, Mihora D, Becket E, Maslowska KH, Schaaper RM, Miller JH (2016) Extreme dNTP pool changes and hypermutability in *dcd ndk* strains. *Mutat Res* **784-785**:16-24.

Ulrich HD (2011) Timing and spacing of ubiquitin-dependent DNA damage bypass. *FEBS Lett* **585**:2861-7.

Ulrich HD, Walden H (2010) Ubiquitin signalling in DNA replication and repair. *Nat Rev Mol Cell Biol* **11**:479-89.

Unrau P, Wheatcroft R, Cox B, Olive T (1973) The formation of pyrimidine dimers in the DNA of fungi and bacteria. *Biochim Biophys Acta* **312**:626-32.

Waisertreiger IS, Liston VG, Menezes MR, Kim HM, Lobachev KS, Stepchenkova EI, Tahirov TH, Rogozin IB, Pavlov YI (2012) Modulation of mutagenesis in eukaryotes by DNA replication fork dynamics and quality of nucleotide pools. *Environ Mol Mutagen* **53**:699-724.

Wan L, Lou J, Xia Y, Su B, Liu T, Cui J, Sun Y, Lou H, Huang J (2013) hPrimpol1/CCDC111 is a human DNA primase-polymerase required for the maintenance of genome integrity. *EMBO Rep* **14**:1104-12.

Wang Z, Rossman TG (1994) Isolation of DNA fragments from agarose gel by centrifugation. *Nucleic Acids Res* **22**:2862-3.

Washington MT, Johnson RE, Prakash S, Prakash L (1999) Fidelity and processivity of *Saccharomyces cerevisiae* DNA polymerase η. *J Biol Chem* **274**:36835-8.

Waters CA, Strande NT, Wyatt DW, Pryor JM, Ramsden DA (2014) Nonhomologous end joining: a good solution for bad ends. *DNA Repair* **17**:39-51.

Waters LS, Minesinger BK, Wiltrout ME, D'Souza S, Woodruff RV, Walker GC (2009) Eukaryotic translesion polymerases and their roles and regulation in DNA damage tolerance. *Microbiol and Mol Biol Rev* **73**:134-54.

Waters LS, Walker GC (2006) The critical mutagenic translesion DNA polymerase Rev1 is highly expressed during G(2)/M phase rather than S phase. *Proc Natl Acad Sci USA* **103**:8971-6.

Watt DL, Buckland RJ, Lujan SA, Kunkel TA, Chabes A (2016) Genome-wide analysis of the specificity and mechanisms of replication infidelity driven by imbalanced dNTP pools. *Nucleic Acids Res* **44**:1669-80.

Weerasooriya S, Jasti VP, Basu AK (2014) Replicative bypass of abasic site in Escherichia coli and human cells: similarities and differences. *PLoS One* **9**:e107915.

Williams LN, Marjavaara L, Knowels GM, Schultz EM, Fox EJ, Chabes A, Herr AJ (2015) dNTP pool levels modulate mutator phenotypes of error-prone DNA polymerase ε variants. *Proc Natl Acad Sci USA* **112**:E2457-66.

Wiltrout ME, Walker GC (2011) The DNA polymerase activity of *Saccharomyces cerevisiae* Rev1 is biologically significant. *Genetics* **187**:21-35.

Xie K, Doles J, Hemann MT, Walker GC (2010) Error-prone translesion synthesis mediates acquired chemoresistance. *Proc Natl Acad Sci USA* **107**:20792-7.

Yagi Y, Ogawara D, Iwai S, Hanaoka F, Akiyama M, Maki H (2005) DNA polymerases η and κ are responsible for error-free translesion DNA synthesis activity over a *cis-syn* thymine dimer in *Xenopus laevis* oocyte extracts. *DNA Repair* **4**:1252-69.

Yang W (2014) An Overview of Y-Family DNA Polymerases and a Case Study of Human DNA Polymerase η. *Biochemistry* **53**:2793-803.

Yang Y, Sterling J, Storici F, Resnick MA, Gordenin DA (2008) Hypermutability of damaged single-strand DNA formed at double-strand breaks and uncapped telomeres in yeast *Saccharomyces cerevisiae*. *PLoS Genet* **4**:e1000264.

Yu SL, Johnson RE, Prakash S, Prakash L (2001) Requirement of DNA polymerase η for error-free bypass of UV-induced CC and TC photoproducts. *Mol Cell Biol* **21**:185-8.

Zhang H, Siede W (2002) UV-induced T-->C transition at a TT photoproduct site is dependent on *Saccharomyces cerevisiae* polymerase η *in vivo*. *Nucleic Acids Res* **30**:1262-7.

Zhang Y, Wu X, Guo D, Rechkoblit O, Geacintov NE, Wang Z (2002) Two-step error-prone bypass of the (+)- and (-)-*trans-anti*-BPDE-N^2-dG adducts by human DNA polymerases η and κ. *Mutat Res* **510**:23-35.

Zhao B, Xie Z, Shen H, Wang Z (2004) Role of DNA polymerase η in the bypass of abasic sites in yeast cells. *Nucleic Acids Res* **32**:3984-94.

Zhao X, Chabes A, Domkin V, Thelander L, Rothstein R (2001) The ribonucleotide reductase inhibitor Sml1 is a new target of the Mec1/Rad53 kinase cascade during growth and in response to DNA damage. *EMBO J* **20**:3544-53.

Zharkov DO (2008) Base excision DNA repair. *Cell Mol Life Sci* **65**:1544-65.

Zhong X, Garg P, Stith CM, Nick McElhinny SA, Kissling GE, Burgers PM, Kunkel TA (2006) The fidelity of DNA synthesis by yeast DNA polymerase ζ alone and with accessory proteins. *Nucleic Acids Res* **34**:4731-42.

Zhou BB, Elledge SJ (2000) The DNA damage response: putting checkpoints in perspective. *Nature* **408**:433-9.

Zhou Y, Wang J, Zhang Y, Wang Z (2010) The catalytic function of the Rev1 dCMP transferase is required in a lesion-specific manner for translesion synthesis and base damage-induced mutagenesis. *Nucleic Acids Res* **38**:5036-46.

Appendices

8.1 Appendix A: dNTP pools measurements in the wild-type and *pol3-Y708A* strains

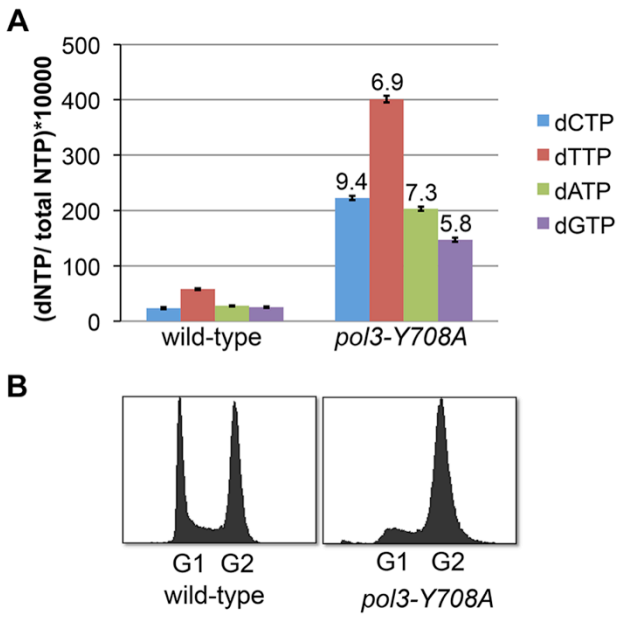

Figure 8.1 Analysis of dNTP pools and cell cycle in a DNA replication mutant that displays constitutively elevated Polζ-dependent mutagenesis.

(A) Intracellular dNTP levels normalized to total NTP in wild-type and *pol3-Y708A* strains. Data are presented as mean ± SD (n = 3 for wild-type strains and n = 4 for *pol3-Y708A* mutants) with the numbers above the bars indicating fold increase compared to wild type. **(B)** Fluorescence-activated cell sorter (FACS) analysis of asynchronous logarithmically growing wild-type and *pol3-Y708A* cultures that were used for dNTP pool measurements in **(A).** Intracellular dNTP levels in asynchronous logarithmically growing yeast strains were measured in the laboratory of Andrei Chabes (Umeå University, Sweden) as previously described (Mertz et al, 2015). (Data are a courtesy of Dr. Andrei Chabes laboratory (Umeå University, Sweden)).

8.2 Appendix B: dNTP pools measurements in the wild-type and *pol3-Y708A* strains treated with 20 mM HU

Measurements of dNTP pools in the *pol3-Y708A* strain treated with 20 mM HU revealed an approximately 25% reduction in dNTP concentrations (Figure 8.2 (A)). An isogenic wild-type strain also showed decreased average dNTP levels in the first 30 min of treatment with 20 mM HU (Figure 8.2 (A)), although at least some of it could be attributed to the changing cell cycle distribution. Particularly, the proportion of G1 cells, which have approximately two-fold lower dNTP pools (Chabes et al, 2003), varied between the time points (Figure 8.2 (B)). In contrast, the cell cycle distribution in the *pol3-Y708A* strain did not change significantly during the two hours in 20 mM HU (Figure 8.2 (B)), so the dNTP measurements shown in Figure 8.2 (A) reflect the actual decrease in intracellular levels.

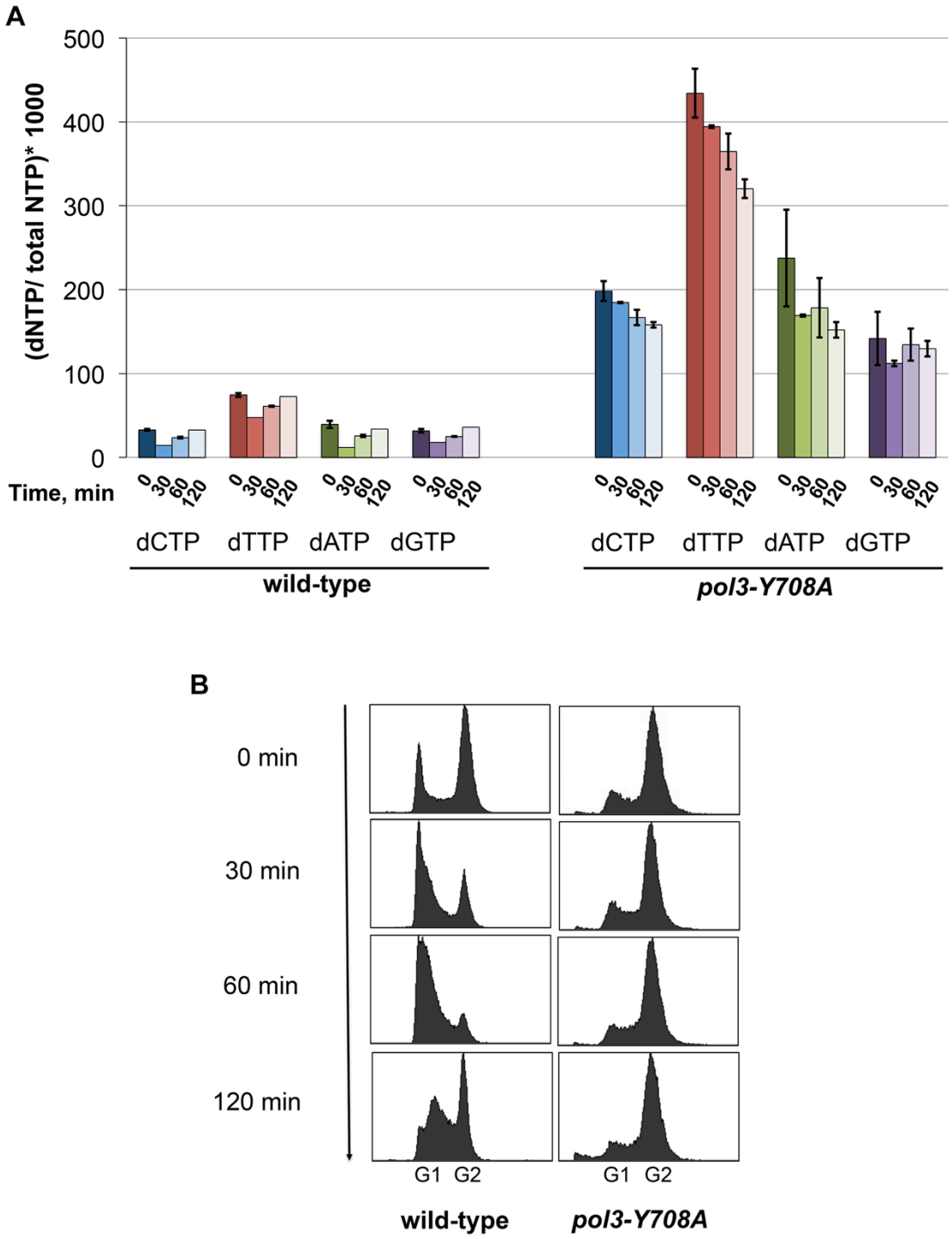

Figure 8.2 Effect of HU treatment on the dNTP levels and cell cycle progression of the wild-type and *pol3-Y708A* strains.

(A) Time course analysis of intracellular dNTP levels in wild-type and *pol3-Y708A* strains treated with 20 mM HU. Time after the addition of HU is indicated on the X axis. The dNTP levels are normalized to total NTPs. Data are presented as mean for two independent measurements. Error bars represent the range of values. To measure

dNTP pools in HU-treated cells, the overnight cultures were first diluted 10-fold and grown in the presence of 20 mM HU for 30, 60, and 120 min. After indicated time points cells were harvested and subjected to dNTP pools measurements according to the previously described procedure (Mertz et al, 2015).
(B) FACS analysis of HU-treated cultures of wild-type and *pol3-Y708A* strains that were used for dNTP pool measurements in *B*. Time after the addition of HU is indicated on the left (Data are a courtesy of Dr. Andrei Chabes laboratory (Umeå University, Sweden)).

8.3 Appendix C: Complex mutations, multiple mutations and large rearrangements induced by Polζ$_4$ and Polζ$_5$ *in vitro*.

Table 8.1 Complex mutations, multiple mutations and large rearrangements induced by Polζ$_4$ and Polζ$_5$ *in vitro*.

Mutation type	Sequence change	Location in *lacZ* sequence
Polζ$_4$, S-phase dNTPs		
Complex	TC → CA	80 – 81
	CCC → TC	-45 – -43
	GTG → TTT	82 – 84
	TCG → TTCA	139 – 141
	TGGCC → GGC (2X)	61 – 65
	TAATAG → CAATAA	152 – 157
	GTTTTAC → TTTTTA	69 – 75
	CCCTTCCCA → TCCTTCCCT	179 – 187
	ATTACGAATTCACTG → CGAATTCAC	48 – 62
	ATTACGAATTCACTGGCC → CGAATTCACGC	48 – 65
Multiple	A → G; T → G	91; 103
	C → A; T → A	134; 147
	G →T; ΔG	102; 123
	G → C; ΔG	148; 169
	A → G; T → G	48; 70
	G → T; C → A	53; 81
	G → T; T → C	-68; -36
	C → A; G → C	81; 118
	T → A; +T	98; 139
	ΔC; ΔC	143; 189
	C → A; G → T	37; 88
	G → T; A → G	102; 153
	T → C; ΔG	104; 159
	C → A; A → T	-55; 1
	T → A; T → C	67; 138
	C → T; G → T	58; 148
	C → A; T → A	-16; 87
	T → C; T → A	-58; 49
	T → A; C → T	-50; 58
	T → A; T → C	-2; 121
	G → A; A → T	-66; 59
	G → A; A → C	9; 171
	G → T; G → T	-68; 102
	G → T; +T	-38; 139
	G → C; G → T	-84; 102
	T → C; G → C	-22; 169
	T → A; GTAA → GTTTT	-54; 151 –154

	G → T; G → C	-84; 148
	GA → TG; G → T	-66 – -67; 149
	T → A; G → C; ΔG	-67; 100; 126
Polζ$_4$, damage-response dNTPs		
Complex	GTG → TTTG	-6 – - 4
	GTG → TTT	82 – 84
	TGC → CC	122 – 124
	CGCAC → T	168 – 172
	TGGCC → GGC (2X)	61 – 65
	AGCTGC → TGCGCA	190 – 195
	CGTCGTG → GTCGTT	78 – 84
	TCCCCCTTT → ACCCCCTTTT (4X)	131 – 139
Multiple	G → A; T → C	99; 112
	A → G; G → T	130; 145
	G → C; A → C	99; 130
	G → T; G → T	53; 84
	G → T; G → A	118; 157
	T → C; G → T	-36; 11
	G → C; C → T	118; 180
	G → T; G → A	-1; 66
	G → T; A → C	123; 190
	G → T; A → C	-66; 28
	C → A; A → T	-55; 39
	G → T; A → G	88; 188
	T → C; G → T	-21; 84
	G → T; ΔG	12; 123
	T → A; G → C	56; 141
	G → T; G → C	53; 169
	A → T; ΔA	-26; 94
	T → G; T → C	-63; 61
	G → C; G → C	-68; 79
	G → A; G → T	-68; 84
	G → A; +T	-77; 139
	G → A; +T	-84; 139
	ΔG; G → C	-47; 178
Polζ$_5$, S-phase dNTPs		
Complex	TA → G	-50 – -49
	GC →T	-38 – -37
	TA → AGC	38 – 39
	TA → AG	38 – 39
	GG → TC	89 – 90
	GC → AT	145 – 146
	ATG → TTT	-11 – -9
	GTG → CTT	82 – 84
	GCG → TCC	100 – 102
	CTG → ATT	146 – 148
	GCA → CCC	169 – 171
	TGCA → G	122 – 125
	GCTG → CCTA	145 – 148
	AATAG → AT	153 – 157

	GTAATAG → T	151 – 157
	TTAATGT → ATAAAGA	-73 – -67
	AAGAGGCCC → GGGGGCC	160 – 168
Multiple	C → G; ΔC	146; 158
	ΔT; C → A	113; 129
	ΔA; C → A	-45; -23
	ΔA; C → A	94; 146
	T → C; G → T	-58; 7
	C → T; CCCCC → TCCCT	68; 132 – 136
	ΔG; G → T; G → T	-38; 41; 53
	C → G; T → G; G → T	-55; 3; 47
	G → T; ΔT	12; 122
	ΔC; A → T; T → C	10; 31; 121
	G → T; G → T; G → C	63; 149; 178
	C → A; C → G	-59; 60
	del(90); T → C; G → A	-167 – -77; -34; 84
	T → C; G → A	-10; 191
Large rearrangements	TGTGTGGAATTGTGAGCGGATAACAATTTCAC → CGT	-7 – 25
Polζ$_5$, damage-response dNTPs		
Complex	TA → CT	38 – 39
	TG → CT	87 – 88
	GG → TC	88 – 89
	GC → CT	149 – 150
	GG → CT	148 – 149
	CCC → GCCT	134 – 136
	TCG → CA	176 – 178
	GCAC → TC	-47 – -44
	CGTG → TGTA	81 – 84
	AAAA → GAAC	91 – 94
	TTA → GTC	103 – 105
	ATGTT → TAGTTT	-11 – -7
	TCGTG → GTGTA	80 – 84
	TCGTG → GGGGGG	80 – 84
	CGCAC → GGCA	168 – 172
	CCGTCG → ACGTCC	64 – 69
	GCACCG → CCACCT	169 – 174
	TCCCAA → AT	183 – 188
	ATCCCCC → TTCCCCT	130 – 136
	AGAGGC → GGAGGGGG	161 – 167
	GTGTGGAAT → TTTGAAAG	-6 – 3
	TCCCCCTTT → CCCCCCTTTTAT	131 – 140
	AGCACATCCCCC → TCC	125 – 136
	ACCCTGGCGTTA → CCCCTGGCGTTC	94 – 105
	ATTACGAATTCACTGG → CGAATTCACTG	48 – 63
Multiple	CCCAGGCTTTACAC → Δ; C → T	-43 – -30; -20
	G → T; C → G	89; 101
	TG → AA; ΔG	-69 – -68; 47
	C → T; A → T	-14; 24

	+T; C → G	139; 177
	G → A; A → G	149; 188
	A → T; ΔC	128; 168
	G → T; A → T	88; 130
	A → T; C → A	24; 68
	C → T; G → T; G → C	134; 151; 178
	G → T; A → G	84; 130
	A → C; TCCCCC → TTCCCCT	94; 131 – 136
	T → G; GCG → CCT	104; 149 – 151
	G → T; C → A	84; 136
	T → A; +T	80; 139
	GTCGTTTTACAACG → TTTTTTAA; TCCCCC → TTCCCCT	66 – 76; 131 – 136
	G → C; A → G	79; 161
	C → A; C → G	65; 146
	A → C; GGC → AGG	85; 164 – 166
	G → T; AACAATTT → GACAATTTT; CGTTTTACAACG → TGTTTTACAACA	-4; 15 –23; 68 – 79
	G → C; G → C; G → T	-9; 11; 88
	G → T; G → C	-18; 88
	C → G; C → G	10; 142
	G → T; G → T	-47; 88
	C → A; A → T	10; 160
	C → T; +T	-30; 139
	+T; GGCGTTA → TTCGGTC	-71; 99 – 105
	G → A; ΔA; G → T	-24; 94; 157
	T → A; C → T	-2; 189
	T → C; G → T; G → A	-36; 149; 164
	A → T; C → T	-74; 136
Large rearrangements	GTTACCCAACTTAATCGCCTTGCAGCACATCCCCCTTTC → TTTTA	102 – 140
	GTTGTGTGGAATTGTGAGCGGATAACAATTTCACACAGGA → AC	-9 – 31
	CGTATGTTGTGTGGAATTGTGAGCGGATAACAATTTCACACAGG → TGTATT	-14 – 31
	GACAGGTTTCCCGACTGGAAAGCGGGCAGTGAGCGCAACGCAATTAATGTGAGTTAGCTCACTCA → TTTTTTT	-150 – -52
	CAGCTGGCACGACAGGTTTCCCGACTGGAAAGCGGGCAGTGAGCGCAACGCAATTAATGTG → ATTAGTA	-127 – -66
	CTTCCGGCTCGTATGTTGTGTGGAATTGTGAGCGGATAACAATTTCACACAGGAAACAGCTATGAC → AA	-23 – 43
	GTTGTGTGGAATTGTGAGCGGATAACAATTTCACAC→ A; A→C	-9 – 27; 59
	TGTTGTGTGGAATTGTGAGCGGATAACAATTTCACACAGG → AG	-10 – 30
	GACTGGAAAGCGGGCAGTGAGCGCAACGCAATTAATGTGAGTTAGCTCACTCATTAGGCACCCC	-105 – -24

	AGGCTTTACACTTTATG → TTTT	
	CTCGTATGTTGTGTGGAATTGTGAGCGGATAA CAATTTCACACAGGAAACAGCTATGACCATGAT TACGAATTCACTGGCCGTCGTTTT → TCTGGTTCGCTTTGAAGCTCGAATTAAAACGCG ATATTTGAAGTCTTTCGGGCTTCCTCTTAATCTT	-16 – 73

Sequence changes are listed in the order of increasing distance between two nucleotide changes. Mutations with the distance between them of ten nucleotides or fewer were considered complex mutations and counted as a single event. All other detectable nucleotide changes were included into calculation of error-rates for individual mutation types in Table 5.1. Δ, deletion; +, insertion.